RF Project 2267
Report 9

THE OHIO STATE UNIVERSITY

RESEARCH FOUNDATION

1314 KINNEAR ROAD COLUMBUS, OHIO 43212

STRESS CORROSION CRACKING OF TITANIUM ALLOYS

R. C. May, F. H. Beck and M. G. Fontana
Department of Metallurgical Engineering

NATIONAL AERONAUTICS AND SPACE ADMINISTRATION
Washington, D.C. 20546

Grant No. NGL 36-008-051

RF Project 2267

Report No. 9

SEMIANNUAL

REPORT

By

THE OHIO STATE UNIVERSITY
RESEARCH FOUNDATION

1314 KINNEAR RD.
COLUMBUS, OHIO 43212

To NATIONAL AERONAUTICS AND SPACE ADMINISTRATION

Washington, D.C. 20546

Grant No. NGL 36-008-051

On STRESS CORROSION CRACKING OF TITANIUM ALLOYS

For the period 1 July 1970 - 31 December 1970

Submitted by R. C. May, F. H. Beck and M. G. Fontana

Department of Metallurgical Engineering

Date September, 1971

FOREWORD

This report covers work through December 31, 1970 on the electrochemistry of titanium in acid solutions and its relation to stress corrosion cracking. Surface hydrides and oxides were found to play a critical role. Embrittlement due to hydrogen absorption occurred upon prolonged exposure. Straining electrode experiments provided no indication for strain-induced dissolution rates of sufficient magnitude to account for the rapid crack velocities observed for titanium stress corrosion in aqueous solutions. Straining at an applied potential of -1000 mV (SCE) produced current transients in the anodic direction which were not observed at less negative potentials.

This report is based on the Ph. D. dissertation of Mr. R. C. May. Work was performed at The Ohio State University under NASA Grant No. NGL 36-008-051.

TABLE OF CONTENTS

LIST OF TABLES

LIST OF FIGURES

LIST OF FIGURES (Cont'd.)

LIST OF FIGURES (Cont'd.)

INTRODUCTION

Stress corrosion cracking (SCC) is a very interesting and extremely complex subject. It has received much attention in recent years because it can produce sudden and drastic failures in metal parts that outwardly appear corrosion free. The phenomenon is an unfortunate but inevitable outgrowth of the development of stronger and more corrosion resistant alloys. It is most often associated with alloys that owe their corrosion resistance to the presence of protective surface films. Titanium has perhaps the most tenacious and quickly formed protective film, and yet the most rapid crack propagation velocity, of all the alloys that are susceptible to SCC.

SCC is a difficult subject to study quantitatively. This is because the critical processes occur inside the metal at the crack tip which is physically separated from the metal surface and the bulk solution and thus is inaccessible to normal external measurements. The overall aim of this investigation was to study, from an electrochemical point of view, the SCC of titanium alloys in aqueous solutions. Titanium alloys are susceptible to stress corrosion crack propagation in neutral NaCl solutions. However, recent experiments have indicated that the solution at the crack tip is much more acidic. With this information in mind experiments were conducted to study (1) the basic electrochemical behavior of titanium in acid chloride solutions and (2) the response of the metal to dynamic straining in the same environment. The aim of this second group of experiments was to simulate, as nearly as possible, the actual conditions which exist at the tip of a crack. One of the foremost theories proposed to explain the propagation of stress corrosion cracks is a hydrogen embrittlement theory involving the precipitation of embrittling titanium hydrides inside the metal near the crack tip. Consequently, information concerning the effects of these internal hydrides is abundant in the literature. On the other hand, the effect of surface hydrides on the cracking process has been largely ignored. However, an initial survey of the basic electrochemical literature indicated that surface hydrides play a critical role in the electrochemistry of titanium in acid solutions. Therefore, a significant part of the present investigation was devoted to a comprehensive analysis of the effect of surface films, particularly hydrides, on the electrochemical behavior of titanium in these solutions. The results of this analysis were quite striking and are presented in Chapter I.

I. THE ELECTROCHEMICAL BEHAVIOR OF TITANIUM IN ACID SOLUTIONS

1. General Aspects

Titanium is potentially a very reactive metal. The equilibrium potential for its dissolution to Ti^{3+} ions is -1450 mV(SCE).[1] Yet, the anodic dissolution of titanium in non-oxidizing solutions occurs in the potential range of -450 to -650 mV(SCE).[2,3,4,12] The fact that dissolution does not occur until a driving force of one volt has been applied implies that the anodic processes are strongly inhibited. Further, the maximum current obtained during anodic polarization in the dissolution potential range is surprisingly small. (i_{crit} for titanium in 3N H_2SO_4 is 110 $\mu A/cm^2$ while i_{crit} for iron in 1N H_2SO_4 is approximately 700,000 $\mu A/cm^2$.[5,6] These facts strongly suggest that the surface of titanium is covered by some sort of protective coating even during active dissolution at the peak of the polarization curve. This protective coating could be an oxide, a hydride, or perhaps chemisorbed oxygen.

Titanium has a high affinity for both hydrogen and oxygen. The standard electrode potential for the formation of the lowest hydride, TiH is +408 mV(SCE). The standard potential for forming the lowest oxide TiO is - 1542 mV(SCE). Therefore, both hydrides and oxides are possible over a very wide range of potential. Thus it is possible to have a hydride present during anodic polarization even in the passive range and to have an oxide present during cathodic polarization. Two surface hydrides[7] and numerous surface oxides[8] have been identified on titanium. Table 1 shows a list of possible surface reactions involving these hydrides and oxides and the standard electrode potential for each reaction. The table was taken largely from Tomashov and Mirolyabov;[5] however, the references listed are the actual sources of the thermodynamic data. There is some question as to the free energy of formation of titanium hydride, TiH_2. It has been listed as -20.6 kcal/mole[9] and -10.0 kcal/mole.[10] The electrode potentials corresponding to both of the free energies are listed in the table. In considering reactions of titanium hydride with other species the value of -20.6 kcal/mole (E°= +208 mV(SCE)) is used. The last group of reactions listed in the table, i.e., those for hydride oxidation, indicates the possibility of hydrides forming on top of oxides and visa versa. Th s phenomenon has been observed by Russian experimentors as well as in the present investigation. The results will be discussed in more detail later.

Since the films on the titanium surface play such an important role in stress corrosion cracking, their characteristics will now be discussed in detail.

Table 1 - Possible Surface Reactions on Titanium and their Standard Electrode Potentials

	No.	Reaction	E°mV (SCE)	E°mV (SHE)	Reference
Titanium Dissolution	a	$Ti \rightleftharpoons Ti^{3+} + 3e^-$	-1452	-1210	1
	b	$Ti + 3Cl^- \rightleftharpoons 3e^-$	-1020	- 778	13
	c	$Ti + 4Cl^- \rightleftharpoons TiCl_4 + 4e^-$	- 630	- 388	13
Hydride Dissolution	d	$TiH \rightleftharpoons Ti^{3+} + H^+ + 4e^-$	- 970	- 730	14
	e	$TiH_2 \rightleftharpoons Ti^{3+} + 2H^+ + 5e^-$	- 782	- 540	14
	f	$TiH \rightleftharpoons Ti^{3+} + 1/2\ H_2 + 3e^-$	-1232	- 990	5
	g	$TiH_2 \rightleftharpoons Ti^{3+} + H_2 + 3e^-$	-1152	- 910	5
Oxide Formation	h	$Ti + H_2O \rightleftharpoons TiO + 2H^+ + 2e^-$	-1542	-1300	1
	i	$2Ti + 3H_2O \rightleftharpoons Ti_2O_3 + 6H^+ + 6e^-$	-1482	-1240	14
	j	$3Ti + 5H_2O \rightleftharpoons Ti_3O_5 + 10H^+ + 10e^-$	-1412	-1170	14
	k	$Ti + 3H_2O \rightleftharpoons TiO_2\ H_2O + 4H^+ + 4e^-$	-1142	- 900	1
	l	$Ti + 2H_2O \rightleftharpoons TiO_2 + 4H^+ + 4e^-$	-1315	-1073	1
	m	$2TiO + H_2O \rightleftharpoons Ti_2O_3 + 2H^+ + 2e^-$	-1362	-1120	1
	n	$3Ti_2O_3 + H_2O \rightleftharpoons 2Ti_3O_5 + 2H^+ + 2e^-$	- 732 - 572 ± 130	- 490 - 330 ± 130	1 15
	o	$Ti_2O_3 + H_2O \rightleftharpoons 2TiO_2 + 2H^+ + 2e^-$	- 572 ±·220	- 330 ± 220	
	p	$Ti_2O_3 + 2H_2O \rightleftharpoons 2TiO_2 \cdot H_2O + 2H^+ + 2e^-$	- 333	- 91	1
Hydride Formation	q	$Ti + H^+ + e^- \rightleftharpoons TiH \quad \Delta G_f^{\circ} = -15.0\ \frac{kcal}{mole}$	+ 408	+ 650	14
	r	$Ti + 2H^+ + 2e^- \rightleftharpoons TiH_2 \quad \Delta G_f^{\circ} = -20.6\ \frac{kcal}{mole}$	+ 208	+ 450	9
		$\Delta G_f^{\circ} = -10.0\ \frac{kcal}{mole}$	- 25	+ 217	10
	s	$TiH + H_2O \rightleftharpoons TiO + 3H^+ + 3e^-$	- 892	- 650	14
	t	$TiH_2 + H_2O \rightleftharpoons TiO + 4H^+ + 4e^-$	- 662	- 420	14
	u	$2TiH + 3H_2O \rightleftharpoons Ti_2O_3 + 8H^+ + 8e^-$	-1012	- 770	14
	v	$2TiH_2 + 3H_2O \rightleftharpoons Ti_2O_3 + 10H^+ + 10e^-$	- 802	- 560	14
	w	$TiH + 2H_2O \rightleftharpoons TiO_2 + 5H^+ + 5e^-$	- 970	- 728	*
	x	$TiH + 3H_2O \rightleftharpoons TiO_2.H_2O + 5H^+ + 5e^-$	- 339	- 97	*
	y	$TiH_2 + 2H_2O \rightleftharpoons TiO_2 + 6H^+ + 6e^-$	- 808	- 566	*
	z	$TiH_2 + 3H_2O \rightleftharpoons TiO_2.H_2O + 6H^+ + 6e^-$	- 283	- 41	*
Others	aa	$O_2 + 4H^+ + 4e^- \rightleftharpoons 2H_2O$	+ 988	+1230	1
	ab	$2H^+ + 2e^- \rightleftharpoons H_2$	- 242	0	1
	ac	$Cl_2 + 2e^- \rightleftharpoons 2Cl^-$	+1118	+1360	1
	ad	$Ti^{3+} + H_2O \rightleftharpoons TiO^{2+} + 2H^+ + e^-$	- 140	+ 100	1

*Calculated by combining data from references 1 and 9.

Note: The potentials listed in the table are standard electrode potentials and do not depend on the direction of the reaction, e.g., ($Ti \rightleftharpoons Ti^{3+} + 3e^-$ represents the potential at which Ti is in equilibrium with a unit activity of its ions).

2. Oxides

The oxide that exists on the titanium surface depends on the oxidation state of the titanium ions. The ions have the highest valence under the most oxidizing conditions, i.e., a high temperature or a large positive potential. The composition of the highest, normally found, oxide on titanium is TiO_2. Hickman and Gulbransen[16] found TiO_2 on titanium exposed to air at temperatures between 300 and 700°C. Yahalom and Zahavi[17] anodized titanium in 0.1M H_2SO_4 at 30°C at a constant current density of 12.5 mA/cm^2. During their galvanostatic treatment the potential across the titanium rose to a value of about 90 volts. They identified the oxide that formed as TiO_2 with the anatase structure.

Data on the structure of films subjected to more mildly oxidizing conditions, such as spontaneous passivation in dilute acid solutions or anodic polarization at low positive potentials, are not abundant in the literature. It has been shown[18] that titanium will spontaneously reform its passive oxide after the latter has been removed in dilute solutions of hydrochloric and sulfuric acids (about 5% or less). When the strengths of the above acids are about 10% or more, anodic polarization must be applied to renew the passivity. Experiments at Ohio State University[19] demonstrated the spontaneous repassivation of Ti-8Al-Mo-1V alloy after abrasion of the surface in 1N HCl + 0.6N NaCl solutions. When the acid strength was 3N repassivation was not spontaneous.[19]

Tomashov[8] has studied the structure of passive oxide films. Table 2 was taken from his paper and shows his data as well as the work of other authors. The literature sources[20-24] are his and quote the original work. (Reference 20 gives details of the method of removing oxide films for electron diffraction.) A few of the findings from the table are extremely noteworthy. First, the film formed in air at room temperature was not found to be TiO_2 but rather TiO with a small amount of Ti_3O_5. (Other workers[29] also found differences between the air formed and solution formed films.) Secondly, spontaneous passivation in dilute solutions of various acids (HCl, H_2SO_4 and HNO_3) as well as 1N solutions of NaCl and NaOH produced the same oxide: $Ti_2O_3 \cdot 3\text{-}4\ TiO_2$. The author[8] also states that this same oxide is formed during anodic polarization of the above solutions provided that the applied potential does not exceed 1 to 2 volts. This finding implied that there is no fundamental difference between the process of naturally forming a film at open circuit and artificially forming it at a positive potential.[8] A third important observation is that the same film was formed in 40% H_2SO_4 (10.6N) at a potential just negative [-.05 volt(SHE)] of the potential for complete passivation as was formed at a potential much more positive [1 volt(SHE)] than that required for complete passivation. This implies that, at least in this case, passivation is not the result of a change in composition of the film but apparently is the result of the film growing to completely cover the surface. (Or perhaps adsorbed oxygen filling in holes in the film.)

Table 2 - The Structure of Oxide Films on Titanium under Different Oxidation Conditions

Conditions and duration of oxidation	Temp. °C	Composition of oxide film	Literature source
Oxidation in air for 10 days	18-20	TiO with a small quantity of Ti_3O_5	20
Corrosion in 92% H_2SO_4 for 100 hr	18-20	Ti_3O_5	21
Spontaneous passivation in solutions: 5% HCl, 5% H_2SO_4, 6% HNO_3, 1N NaCl, 1N NaOH for 10 days	18-20	$Ti_2O_3 \cdot 3\text{-}4TiO_2$	Author's data (8)
Anodic oxidation in 40% H_2SO_4 potentials of -0.05 and +1.0 V for 5 hr	18-20	$Ti_2O_3 \cdot 3\text{-}4TiO_2$	The same
Oxidation in Air	875-1050	Laminated scale of TiO, Ti_2O_3, and TiO_2 rutile	22
Oxidation in 10% CrO_3 for 10 hr	Boiling	TiO_2, anatase and rutile	23
Oxidation in aqua regia for 0.5 hr	Boiling	TiO_2, anatase	23
Oxidation in 50% HNO_3 for 2 hr	Boiling	The same	23
Anodic oxidation in 0.1N H_2SO_4. At a potential of +8.0 V for 5 hr	18-20	The same	24
Oxidation in 65% HNO_3 for 5 hr	Boiling	TiO_2, anatase with a small quantity of rutile	Author's data (8)
Anodic oxidation in 40% H_2SO_4. At a potential of +8.0 V for 15 min	18-20	The same	The same

3. Hydrides

Hydrides have been observed to form on the surface of titanium in aqueous solutions by a number of workers. Sanderson and Scully[25] found surface hydrides in aqueous NaCl (pH = 1) when the metal was plastically deformed. Ogawa and Watanabe[34] identified surface hydrides after a brief immersion in hydrofloric acid. Tomashov[5] found hydrides after cathodic charging in $3N_2H_4SO$. Otsuka[26,27] observed hydrides on the surface of specimens exposed to hydrochloric acid solutions of varying concentrations, from 5% (1.4N) to 31.1% (9.9N). In later work, Otsuka[7] identified the hydrides by electron diffraction and found that the composition was a function of the concentration of acid. Specimens immersed in 15% HCl (4.42N) for 20 hours were coated by a hydride of composition TiH. Specimens exposed to 12N HCl for the same length of time formed hydrides of composition TiH_2. Both hydrides were found to be fcc structure with the lattice constant varying with the hydrogen content from 4.40Å for TiH to 4.46Å for TiH_2.

When a specimen coated with a hydride was abraded with emery paper the film was found to be "much harder and more glossy" than the titanium substrate.[27] The film was also found to be tightly bound to the titanium in that it was difficult to abrade it off.[27] The presence of the hydride film can easily be recognized by immersing a coated specimen in hydrofloric acid. When this is done the hydride layer turns a black color.[5,27]

When a hydride is formed in a very strong acid (12N HCl)[7] or by prolonged cathodic charging in a weaker acid ($5mA/cm^2$ for 18 hr. in 0.5N H_2SO_4)[5] a noticeable change occurs in the appearance of the metal surface. The metal surface darkens and assumes a rough, porous appearance. This is thought to be due to the dissolution of the metal (especially in the strong acid) and to the absorption of a large quantity of hydrogen.

In a series of corrosion tests Otsuka[7] also demonstrated that the corrosion rate (as measured by weight loss) of titanium specimens in hydrochloric acid decreased when the hydride was present. Straumanis and Chen[28] found the same tendency in dilute sulfuric acid solutions. These corrosion tests as well as visual observation and physical abrasion of the hydrided surface[7,8,26,27] indicate that the hydride layer is a physically and chemically coherent phase which is tightly bound to the metal surface.

Quantitative data on the rate of formation of titanium hydride is very scarce. Most of the available data has been concerned with the identification of the hydride phase and consequently long exposure times have been allowed to provide a layer thick enough to identify. Quite thick hydrides have been grown under various conditions. For example, Otsuka[7] reported a hydride layer at least 1μ thick on a titanium specimen left in 6N HCl at room temperature for 8 days. The hydride was thickest at crevices with a maximum thickness of 7μ. As would be expected due to the cathodic nature of the hydride formation reaction,

cathodic charging greatly increases the rate of hydride formation. A hydride layer approximately 2μ thick was grown on a titanium surface in 1 hour in 3N H_2SO_4 when a cathodic current density of 5 mA/cm^2 was applied.[5] Hydrides were also found on a titanium surface after exposure for only 2 hours in 0.1N NaCl during which the metal was cathodically charged at a current density of 10 mA/cm^2.[7]

Referring back to Table 1 one can see that hydride formation either from bare titanium metal or from an oxide, requires the reaction of H^+ ions. Therefore the rate of hydride formation should increase with the concentration of the acid. This has been qualitatively observed.[7]

The only available quantitative data on the rate of growth of hydrides was reported by Tomashov et al.[152] for titanium and a Ti-4.35Al alloy in 0.03N H_2SO_4 + 0.5N Na_2SO_4 solutions. Hydrides were formed by cathodic charging at current densities from 20 to 80 mA/cm^2. They observed a parabolic growth rate for hydrides on both the metal and the alloy.

To affect the rates of reactions taking place at its surface a hydride need only be a few angstroms thick. Using the data of Tomashov,[5] cited previously, and assuming a parabolic growth rate, it is easily seen that if a layer 2μ thick was produced by charging for 1 hour in 3N H_2SO_4, a layer, say 20 Å thick would form in a matter of milliseconds. The same sort of comparison applied to the 1μ thick hydride layer formed under open circuit conditions in 6N HCl in 8 days indicates that a thickness of 20 Å would require only a few seconds.

Information about the actual hydride formation reactions that will occur under different conditions can be obtained by referring again to Table 1. One can see that there are three possible types of reactions that can produce surface hydrides. One is the reaction of hydrogen ions with titanium metal to form hydride (reactions q and r). The requirements for this type of reaction are a bare titanium surface, hydrogen ions, and a potential below +408 mV(SCE). These conditions are met whenever titanium is immersed in an acid of sufficient strength to dissolve the passive film. The second group of reactions are those in which a hydride forms directly upon reduction of an oxide (reactions s - z). This type of reaction does not require a bare titanium surface but it does require a negative potential the magnitude of which varies according to the oxide involved. The steady state corrosion potential which occurs on passive titanium immersed in weak acids is not negative enough to form hydrides by this mechanism. Therefore, one would expect that cathodic charging would be required to form hydrides in neutral salts or weak acid solutions. A final possibility is a reverse dissolution reaction where a hydride is formed by reduction of titanium ions (reactions d - g). Reactions of this type require a very large negative potential and the availability of titanium ions. This would not be likely on a bare surface even with a large negative applied potential because the driving force for hydride formation by reactions q or r would be much larger and hydrides should form by that mechanism. A

reverse dissolution reaction could occur on an oxide surface if a high concentration of Ti^{3+} ions were present - perhaps in a crevice.

In summary, the available information indicates that hydrides should form quite rapidly whenever titanium is immersed in an acid of sufficient strength to dissolve the passive film - the specific rate increasing if the acid is made stronger or a negative potential is applied. The formation of hydrides in weak solutions where titanium is passive would require cathodic polarization.

Data on the properties of titanium hydride are difficult to find. Otsuka[7] states that the hydride layer formed during exposure to hydrochloric acid is electrically conductive. This is in contrast to the oxides which are generally highly nonconductive.[174] The difference in conductivity could be important in explaining reaction rates on oxides versus hydrides. However, only general comparisons can be made since the conductivity of an oxide on a metal surface may be quite different from the conductivity of the same oxide in the bulk phase. This is especially true if the surface oxide is thin enough so that electron tunneling effects become significant.

4. Thickness of Surface Films

Oxide films formed on exposure of titanium to air at room temperature are very thin. Tomashov et al.[30] found the air-formed film thickness to be 18.9 Å after several days exposure. Other workers[31,32] found thicknesses from 12 Å to 45 Å. Andreeva[33] using an ellipsometric technique found the oxide thickness immediately after interaction of titanium with air at room temperature to be 12-16 Å thick. After 70 days the thickness was 50 Å. Further growth of the film although very slow still proceeded. In 545 days the film thickness was 80-90 Å and after 4 years it was 250 Å.[33] (It should be pointed out that this is rather odd film growth kinetics, very slow at the beginning then increasing with time.) In Andreeva's investigation the "natural" or air films were measured on metal substrates that were vacuum deposited. Air was then let into the system and film thicknesses measured. After the film was formed, if the system was pumped down again to a pressure of 10^{-6} to 10^{-7} mm of Hg a part of the film was desorbed. This indicates that the film consists of a strongly bound, chemisorbed, layer which is underneath a weakly bound layer.[33] The thickness of the physically adsorbed layer was 1/4 of the total film thickness on the titanium. This ratio remained reasonably constant as the film thickened. Andreeva[33] also made measurements on polished specimens. Specimens were polished and kept in air at room temperature for 180 days during which time changes in the film thickness were monitored. The film formed after polishing does not change with time and stays at a value of 15 Å to 22 Å. (The thickness of the natural oxide film is not considered.) When specimens are subjected to a vacuum all but 5 Å of the film is desorbed.

In this same paper measurements of film thicknesses were also made during exposure to electrolytic solutions. Polished specimens were used and measurements apply only to changes in thickness over and above the "natural" film thickness. First, measurements were made at room temperature in two solutions in which titanium is naturally passive: 1N Na_2SO_4 and 0.5N H_2SO_4. Both the open circuit potential and film thickness were followed as a function of time. In both solutions the film thickened with time and, as it did so, the potential shifted in the positive direction. But the magnitude of the film thickness was quite different in the two solutions, being 4 times thicker in the acid solution. Other measurements were made in solutions where the surface oxide was unstable. In 40% H_2SO_4 (10.6N) the open circuit potential and the film thickness were monitored as a function of time. The potential followed the usual pattern of a gradual decay in the active direction until it reached a potential where a rapid transition to the active state occurred. The film thickness on the other hand remained fairly constant until the critical potential was reached. Then, as the activation process proceeded, the film thickness increased greatly (from about 30 Å to 250 Å) then decreased suddenly as the specimen became completely active. This same tendency of the film to thicken considerably during the transition from the passive to the active state was observed when activation was carried out by cathodic polarization. Cathodic polarization tests were run in 40% H_2SO_4 (10.6N) and 20% HCl (6N). The polarization was done potentiostatically and, as the applied potential was shifted from the open circuit value of about 0 mV(SCE), the film thickness remained reasonably constant until a potential was reached at which the cathodic current density began to increase sharply. At this point the film grew quite rapidly and then dissolved. This film thickening is apparently associated with the hydration of the oxides or the growth of a hydride or perhaps with the reduction of higher to lower titanium oxides.[43] This latter possibility is not likely since the air formed film was found, as previously mentioned, to be TiO and, in the above solutions, higher oxides will not form spontaneously.

Anodic polarization tests were also run. These were conducted galvanostatically and the potential and film thickness were measured as a function of the applied anodic current. Tests were run in 10% (2.2N) H_2SO_4 and 75% (26N) H_2SO_4. The film thicknesses and anodic potentials both increased as the applied current increased. At any particular current the film was thicker in the stronger acid.

5. Polarization Behavior of Titanium - Effect of the Surface Films

There are a large number of papers in the literature which describe the electrochemistry of titanium in acid solutions.[2-4,7,12,35-39] However, very few of these consider the effect of a surface film, particularly a hydride, on the polarization behavior. Tomashov[5] has run a series of experiments to determine the influence of the hydride on the anodic polarization behavior of titanium. He compared anodic polarization curves in 3N H_2SO_4 between specimens pretreated to form a 2μ thick

hydride layer (cathodic charging for 1 hour in above solution at 5 mA/cm^2) and untreated specimens. Figure 1 shows the results. The untreated specimen (curve 1 on the figure) had a maximum current density almost 2 times greater than the hydride coated specimen (curve 2). Another specimen was given a prolonged charging treatment (18 hours at 5 mA/cm^2 in 0.5N H_2SO_4). It had a hydride layer about 10μ thick on the surface. When it was polarized anodically the maximum current density was again high, even higher than the untreated specimen (curve 3). Both of the hydride coated specimens reached the peak of the curve at a slightly more noble potential than the untreated specimen. Also both showed a small cathodic loop near the potential for complete passivation. Tomashov[5] explained the lower peak for the coated specimen as an inhibition of the anodic dissolution process by the presence of the hydride. The high peak obtained after a long charging time was suggested to be the result of a change in the surface of the specimen due to prolonged hydrogen absorption. The surface became darker and rougher. Essentially, the actual reaction area became larger and therefore the measured current was larger.

One can more clearly see what is happening during the polarization process with a graphical explanation by means of Evans Diagrams. These schematic diagrams are shown in Figure 2 and present an alternate explanation of the reduction of the peak current density due to the hydride. *The curves plotted represent not the actual currents that are* measured but the real kinetic curves which give rise to the measured ones. The anodic currents here are taken to be composed of two reactions (1) a dissolution reaction which occurs at potentials below the peak and (2) an oxide formation reaction which occurs at potentials above the peak. The cathodic currents are assumed to arise from the hydrogen evolution reaction at all potentials. The measured current is always a net current $I = I_a - I_c$. For example, the plotted curve for case 1, untreated titanium, can be followed by starting at the corrosion potential where the cathodic (hydrogen evolution) and anodic (dissolution) currents are equal (point a) then measuring the difference $I_{a1} - I_{c1}$ with increasing potential. The maximum current, I_1, is shown on the graph and occurs at a potential corresponding to the peak of the anodic curve. Curves I_{c2} and I_{a2} correspond to curve 2 on Figure 1 and depict the situation when a hydride is formed during relatively short charging times. The cathodic curve, I_{c_2} is shifted to higher currents. This would be true because the hydrogen evolution reaction goes faster on a hydride surface than it does on a titanium surface. There is evidence that this may occur in some cases.[37,40] It will be discussed in more detail later. The anodic curve I_{a2} is assumed to remain essentially the same except that the potential for the oxide formation reaction (the peak of the curve) is shifted slightly in the noble direction. Measuring the difference $I_{a2} - I_{c2}$ in the same way as described above results in a smaller maximum current, I_2, and a shift in the maximum current to more noble potentials. Also, at potentials slightly above the peak a situation arises during which the cathodic current I_{c2} is larger than the anodic current I_{a2}. This produces the cathodic loop as was observed in Figure 1.

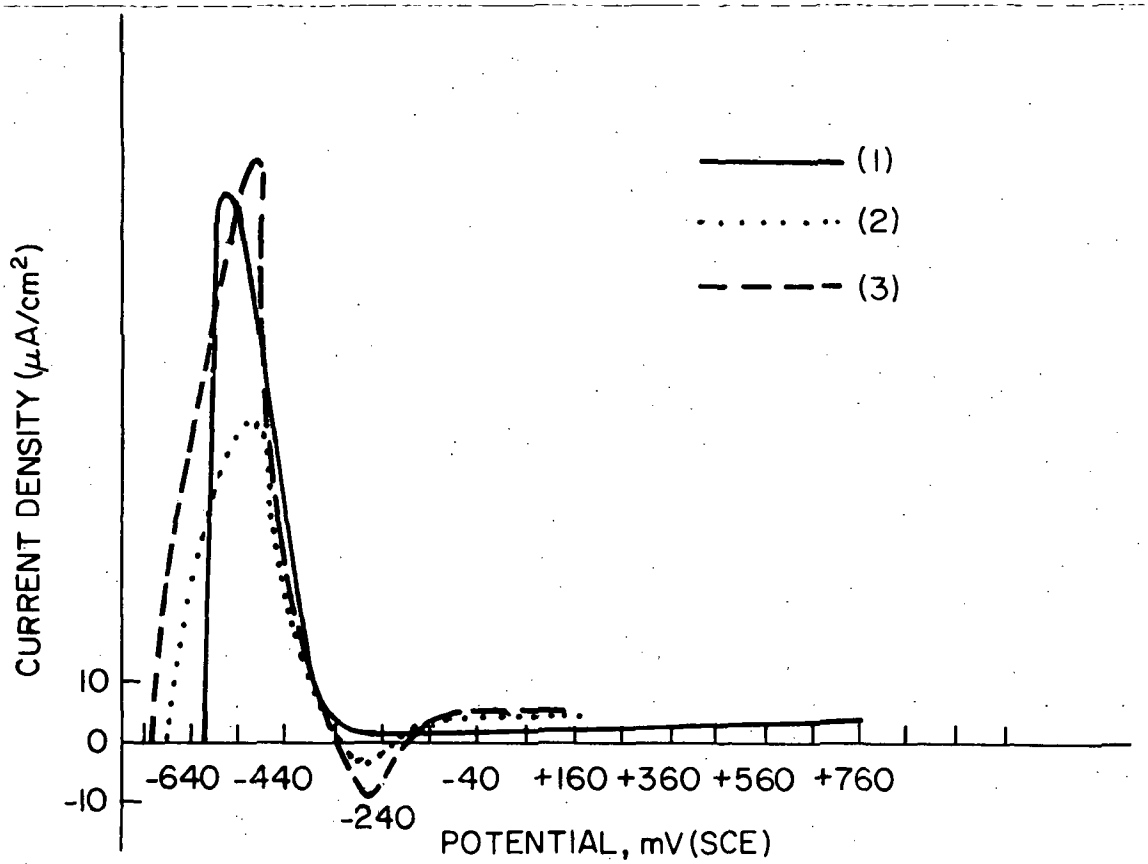

Figure 1 - Anodic Polarization Curves for Titanium in 3N H_2SO_4. (1)-untreated titanium; (2)-titanium with a 2-μm thick hydride layer formed during cathodic charging for 1 hr. at 5 mA/cm^2; (3)-titanium with a 10-μm thick hydride layer formed during cathodic charging for 18 hrs. at 5 mA/cm^2. (Ref. 5).

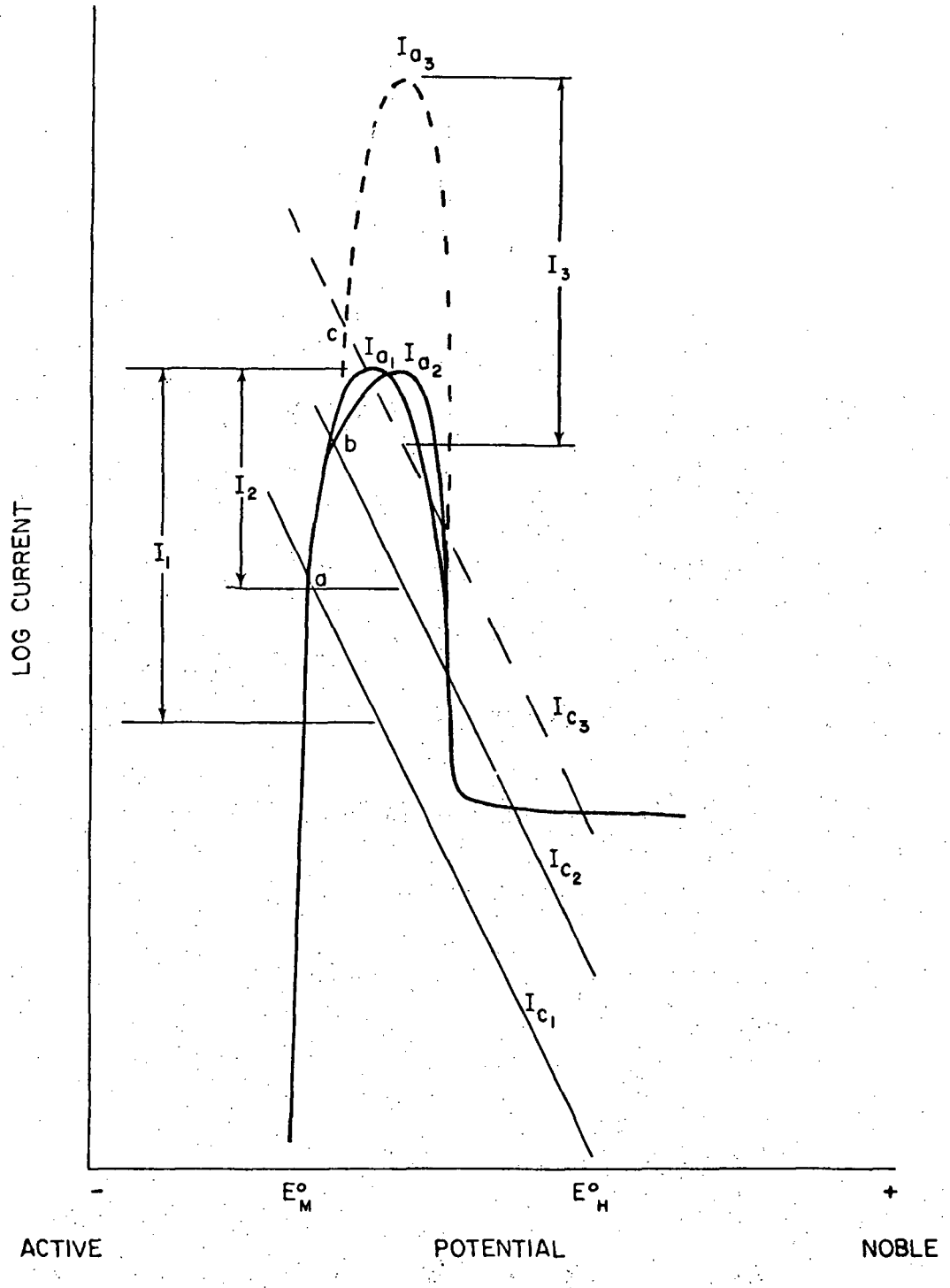

Figure 2 - Graphical Explanation of the Anodic Polarization Curves of Figure 1.

During the prolonged charging of a specimen (case 3) the actual surface area for reaction likely does increase due to the large amount of hydrogen absorbed, as suggested by Tomashov.[5] He found that if the surface of a specimen which had undergone prolonged charging were rubbed lightly with aluminum oxide powder the porous hydride was removed and the polarization curve changed back to curve 2, Figure 1. This can also be explained graphically. In this case, the cathodic curve is thus shifted further, to I_{c3}, which represents the combined effect of the increased kinetics of the hydrogen evolution reaction on the hydride surface plus the increase in actual reaction area. But the area addition will increase the anodic current also. Further, the surface after prolonged cathodic charging was found to have microcracks.[5] This suggests that the kinetics of the dissolution reaction may increase. These effects are shown on Figure 2 by a large increase in anodic current (see I_{a3}) which arises from both an increase in kinetics and an increase in area. Following the difference $I_{a3} - I_{c3}$ from the new corrosion potential (point c) one sees that the maximum current, I_3, is again large as in case 1. Following $I_{a3} - I_{c3}$ further to potentials where the cathodic loop occurs one can see that the magnitude of the net cathodic current in the loop will be larger than case 2. Reference back to Figure 1 shows that this occurs. One further observation from Figure 2 can be made by looking at the corrosion potentials of the three cases. It can be seen that case 3 has the most noble corrosion potential (point c), followed by case 2 (point b), followed by case 1 (point a). This observation is also confirmed by Figure 1. Thus the Evans diagrams appear to present a very complete explanation of the observed polarization behavior.

6. The Dissolution Reaction

Next the three different reactions which combine to give the polarization behavior will be discussed in some detail, particularly in relation to the effect of the hydride layer. The first reaction is anodic dissolution. The exact potential at which dissolution occurs depends upon the specific acid and the pH but it can be stated that in nonoxidizing acids titanium dissolves in the potential range of about -450 mV to -650 mV(SCE). As mentioned previously the standard electrode potential for the dissolution of titanium to trivalent ions is -1452 mV(SCE) and so the over-potential for dissolution is almost 1 volt. One explanation of this inhibition in the dissolution reaction is that the titanium is coated with a hydride and the dissolution rate of the base metal is controlled by the dissolution rate of the hydride.

Four possible hydride dissolution reactions will be considered (see Table 1). They are listed below with their respective standard potentials (taking the pH as 0).

$$(1)\quad TiH \rightarrow Ti^{3+} + H^{+} + 4e^{-} \qquad E^{o} = -970 \text{ mV(SCE)}$$

$$(2)\quad TiH_2 \rightarrow Ti^{3+} + 2H^{+} + 5e^{-} \qquad E^{o} = -782 \text{ mV(SCE)}$$

(3) $TiH \rightarrow Ti^{3+} + \frac{1}{2}H_2 + 3e^-$ $\quad E^o = -1232$ mV(SCE)

(4) $TiH_2 \rightarrow Ti^{3+} + H_2 + 3e^-$ $\quad E^o = -1152$ mV(SCE)

One would expect that reactions 1 and 2* would be inhibited in strong acid solutions because they require the production of more H^+ ions in a solution already concentrated with protons. This tendency is confirmed by considering the standard electrode potentials. At a dissolution potential of say -500 mV(SCE) there would be a much larger driving force for reactions 3 and 4 to occur than for reactions 1 and 2. Experimental verification of the mechanism of hydride dissolution was demonstrated in a recent paper by Tomashov, et al.[42] In the experiments a hydride layer 5μ thick was put on the surface of a titanium specimen by cathodic charging at 5 mA/cm^2 for 3 hours in 10N H_2SO_4. The hydrided specimen was then held in the same solution at -442 mV(SCE) which is the potential at the peak of the anodic polarization curve. Another titanium specimen which was not charged to produce a hydride was also held under identical conditions for comparison. The amount of corrosion was determined by analysis of the solution by a calorimetric method using hydrogen perioxide. A calculation was made of the amount of metal dissolved via Faraday's Law from the measured current flow during the 3 hour test and this value was compared with the amount of metal found in solution. It was found that close to 100% of the current could be accounted for by the formation of trivalent ions. This indicates that titanium hydride dissolves by reaction 3 or 4 because if reaction 1 or 2 occurred then some of the charge passed would be used for the formation of protons with an accompanying decrease in the concentration of titanium in solution. Further, the results for the untreated specimen were very nearly the same indicating that it also dissolves as a trivalent ion.

Other very striking results were obtained during the same experiment. First, a calculation of the corrosion penetration distance from the amount of titanium passed into solution during a 30 hour test indicated that the metal/solution boundary should have moved about 8.3μ which is considerably deeper penetration than the 5μ thick hydride on the surface. However, metallographic examination of the specimens after the test showed that the hydride was still uniform, pore-free and practically the same thickness as it had been originally! Secondly, no hydrogen evolution was observed on the surface of the specimen. This would indicate that the hydrogen must diffuse into the metal as its concentration on the surface increases due to dissolution of titanium. The hydrogen content of the metal was determined. (The method used was vacuum extraction at 1000-1200°C and a pressure of 10^{-6} mm Hg.) The hydrogen determination was done both after the preliminary cathodic charging and after the total treatment of charging and anodic dissolution. The amount

*Numbers refer to reactions in the text while letters refer to reactions in Table 1.

of hydrogen in the metal was found to be nearly the same in both cases. In other words, as the dissolution proceeds the hydride layer merely moves into the metal.

The dissolution current density during the above tests is rather low, approximately 250μ A/cm^2. If a hydride layer is dissolved in a very strong sulfuric acid solution (25.6N) where the dissolution current density is approximately 10 times higher, then visible hydrogen evolution occurs and the hydride phase is dissolved.[43]

The fact that the dissolution behavior of the hydride coated specimen and the untreated titanium were identical is very striking. It supports the hypothesis put forth above (Figure 2) that the decrease in the peak current during polarization with a hydride coated specimen is likely due to the increase in the rate of the cathodic reaction on the hydride and not to a change in the dissolution rates. One way to explain the identical dissolution rates of untreated metal and hydride is to assume that even the untreated metal has a thin hydride layer on it. As was discussed previously in the section on hydrides, very short times (a few seconds) appear to be enough to form in a very thin hydride say 20 Å thick. Thus a thin layer could form on untreated titanium after the specimen has activated while the experimentor is waiting for a steady state corrosion potential to be reached. The thickness of the hydride layer could not affect the dissolution rate because the mechanism does not involve diffusion of titanium through the hydride layer but only diffusion of hydrogen into the metal, i.e. movement of the hydride phase into the metal. Therefore, if the rate of diffusion of hydrogen in the hydride layer is faster than the rate of metal ionization, i.e., if the metal ionization were rate controlling, then the overall rate of the dissolution reaction would not depend on the thickness of the hydride.

The hypothesis that a hydride layer controls the dissolution of "active"* titanium in acid solutions is supported by the work of Sukhotin and Tungusova.[41] They formed a hydride of composition TiH_2 by heating titanium in an atmosphere of hydrogen at 550°C. They then compared the anodic polarization curves for the hydride and for titanium in 0.2N H_2SO_4 at 95°C and in 2N H_2SO_4 at 25°C. The hydride and the titanium produced almost identical polarization curves. The authors concluded that passivation of titanium is due to the formation of a protective oxide on the surface of an existing hydride layer.

These polarization experiments and the hydride dissolution experiments combined with the rapid rates of hydride formation are a strong indication that a hydride layer is present in concentrated acid solutions at all times. However, if this is true it is difficult to explain the

*The term "active" means not passive. The quotation marks are used because there is strong evidence that, as discussed below, titanium is covered with an oxide film even in concentrated solutions in which it is not passive.

lowering of the measured anodic polarization peak observed by Tomashov in his earlier experiments (Figure 1, curve 2). The question is, why should the cathodic kinetics be greater on one hydride surface than on the other. It would seem that the thickness of the layer should not affect the rate of the cathodic reaction occurring at the surface. Although this apparent anomaly cannot be resolved with the available information, it is clear that the hydride layer exerts a profound influence on the anodic polarization behavior of titanium and, in fact, controls the rate of anodic dissolution.

The dissolution of titanium to trivalent ions has been observed by many workers. Oliver and Ross[45] experimentally measured the redox potential for the reaction

$$(5) \quad Ti^{3+} + e^- \rightleftarrows Ti^{2+}$$

and found it to be -2240 mV(SCE). This fact precludes the oxidation of titanium to divalent ions. Armstrong et al.[37] deduced that titanium dissolved directly as Ti^{3+} ions from their experiments in sulphuric acid solutions at 70°C. Russian workers[44] came to the same conclusion from their experiments in a variety of solutions. Beck[46] found the same result in 6N HCl solutions.

Generally, the rate of dissolution of titanium increases as the concentration of acid increases. This is most often reported as an increase in the current at the peak of the anodic polarization curve (i_{crit}). In HCl solutions, i_{crit} increases with H^+ concentration throughout the entire range from very dilute to highly concentrated solutions.[3,7,29,35,47] The corrosion rate, as measured by the amount of metal dissolved in the solution, is directly proportional to i_{crit} and also increases with H^+ concentration.[7,48,49,50] The same observed increases in i_{crit} and corrosion rate with H^+ concentration occur in sulfuric acid solutions up to about 40% (10.6N).[40,51,52] Above 40% (10.6N) H_2SO_4 the rate of dissolution is very complex.[39,54,55]

Several experimentors have measured the order of the dissolution reaction with respect to H^+ concentration. The order is obtained by plotting values of log i_{crit} versus log $[H^+]$ while holding the temperature, applied potential, and concentrations of other species constant. A straight line should result; the slope is the reaction order. Thomas and Nobe[36] obtained a value of 0.84 in sulfuric acid solutions from pH = 0.25 to pH = 2.0. Peters and Myers[56] measured a value of 0.77 in much stronger sulfuric acid solutions (1, 5, and 10N). Both the above studies were conducted at room temperature. Armstrong et al.[37] stated that the dissolution rate was approximately first order with respect to H^+ ions for their experiments in sulfuric acid at 70°C. They varied the concentration over a range from approximately 10% (2.2N) to 64% (20N). However their results may be dubious since, as mentioned above, the mechanism of dissolution is thought to change in concentrated sulfuric acid above about 40%.[33,53] The reaction order was not calculated by any

of the workers studying hydrochloric acid solutions. However, the data from two papers were in a form in which this calculation could be made and this was done. Using data from Levy and Sklover[35] an order of 2.82 was calculated for 12% (2.5N) and 20% (6N) HCl solutions at 65°C. Data from Brynza et al.[47] gave a value of 1.65 for HCl solutions from 5% (1.4N) to 20% (6N) at 80°C. The reaction order with respect to H^+ ions is thus higher in hydrochloric than in sulfuric acid solutions.

The most noteworthy aspect of the above discussion about the dissolution reaction is that it appears to be controlled by the dissolution of a titanium hydride. The standard electrode potential for the hydride dissolution according to reaction 3 or reaction 4 is -1232 mV(SCE) or -1152 mV(SCE), respectively. Although these potentials are more noble than the standard potential of dissolution of bare titanium to trivalent ions [-1452 mV(SCE)] they are still over one-half volt more negative than the potentials at which dissolution occurs. Thus the large inhibition of the anodic dissolution of titantium in acid solutions cannot be accounted for solely on the basis of a surface hydride. Oxygen bonds (an oxide or chemisorbed oxygen) must be involved. This is emphasized by the very small currents measured during dissolution. Thus during anodic dissolution the hydride layer must be covered by an oxide. Reference back to Table 1 shows that the equilibrium potentials for the formation of lower oxides from a hydride surface are below the range of active dissolution and thus it is certainly possible to have an oxide covered hydride. The increase in dissolution current as the acid concentration increases, as discussed in the previous section, is easily explained for an oxide covered surface. During dissolution, at the peak of the anodic polarization curve, the surface is, of course, not passive. The oxide present is not the passive oxide but a lower oxide which is more soluble in the solution. As the acid concentration increases the oxide becomes increasingly soluble and dissolves slightly producing a less protected surface and a higher dissolution current.

The hypothesis that a surface oxide is present during the anodic dissolution of titanium is supported by the behavior of the current as a function of time when the potential is suddenly increased. When a metal is in the passive range, a sudden increase in the potential results in a current spike followed by a gradual decay to a steady value. This type of behavior is common and has been associated with the presence of a passivating surface layer. But for titanium specimens in 3N H_2SO_4 this same type of behavior occurs in the active dissolution range as well as in the passive range.[5] The only difference is that the current decays somewhat faster in the active range and the steady state value is reached more quickly. (It should be noted that even on a bare metal surface if the potential is suddenly increased the current will increase sharply then decay due to changes in the charge of the double layer.[62] However this process is very fast and decay times are measured in milliseconds whereas the decay times in the above processes are much longer.) Galvanostatic experiments were also run in 3N H_2SO_4.[5] Here the potential versus time curves are plotted when the current is

suddenly increased. These results also supported the presence of an oxide layer during anodic dissolution.[5] Suppose an oxide is inhibiting the corrosion of titanium; then, if the oxide is reduced by cathodic polarization, the corrosion rates should increase. This has been found to occur in sulfuric and nitric acid solutions.[83,84] It will be discussed in more detail later.

As a final consideration of the dissolution mechanism another possibility should be discussed. Namely, that under certain conditions the process may be a chemical rather than an electrochemical one. This has been considered by several Russian workers.[58,59,60] This came about when it was discovered that often the dissolution rate as determined by analysis of the amount of metal in solution was much higher than that calculated from current flow. Specifically, this was observed for a Fe + 12-14Cr alloy in 0.1N H_2SO_4 at 90°C.[59] Figure 3 shows the experimental results. It is seen that the analytically determined corrosion rate is higher than the observed current at all potentials. One must remember of course that the observed current is a net current and thus does not always give a true measure of the dissolution current. This explains the discrepancy at potentials near the corrosion potential. However it does not explain the difference at potentials removed from the corrosion potential. The difference is particularly striking at negative potentials where the dissolution rate stays high even though a large cathodic current is flowing. The authors[59] suggested a general reaction for chemical dissolution of a metal M

$$(6)\quad M + nH_2O \rightarrow M^{n+} + nOH^- + n/2\ H_2$$

The importance of these results is emphasized when it is remembered that the dissolution of Fe-Cr alloys is sulfuric acid has long been tacitly assumed to be electrochemical.

The possible occurrence of a chemical mechanism in the corrosion of titanium alloys has not been considered in the literature. At anodic potentials, experimental evidence indicates that dissolution is electrochemical since the analytically determined corrosion rates correspond very closely to the current flowing. However, chemical processes could be associated with increased dissolution at cathodic potentials which, as mentioned above, was observed for titanium in nitric and sulfuric acids.[83,84]

7. Passivation

If, during the course of anodic dissolution of titanium in strong acid solutions, the metal is polarized to a large enough extent then the rate of dissolution decreases sharply and the metal becomes passive. This has been associated with the formation of higher oxides which have limited solubility in the acid (see Table 2). If a hydride is initially present on the surface then the oxide should form on top of it. Tomashov[5] has studied the growth of an oxide over a hydride. First, he formed a 3.5-4.0μ thick hydride on the titanium surface by cathodic

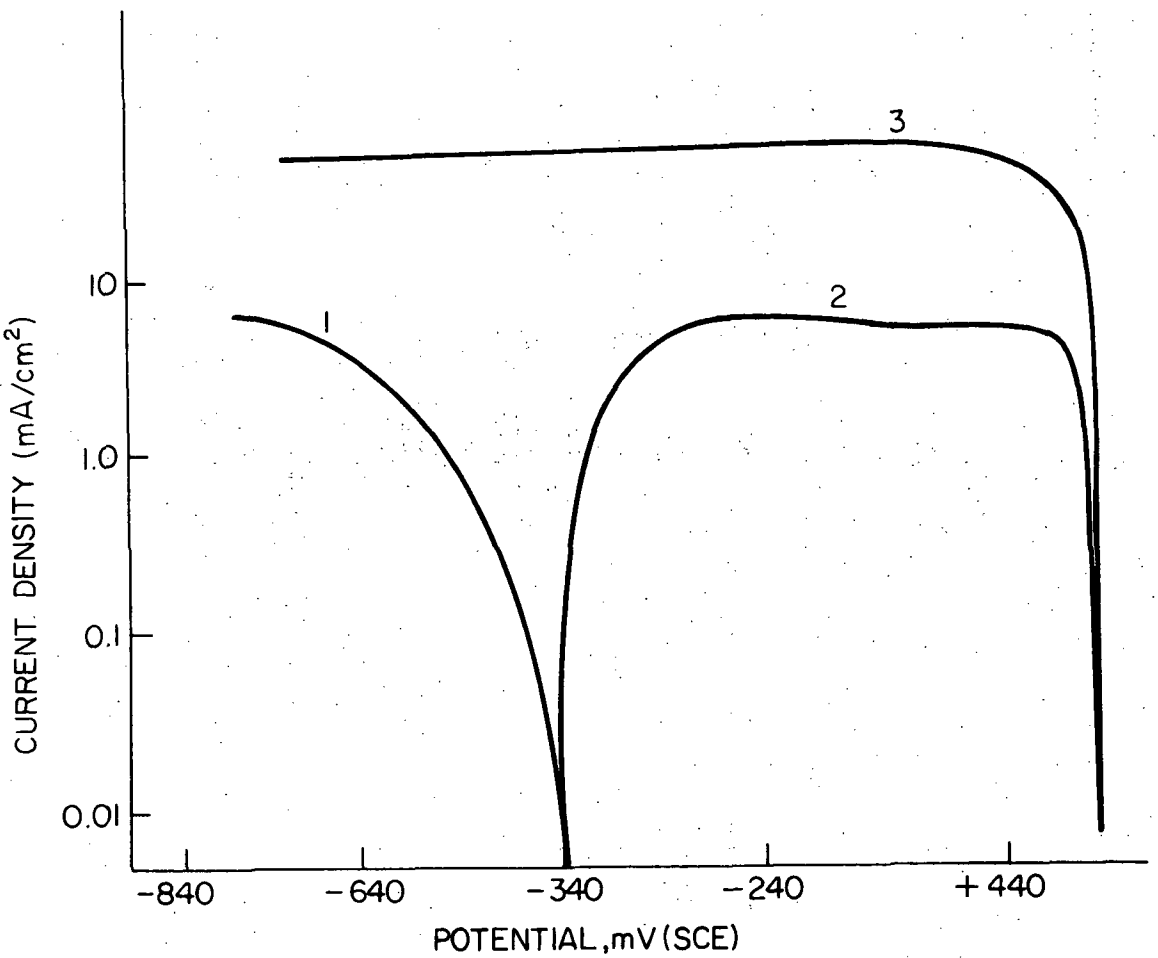

Figure 3 - Cathodic (1) and Anodic (2) Polarization Curves and the Dependence of the Dissolution Rate Determined Analytically on the Potential (3) for an Fe + 12-14 Cr Alloy in 0.1N H_2SO_4 at 90°C. (Ref. 59).

charging of the specimen for 1.5 hours in 3N H_2SO_4 at a current density of 15 mA/cm^2. The oxide was then formed in 18% H_2SO_4 + 10% H_3PO_4 at a temperature of 100°C by applying an anodic current of 10^{-2} A/cm^2 for 8 hours. This anodizing treatment would produce an oxide film about 4μ thick on a titanium surface without a hydride layer.[5] The subsequent metallographic examination of the specimen was very interesting. The thickness of the hydride layer remained the same after the anodizing treatment. Also, the thickness of the oxide formed on the hydride was the same as would be formed on unhydrided titanium (within experimental error). Thus the hydrogen in the hydride is apparently not oxidized during anodizing and the oxide forms by diffusion of titanium through the hydride. Also since the oxide layer was as thick on the hydride as on the titanium, the diffusivity of titanium through the hydride must be faster than through the oxide so that the rate of oxide growth is not affected by the hydride. The thickness of the hydride, it should be recalled, was also observed to remain constant during anodic dissolution. Thus it appears that once a hydride forms on the surface it tends to remain there and dissolution and oxidation reactions must occur on the hydride surface.

The actual mechanism by which metals become passive is the subject of much controversy. There are two major theories. One is that passivity is due to the chemisorption of oxygen or OH^- ions on the metal surface.[64,65] The adsorbate need be only a monolayer or less (if it adsorbs at active dissolution sites, say kink sites). The adsorbed atoms affect charge transfer and essentially increase the over-voltage needed for metal atoms to dissolve. The small current flowing when the metal is passive is thus the same as in the active state, i.e. the dissolution reaction. The steady state then, represents a non-changing, highly inhibited dissolution rate. The exact mechanism by which the adsorbed species inhibits dissolution is not completely clear. It has suggested that the oxygen adatoms affect the dissolution indirectly in that their presence prohibits the presence of water or anions which would bring about hydration or dissolution.[63]

The second theory is the oxide film theory. The oxide film essentially forms a barrier between the metal and the corrosive environment. In this theory, the current flowing in the passive region is due to the formation of more oxide. The only way that metal cations get into solution is by the dissolution of the oxide which is usually considered a chemical process. A steady state condition exists when the rate of electrochemical film formation is equal to the rate of chemical film dissolution.

The fact that oxide films have been found and identified on the surface of titanium in the passive region (see Table 2) would appear to be proof that the oxide film theory is the correct passivation mechanism for titanium. But the presence of an oxide film at potentials more noble than the passivation potential does not necessarily prove that these films were present at a critical potential when passivity was incipient. In other words, there is no doubt that oxides are

present in the passive potential range but there is some doubt as to whether they are responsible for the initial passivity.

Support for the adsorption theory is found in experiments run by Tomashov and Strukov[66] in 10N H_2SO_4. They showed that an oxide current equivalent to less than a monolayer of oxygen was required to change titanium from the active to the passive state. However in these experiments the state of the surface before the application of the passivating current was not directly controlled. There could have been adsorbed oxygen or even a thin film there already.[175] As discussed previously, the large inhibition of the anodic dissolution of titanium in acid solutions predicts the presence of some sort of partially passivating layer in the active region.

Reference back to Table 2 shows that the same oxide film was found at a potential just negative of that for complete passivation as was found at a potential deep in the passive range. This finding gives strong support to the oxide film theory of passivation.

It is well known that when the potential of a stable, passive metal is suddenly increased, the passive current increases sharply then decays slowly back to the steady value. The two passivity theories have different explanations for this transient current. In the adsorption theory, the current flowing at steady state is a real dissolution current so the current transient represents an increase in dissolution and a gradual change of the surface to a new state corresponding to the new applied potential. Since the amount of oxygen adsorbed on the surface is so small the current associated with the removal or addition of oxygen should be negligible.

In the film theory the metal dissolution rate is independent of potential. The current transient represents a change in the rate of the oxide formation. The thickness of the oxide will thus increase (for a positive potential shift) until it is thick enough so that once again its formation rate, determined now by the new potential difference and regulated by diffusion, is equal to the constant chemical dissolution rate. Thus there should be no new metal ions in solution, just a thicker oxide. Obviously, the validity of either hypothesis can be checked by analytically following the dissolution process during a current transient. An experiment of this nature was carried out by Novakovskii and Likhachev[67] for iron electrodes in 0.1N H_2SO_4 using the radioactive isotope Fe^{59} to follow the dissolution. They measured an increase in the dissolution rate during the current transient. This increase represented 80-90% of the current change. This finding refutes the theory that the film dissolution rate is a constant, independent of potential. This change in dissolution rate during transient conditions was also found for passive zinc[68,69] and platinum.[70] The same results were found for titanium via a different method by Novakovskii and Ovcharenko[71] in 0.2N H_2SO_4. They monitored changes in film thickness, using inverse capacitance measurements, at the moment of a potential

shift. They found that the increase in film thickness could only account for a fraction of the current transient. They concluded that a large portion of the current must be used for film dissolution. It must be pointed out that these findings cannot refute the existance of oxide films on the surface of passive metals, particularly passive titanium where films have been identified. They do give grounds for the assertion that film formation and metal dissolution are similar processes which occur in parallel on passive electrodes.[71] Both processes are electrochemical and thus both are affected by changes in potential according to normal electrochemical kinetics.

The above experiments indicate that the dissolution rate of passive titanium in a transient situation is changed in a manner predicted by electrochemical kinetics. However, other experiments involving measurements of steady state dissolution rates in the passive state indicate that there are still some unexplained features in the behavior of passive titanium.[73] In these experiments the steady state dissolution rate for titanium in 1N H_2SO_4 was determined analytically at potentials in the passive range. The dissolution rate was found to be almost an order of magnitude higher than the passive current flow would indicate. Thus, chemical dissolution processes must be occurring on passive titanium in the steady state condition.

It appears from the above results that the dissolution of titanium in the passive range is quite complex involving both electrochemical and chemical processes. In evaluating the differences care must be taken to consider all the variables before making conclusions. The dissolution behavior may vary greatly as experimental conditions are changed. For example an increase in the acid concentration would be expected to affect the rate of chemical dissolution much more than the rate of electrochemical dissolution.

8. The Hydrogen Reduction Reaction

Cathodic reactions play a vital role in the corrosion of a metal in an acid solution. Under open circuit conditions charge neutrality requires that any anodic reaction must be accompanied by a cathodic reaction of equal rate. Thus, often the dissolution rate of a metal may depend on the rate of a cathodic reaction going on at its surface. Cathodic reactions are particularly important in the titanium system because the highest susceptibility to stress corrosion cracking occurs at cathodic potentials and because the main cathodic reaction, hydrogen ion reduction, may be directly involved in the cracking process.

The reduction of hydrogen ions results in the formation of neutral hydrogen atoms. These atoms usually combine to form gas molecules according to the overall reaction

$$(7) \quad 2H^+ + 2e^- \rightarrow H_2$$

However, as is proposed in one prominent stress corrosion theory to be discussed later, the nascent hydrogen may instead enter the lattice and embrittle the metal.

The hydrogen evolution reaction (equation 7) is one of the most well-studied of all electrochemical reactions. The kinetics of the HER on titanium in aqueous solutions have been investigated by a number of workers. One common experimental measurement is a cathodic polarization curve. This is a plot of log i versus applied potential. If all the other reduction reactions except the HER are eliminated (or have very slow reaction rates) the polarization curve should have a linear region (see Appendix). The slope of the line in this region is called the Tafel slope and its value is related to the mechanism of the electrochemical reaction.

Most of the available data for the HER reaction on titanium is for sulfuric acid solutions. Straumanis et al.[57] found that the Tafel slope decreased with increasing acid concentration, from a value of 241 mV/decade in 0.02N H_2SO_4 to 119 mV/decade in 10N H_2SO_4. Thomas and Nobe[53] reported a value of 150 mV/decade in 1N H_2SO_4 and Artemova[144] a value of 135 mV/decade in 2N H_2SO_4. Both these values agree well with the data of Straumanis et al.[57] However, other workers found values which did not fit with the above trend. Andreeva and Kazarin[39] reported a value of 160 mV/decade in 10.6N H_2SO_4 and Petrenko[145] observed a value of 119 mV/decade in 2N H_2SO_4. These differences are probably related to different surface layers on the titanium. As mentioned previously surface hydrides are formed very rapidly on titanium in sulfuric acid. Observations[7] indicate that, in strong acid solutions say 5N or greater, they should form in a matter of seconds. However, in weak acids say 1N it may take much longer. Without more data on the kinetics of hydride formation and more complete details on the exact experimental procedures, it is not possible to be certain of the state of the surface in the above experiments. A few qualitative correlations can, however, be made. Straumanis et al.[57] indicate that there was not a long delay from the time when the specimens were put into the solution until tests were begun. Therefore they probably did not have a surface hydride except in the strong acid solutions. On the other hand Petrenko[145] cathodically charged his specimens for 1 hour at a current density of 5 ma/cm^2 before testing. His surface almost certainly was covered with a hydride and his value of 119 mV is identical with the observations of Straumanis et al. in 10N solution. Hackerman and Hall[38] reported a slope of 154 mV in NaCl solutions. This value appears too low for neutral solutions, however, the authors took extreme care to attain steady state during their experiments, waiting a matter of days in some cases. Their lower value could therefore be the result of a hydride. In this connection Hackerman and Hall[38] reported a visible change in the surface condition after prolonged experiments.

The order of the HER with respect to H^+ ions has been reported in two papers. Kolotyrkin and Petrov[146] reported that the reaction rate

had a first order dependence on proton concentration in acid solutions (H_2SO_4) and was independent of proton concentration in alkaline solutions. Thomas and Nobe[53] obtained a reaction order of 0.6 with respect to hydrogen ions in 1N H_2SO_4 solutions.

A somewhat detailed look at various steps that make up the HER reaction is appropriate at this time. The overall process (reaction 7) is thought to occur by the following steps, written for titanium:

$$(8)\quad Ti + H^+ + e^- \leftrightarrows Ti\text{-}H_{ads}$$

then

$$(9)\quad Ti\text{-}H_{ads} + H^+ + e^- \leftrightarrows Ti + H_2 \uparrow$$

or

$$(10)\quad Ti\text{-}H_{ads} + Ti\text{-}H_{ads} \leftrightarrows 2Ti + H_2 \uparrow$$

The first reaction is the discharge reaction in which a proton accepts an electron from the metal and is adsorbed. This reaction always occurs[141,147] and is followed by either electrochemical desorption (reaction 9) or recombination (reaction 10). The former reaction occurs when a proton hits a site which already has an adsorbed hydrogen atom on it. Thus it is favored when the fractional surface coverage θ is high and when adsorption bonds are strong so that lateral movement of adsorbate is difficult. The recombination reaction is not electrochemical and occurs by the reaction of two adsorbed atoms already on the surface. It is favored when θ is small and the adsorbed atoms are mobile. On the titanium surface the process is believed to occur by reactions 8 and 9 i.e. discharge followed by electrochemical desorption.[53,141] The latter reaction is thought to be rate controlling[53,141] so that the overall reaction should result in a large fraction of the surface covered by adsorbed hydrogen atoms - a condition that would promote the adsorption of hydrogen into the lattice.

Next, consider the effect of a surface hydride on the HER. To date there have been no experiments studying the HER on a hydride surface although a few workers[37,40] have noted an increase in the rate of the HER under certain conditions and have suggested a surface hydride as the reason. Consider a 5N HCl solution as an example. The composition of the surface hydride in that solution would be close to TiH.[7] This hydride has an fcc structure and a density of 0.075 moles/cm^3 compared to 0.094 moles/cm^3 for titanium.[148] In terms of atoms of titanium per unit area of surface this difference is not great (about 8%). Hydrides have been found to be tightly adherent to the titanium surface and electrically conductive.[7] So in considering electrochemical reactions at its surface the hydride can be thought of as merely a slightly expanded titanium lattice with hydrogen occupying interstitial positions. Therefore, the HER mechanism on a TiH surface would be expected to be the same as on the base metal.

Surface oxides would exert greater influence on the rate of the HER because they are not good electron conductors. Meyer[149,150] and Posey et al.[151] have developed electrode kinetic equations for reduction reactions occurring on metals covered with a thin oxide film. The equations involve a dual barrier model[149] which assumes that reaction rates are determined by the charge transfer both across the double layer and across the film. Thomas and Nobe[53] have applied this model to their study of the HER on titanium in 1N H_2SO_4 and found it to be consistent with their results.

9. Effect of Temperature

Reaction rates generally increase as the temperature is raised. According to absolute reaction rate theory the rate of a reaction is related to the temperature by an equation of the form

$$(11) \quad \text{rate} = A\, e^{-Q/RT}$$

where A = constant and Q = activation energy.

From this equation, if the logarithm of the rate is plotted versus 1/T a straight line should be obtained. The activation energy can then be calculated from the slope. In making plots of this nature care must be taken to keep all other variables (activities, electrode potentials, etc.) constant as the temperature is changed.

Consider an electrochemical, anodic dissolution reaction which is activation controlled. The activation energy is found by plotting log i versus 1/T, where i is the current density. The activation energy, thus determined, is

$$(12) \quad \Delta G_e^{\dagger} = \Delta G_a^{\dagger} - \alpha F \Delta\varphi$$

where $\Delta G_a^{\dagger}$ = chemical activation free energy, cal/mole

α = transfer coefficient, included term for number of electrons transferred if the reaction is a multistep one, equiv/mole

F = Faraday constant, 23,060 cal/volt equiv

$\Delta\varphi$ = the actual potential difference between the metal and the solution, volts

$\Delta G_e^{\dagger}$ represents an electrochemical activation energy since it includes a potential dependent term. For a description of the origin of the terms see the Appendix. This activation energy reflects the reaction mechanism. It describes the intrinsic rate of the electron transfer reaction which occurs across the double layer. The key terms are $\Delta G_a^{\dagger}$ which is the activation barrier for a chemical transfer and α, which describes how the transfer is affected by the potential gradient between the surface and the solution F is, of course, a constant and $\Delta\varphi$ can be

kept constant by the experimentor. Therefore a change in the electrochemical activation energy at constant $\Delta\varphi$ reflects a change in the energetics of the electron transfer process. One can note that there are no concentration terms in the activation energy. Changing the concentration of a reactant will of course change the overall rate of the reaction but should not affect the intrinsic rate of the transfer process. If it does then it has in effect changed the mechanism of the reaction. It must be remembered that the electrochemical activation energy $\Delta G_e^\dagger$ is the sum of two terms. In order for the mechanism to be identical in two situations each term in the sum must be the same.

Obviously, the electrochemical activation energy is a very valuable parameter. It becomes somewhat less useful when one realizes that is is impossible to quantitatively separate the two terms of equation 12 and evaluate the chemical activation term $\Delta G_a^\dagger$. This is because the potential difference $\Delta\varphi$ cannot be measured exactly. Another problem arises in the experimental determination of $\Delta G_e^\dagger$. As mentioned previously, when measuring the reaction rate as a function of temperature, care is taken to keep all other variables constant. But this may not be possible. For example, although the concentration of a species can be controlled, its activity coefficient cannot be and may be a function of temperature. The situation is brightened by two factors. First, these temperature dependent terms in the preexponential factor (A in equation 11) exert much less influence on the current than exponential temperature terms. Secondly, large discrepancies in the constancy of the pre-exponential terms should result in a non-linear log i versus 1/T plot.

Values of the electrochemical activation energy for titanium dissolution in the "active" state have been reported in hydrochloric and sufluric acids. Levy and Sklover[35] calculated a value of 20kcal/mole in 6N HCl. The data of Togano et al.[49] produced a value of 15 kcal/mole in the same solution. (This value was calculated by the present author and there may be some error in the result due to the uncertainty in taking the data from the published graph.) In 4.7N H_2SO_4 a value of 19.4 kcal/mole was reported for Ti-6Al-6V-2Sn alloy.[52] Griess[75] reported a value of 11 kcal/mole for titanium in 0.9M NaCl + 0.1M HCl. These values are somewhat higher than activation energies found for active dissolution of other metals. A value of 6 kcal/mole was reported for iorn in 1N H_2SO_4.[78] Values for nickel were reported between 10 and 11 kcal/mole, independent of the pH.[78,79,80] Murata,[74] however, measured a value of 19.5 kcal/mole for nickel wires in 1N H_2SO_4 (pH = 0.35).

Values of the activation energy for dissolution in the passive range appear to be generally lower than in the active range. Togano et al.[49] measured changes in the passive current density of titanium in hydrochloric acid solutions at 1500 mV(SCE) in the temperature range from 35 to 90°C. They obtained values of 2.06 kcal/mole and 2.33 kcal/mole for 10% (2.87N) and 20% (6N) concentrations, respectively. In 30% (9.5N) HCl they obtained a discontinuity in the activation energy.

For temperatures between 35 and 50°C the value was 3.42 kcal/mole, while between 50 and 70°C it was 10.2 kcal/mole. For passive iron in 0.15N boric acid + 0.15N sodium borate (pH = 8.3) a value of 3.5 kcal/mole was reported.[77]

Consider the anodic dissolution reactions for titanium in strong acid solutions where the metal is not passive, and the activation energy is on the order of 19 kcal/mole. Although a quantitative mechanism cannot be deduced from this information, a few observations can be made. First, an activation energy of this magnitude rules out the possibility that the dissolution was controlled by transport in the electrolyte. Transport in the solution would be directly proportional to the diffusivity and its activation energy would be much less than 19 kcal/mole.[76] Secondly, if the dissolution is activation controlled then the activation energy would be described by equation 12. If a particular reaction is assumed to be occurring then an approximate value of the electrochemical term can be calculated and an estimate of the chemical activation energy determined. For example, assume the reaction is

$$(4)\quad TiH_2 \rightarrow Ti^{3+} + H_2 + 3e^-$$

Then, the transfer coefficient can be approximated by the term $(1-\beta)z$ where β is the symmetry coefficient (see Appendix), usually close to 1/2 and z is the number of electrons in the reaction equal to 2 in this case. An estimate of $\Delta\varphi$ can be made from the overpotential at which the dissolution occurred. In 6N HCl, i_{crit} occurred at a potential of -450 mV(SCE).[35] From Table 1, E° for the above reaction is -1152 mV(SCE). The overpotential is therefore 700 mV. Equation 12 becomes, using the value of $\Delta G_e^\dagger$ from Levy and Sklover,[35]

$$\Delta G_e^\dagger = 20{,}000 \cong \Delta G_a^\dagger - (1-1/2)(3)(23{,}060)(0.7)$$

and

$$\Delta G_a^\dagger \cong 43{,}200 \text{ cal/mole}$$

$$\approx 43.2 \text{ kcal/mole}$$

So if the dissolution is activation controlled, it must involve a large chemical activation energy.

Another possible interpretation of the dissolution reaction is that it is occurring through a surface oxide layer. The presence of some sort of protective layer on the titanium surface even during anodic dissolution is highly likely as discussed previously. If the oxide were continuous then the reaction rate would likely be determined by transport of cations through the film. If the film is thin so that the field across it is high the equation for the ionic current at point x in the oxide takes the form[81]

$$(13)\quad i(x) = \frac{zFDC(x)}{a} \exp \frac{z\lambda VF}{RT}$$

where D = the diffusivity cm^2/sec

C(x) = the concentration of mobile cations at point x, $mole/cm^3$

a = the lattice parameter, cm

λ = distance from the stable position for an ion to the maximum energy position during a jump, cm

V = field strength in the oxide, volts/cm

But the diffusivity is a function of temperature,

$$(14)\quad D = D_o\, e^{-Q_D/RT}$$

where D_o = a constant, cm^2/sec

Q_D = activation energy for diffusion, cal/mole

Putting this value for D into equation 13 the current becomes

$$(15)\quad i(x) = \frac{zFD_oC(x)}{a} \exp - \frac{Q_D - z\lambda VF}{RT}$$

To see if this equation would fit the available literature on titanium dissolution rates, values for titanium oxide were substituted. The only titanium oxide diffusion data available in the literature is for the diffusion of iron in titanium dioxide, TiO_2. The values given were $D_o = 0.192\ cm^2/sec$ and $Q_D = 55.4$ kcal/mole.[82] Therefore, the diffusion of Fe in the oxide must be assumed to approximate that of titanium. TiO_2 is likely not the oxide present during anodic dissolution in the "active" range. But a look at the structures of the lower oxides indicates that diffusion through them would certainly be no faster than through TiO_2 and may be much slower. (Ti_2O_3 has a hexagonal, corundum type structure; TiO has a face centered cubic structure; TiO_2 has a tetragonal structure.) In making the calculation the oxide was assumed to be Ti_2O_3 and the current then was assumed to be due to the transport of Ti^{3+} ions across the oxide. All the cations were assumed to be mobile and their concentration taken as that for Ti^{3+} in TiO_2, 6.25×10^{-2} moles/cm^3. This concentration was assumed to be constant throughout the oxide. The lattice parameter, a, equals 5×10^{-8}cm. If the value of activation energy, 20 kcal/mole, measured by Levy and Sklover is put into the equation a current of 551 $\mu A/cm^2$ is obtained at 35°C. Their measured current at that temperature was approximately 125 $\mu A/cm^2$ which is the same order of magnitude so that it is feasible that dissolution occurred through an oxide.

An estimate of the thickness of oxide which would produce the measured activation energy can now be made. Assume the field strength V equals the potential difference $\Delta\varphi$ divided by the film thickness δ. $\Delta\varphi$ is approximated by the over potential. The overpotential, here would be the difference between the applied potential [-450 mV(SEC)] or standard electrode potential for formation of Ti_2O_3 [-1482 mV(SEC)] or 0.103 volts. The value for λ can be taken as approximately 1/2 the lattice parameter ($\lambda = 2.5 \times 10^{-8}$mm). Putting these values into the expression for the measured activation energy from equation 15 ($Q_D - z\lambda VF$), one obtains an oxide thickness of 5Å. Thus, if the dissolution rate is controlled by transport through an oxide it must be extremely thin. Further, the value of the current in equation 15 is very sensitive to oxide thickness. If the film increased to only 10Å thick, the current reduces to a value of 10^{-11} $\mu A/cm^2$.

10. General Anodic Properties - Comparisons

In the preceeding sections the various surface layers that exist on titanium have been discussed and an attempt has been made to relate their properties to surface reactions, particularly to the dissolution reaction. With this information in mind it is now pertinent to compare the corrosion properties in various acids. Inhibiting effects of various additions and potential effects will be discussed as well as the changes which occur when pure titanium is replaced by an alloy.

A comparison of the corrosion behavior between sulfuric and hydrochloric acids is particularly interesting since stress corrosion cracking occurs in HCl but not in H_2SO_4 solutions. In general, the behavior of titanium in HCl and H_2SO_4 solutions is very similar. For acid concentrations up to about 10N their anodic polarization curves have identical shapes. The potential ranges over which dissolution and passivation occur are the same. This is not surprising since the same oxide was found in each acid (see Table 2). Further similarities are found by observing the changes when the temperature of acid concentration is increased. For both acids an increase in temperature increases the maximum dissolution current, i_{crit}, but does not change the potential at which the current peak occurs, Ep.[11,35,49] Increases in temperature and/or concentration cause a shift in the potential for complete passivation, Ecp, in the noble direction for both solutions.[7,11,51] Increases in concentration alone tend to shift Ep slightly in the noble direction in sulfuric acid[36,52,56] although the shift was not observed by one experimentor.[51] In hydrochloric acid solutions the shift does not occur for pure metal[7,35] but does occur for alloys.[35]

In both solutions the steady state corrosion potential, E_{corr}, tends to shift in the active direction as the solution becomes more aggressive (higher concentration and/or higher temperature).[7,11,47,51] This does not seem to occur if the solution is too dilute. Changing the pH of H_2SO_4 to 0.35 to 2.0 produced no change in the open circuit potential.[36] Peters and Myers[56] found a small shift of E_{corr} in the

opposite (noble) direction with increases in acid concentration in 1-10N H_2SO_4. However, they cathodically polarized their specimen at -1500 mV(SCE) for 5 minutes before testing. Their shift may be due to more rapid hydride formation in the more concentrated acid.

The corrosion rates in HCl are somewhat higher than in H_2SO_4 for the same normality.[7,47,89] In strong solutions of either acid (about 10% or more)[18] the air formed film is not stable and the metal will activate naturally. However, in 6N H_2SO_4, if a specimen is polarized at +500 mV(SCE), then the circuit is opened, the passive film will not dissolve naturally and the corrosion potential remains at a noble value.[7] A specimen given the same treatment in 6N HCl will activate naturally.

Some very interesting observations were made by Thomas and Nobe[36] when they added 0.5 to 5.8% NaCl to a 1N H_2SO_4 solution. Although the NaCl produced no change in E_{corr} it lowered i_{crit} and produced a cathodic loop in the passive range. It also lowered the passive current flow. Even when the passive film was formed with no Cl^- present and the NaCl subsequently added, the passive current still decreased. Further, they found that after anodic polarization they could activate a specimen by cathodic polarization in a pure H_2SO_4 solution but not in a H_2SO_4 and NaCl solution. Thus when added to a sulfuric acid solution the chloride ions tend to have a passivating effect. Levy[52] also found that additions of Cl^- to H_2SO_4 facilitated passivation.

It appears, then, that a comparison of the behavior of titanium in HCl and H_2SO_4 does not explain why the chloride ion should be so deleterious in causing stress corrosion cracking. The answer may lie in the fact that polarization tests do not describe any localized effects on the metal surface. For example, if additions of Cl^- to H_2SO_4 solutions were causing localized attack, the overall current flow could still easily be lower than a situation where general dissolution was occurring.

The tendency toward localized corrosion in the presence of chloride ions is supported by observations of pitting in the passive range (at potentials greater than about 1 volt) during anodic polarization in HCl[35] but not in H_2SO_4[52] solutions. Also, Kolotykin and Strunkin[89] observed pitting when an alternating current was applied to HCl + Cl_2 solutions but observed only an increase in overall corrosion when the same current was applied to H_2SO_4 + Cl_2 solutions. Owen[143] observed pitting in the Ti-6Al-4V alloy in 5N HCl solutions whereas the dissolution of Ti and Ti-Al alloys was found to be uniform in sulfuric acid solutions.[97]

Kirkin and Zhuk[85] studied the corrosion behavior of titanium and Ti-Al alloys (up to 5% Al) in acetic acid solutions (0.84N to 14.3N) and in nitric acid solutions (0.81N to 12N) at temperatures between 25 and 80°C. They measured anodic polarization curves as well as conducted weight loss measurements. Analysis of the polarization curves

showed that titanium was in the passive state in both acids at all concentrations and temperatures tested. The corrosion rates were also very low under all conditions. The corrosion resistance was reduced slightly when titanium was alloyed with aluminum. This was indicated by a higher passive current and by a larger weight loss. This passivity of titanium, even in very concentrated nitric acid solutions, is easy to understand since nitric acid is very oxidizing and titanium is generally passive in oxidizing acids.

The corrosion of titanium in reducing acids such as H_2SO_4 and HCl is easily inhibited. Oxidizing agents such as K_2CrO_4 inhibit.[90] The presence of oxygen in the solution often is enough to passivate the metal. Bubbling gaseous chlorine through the solution will passivate titanium in 6N NCl at 60°C.[89] Salts of other metals are very effective inhibitors. Schlain and Smatko[91] found that ions of iron, copper, gold, platinum, mercury, zinc, aluminum, cobalt, and magnesium passivate titanium in hydrochloric acid.

The mechanism by which these additions inhibit the corrosion is not completely agreed upon. Uhlig and Geary[92] attribute the inhibition to the saturation of valence forces of the titanium surface by the adsorption of ions. The ions as they adsorb receive a certain amount of negative charge from the metal. This leaves the metal surface with an excess positive charge and a more noble potential. Inhibition by OH^-, Cu^{2+}, Fe^{3+} and O_2 is attributed to this effect. Another explanation for the inhibition is that the presence of O_2 or a metal salt adds another reduction reaction to the processes occurring at the surface. This causes a shift of the potential in the noble direction. If the resulting potential is above that for formation of a protective layer, the metal passivates. Further, the potential required to achieve passivity is much more active for titanium than for most other metals and so it is very easily passivated in this manner. For example, in 1N H_2SO_4 titanium is completely passive at a potential of about -300 mV(SCE)[52] while iron in the same solution requires a potential of +500 mV(SCE).[6] The overall corrosion potential is shifted even further when noble ions such as Pt^{4+} are reduced because they plate out on the surface creating more effective cathodic area and further enhancing the reduction processes.

Another interesting inhibitor which has been considered by a number of workers is Ti^{4+} ions. Weiman[93] found that the weight loss of titanium specimens decreased when he added Ti^{4+} ions to sulfuric hydrochloric and nitric acids of varying strengths and temperatures. He hypothesized that Ti^{4+} chemically inhibits the dissolution. Andreeva and Yokovleva[94] also found the Ti^{4+} ions to be inhibiting. They postulated a chemical equilibrium between Ti^{4+}, in the form of titanyl ions (TiO^{2+}), and the oxide, TiO_2.

$$(16)\quad TiO_2 + 2H^+ \rightleftarrows TiO^{2+} + H_2O$$

As the oxide dissolves it produces titanyl ions. By the law of mass action, increasing the concentration of TiO^{2+} will push the equilibrium to the left and retard dissolution.[94]

Tomashov et al.[95] also believe that the Ti^{4+} ions are present in the form of titanyl ions. However, they believe that these ions inhibit via an electrochemical reaction. They postulate that, in the presence of protons, the ions are electrochemically reduced to trivalent ions according to the reaction

$$(17)\quad TiO^{2+} + 2H^{+} + e^{-} \rightarrow Ti^{3+} + H_2O$$

This reaction shifts the overall corrosion potential in the noble direction in the same way as discussed above, thus passivating the metal. Although the standard potential for this reaction is not very high compared to say O_2 reduction [-142 mV(SCE) versus 988 mV(SCE) respectively], the solubility of titanyl ions is several orders of magnitude higher than that of dissolved oxygen.[95] Thus, if the concentration of TiO^{2+} ions is sufficiently large, they can produce quite a large cathodic current and be quite effective in shifting the corrosion potential to the passive region.

Tomashov et al.[95] also found that, in the presence of oxygen, the dissolution processes were much slower when the volume of solution was small and allowed to stagnate without being changed. In this case a concentration of Ti^{3+} ions develops from the metal dissolution. These ions are then postulated to be oxidized by the dissolved O_2 to produce more titanyl ions.[95]

$$(18)\quad Ti^{3+} + 1/2\ O_2 + H_2O \rightarrow 2TiO^{2+} + 2H^{+}$$

Titanium tends to become active in crevices, even in solutions where it is normally passive. Ruskol and Klinov[96] studied this phenomenon in sulfuric acid solutions. They also suggested that Ti^{4+} ions were passivating but hypothesized that Ti^{3+} ions were aggressive and activated the titanium. They found that the concentration of Ti^{3+} ion in the crevice increased as a function of time. At the same time the dissolved oxygen content decreased. The exact mechanism by which the trivalent ions activated the titanium was not elucidated by their data. However, it was suggested that the Ti^{3+} ions act as reducing agents and thus effictively shift the corrosion potential in the active direction. In other words, in the absence of oxygen the Ti^{3+} ions are electrochemically oxidized. This could occur by reversing the direction of reaction 17.

$$Ti^{3+} + H_2O \rightarrow TiO^{2+} + 2H^{+} + e^{-}\quad E^{o} = -142\ mV(SCE)$$

The equilibrium potential for this reaction is given by

$$(19)\quad E(\text{volts}) = E^{o} - 0.1182\ pH + 0.059 \log \frac{[TiO^{2+}]}{[Ti^{3+}]}$$

Consider a crevice in which the concentration of trivalent ions has built up to say 10^{-1} moles/liter. Assume the pH is 1.5 and the concentration of titanyl ions is low for example, 10^{-6} moles/liter. Putting these values into equation 19, the equilibrium potential becomes -614 mV(SCE). This potential is below the passivation potential for titanium in sulfuric and hydrochloric acids. Thus, if the kinetics of the reaction were rapid it could serve as an effective means of shifting the corrosion potential into the active dissolution range.

Although titanium is easily passivated and is usually relatively inert in acid solutions, a few species cause rapid dissolution when added to the environment. One of the most interesting of these is floride compounds. Straumanis and Chen[28] found that small additions of ammonium floride greatly increased the dissolution rate of titanium in HCl, H_2SO_4, HBr, and HI solutions. Titanium is also very active in hydrofloric acid. Even dilute solutions of this acid readily dissolve the metal and they are often used as etchants. The corrosion potential of titanium in 0.5N HF has been measured to be approximately -1000 mV(SCE)[28,55], an extremely low corrosion potential. It has been suggested[72] that hydrofloric acid dissolves the oxide and the floride ions form complexes with the metal. An example is

$$(20)\quad TiO_2 + 6HF \rightarrow [TiF_6]^{2-} + 2H_2O + 2H^{+}$$

Although titanium dissolves rapidly in floride-containing solutions, interestingly enough, the floride is the only halogen in which titanium will not stress corrode. Perhaps the dissolution in HF is not localized enough to promote cracking.

Other solutions which attack titanium are hot concentrated low-pH chloride salts (eg. boiling 30% $AlCl_3$ or 70% $CaCl_2$).[88] Very powerful oxidizers are corrosive. Examples are red fuming nitric acid[86] and 90% H_2O_2. Titanium is pyrophoric in anhydrous RFNA if the NO_2 content is high.[87] Dry chlorine gas will also attack the metal.[88] The addition of water inhibits the corrosion in both the fuming nitric and the Cl_2.

Generally, the purpose of adding alloying elements to a pure metal is to improve its mechanical properties. The corrosion resistance is usually lowered, especially if the alloying elements promote the formation of a second phase. Aluminum is a common alloying element used to improve the mechanical properties of titanium. Aluminum additions lower the corrosion resistance of titanium in nitric acid[85] and in sulfuric acid.[97] Strunkin[98] et al. found that Ti-5Al-2.5Sn had notably lower corrosion resistance than the pure metal in hydrochloric acid. However, they found that the addition of oxidizing agents (Cl_2 and $K_2Cr_2O_7$) significantly increased the corrosion resistance of the alloy.

When the oxidizers were available in sufficient amounts the dissolution rate of the alloy was no greater than the metal. Levy and Sklover[35] plotted anodic polarization curves of various alloys in HCl solutions. They found the dissolution rates (as measured by i_{crit}) to be higher for the alloys than the metal. For an α-β alloy, Ti-6Al-6V-2Sn, they found that the dissolution rate increased as the strength level, and concurrently, the ratio of alpha phase to beta phase increased. Also at high positive potentials [greater than 1000 mV(SCE)] the α-β alloys were pitted while the pure metal was not. An all beta alloy Ti-13V-11Cr-3Al did not pit. Similar polarization experiments were run by Levy[52] in sulfuric acid solutions. These results indicated that the corrosion rate of the α-β alloy Ti-6Al-6V2Sn was greater than the pure metal. The same increase in the dissolution rate with increasing strength was again found for this alloy. The corrosion rate of the β alloy Ti-13V-11Cr-3Al was not significantly different than the pure metal. As was mentioned previously, no pitting occurred in the sulfuric acid solutions. However, Peters and Myers[56] concluded that there was no significant difference in the dissolution behavior between the metal and its alloys. Their experiments were also run in sulfuric acid. Alloys tested were Ti-5Al-2.5Sn, Ti-6Al-4V, Ti-8Al-1Mo-1V and Ti-13V-11Cr-3Al.

In experiments[83] studying the growth of hydrides in 3N H_2SO_4 it was found that the hydrides were thicker on pure titanium than on a Ti-4.35Al alloy. Also the thickness of the hydrides on the alloy was very uneven showing a great deal of scatter in measured values from test to test.

The effect of applied potential on the dissolution rate of titanium is very interesting. As has been indicated previously, the highest dissolution rate occurs at potentials corresponding to the peak of the anodic polarization curve. However, some very informative observation were made in experiments in which corrosion rates were measured during cathodic polarization of titanium and a Ti-4.35Al alloy in 3N H_2SO_4.[83] For the pure titanium, as the cathodic current density, i_c, was increased from 0.5 mA/cm^2 to 2 mA/cm^2, the corrosion rate decreased. When i_c was increased further (to a final value of 30 mA/cm^2), the corrosion rate increased. However, even at 30 mA/cm^2 the corrosion rate was lower that it was under the open circuit condition. When the Ti-4.35Al alloy was tested the corrosion rate was found to increase greatly as the cathodic current density increased. When i_c was 32 mA/cm^2 the corrosion rate was twice as large as it was under open circuit conditions. The corrosion rates were given in the paper as mg/cm^2 over a 48 hour test period. To compare then with other dissolution rates, they were converted to current using Faraday's law and assuming dissolution to trivalent ions. The values for the alloy were 140 μA/cm^2 at i_c = 32 mA/cm^2 as opposed to 70 μA/cm^2 when i_c = 0. These rates are the same order of magnitude as those reported during dissolution in the active, anodic range. The same behavior was also found in less concentrated sulfuric acid solutions, 0.1N and 0.05N H_2SO_4. The phenomenon is believed to be due to the reduction of a protective surface layer.[83] This same increase in dissolution rates as the cathodic current

is increased was found for titanium in nitric acid solutions by Karasev and Stabrovskii.[99] The corrosion rate was determined by weight loss measurements. The tests were run in 2, 4 and 6N HNO_3 at temperatures of 20 to 80°C and with cathodic current densities of 200,400 and 600 mA/cm^2. The highest dissolution rates were measured when the cathodic current was the largest. In a typical example, at 20°C in 4N HNO_3 as the current was increased from 200 to 400 to 600 mA/cm^2 the dissolution rate increased from 750 to 1580 to 2260 $\mu A/cm^2$ (converted to current density from gm/m^2 hr in the same way as above). These dissolution rates are an order of magnitude larger than normal dissolution rates for "active" titanium in acids. For example in 3N H_2SO_4 i_{crit} from polarization data is only 110 $\mu A/cm^2$.[5] The cathodic current densities used in this experiment were much larger than those used in the experiments in sulfuric acid discussed above.[83] Apparently the larger cathodic currents produce a more complete removal of the protective film. The observation of increasing dissolution rates with increasing applied cathodic current gives strong support to the hypothesis that there is a protective film on titanium even during "active" dissolution.

II. THE STRESS CORROSION CRACKING OF TITANIUM ALLOYS IN AQUEOUS SOLUTIONS

1. General Aspects

Stress corrosion cracking is an extremely complex phenomenon. It occurs in a large number of seemingly unrelated metal-environment systems. Titanium alloys will crack in such diverse environments as aqueous chloride solutions, methanol-chloride solutions, dinitrogen tetroxide, and certain liquid metals. Even in a particular metal-environment system the cracking process is very complicated, involving complex interaction between a stressed surface and a corrosive environment. In the following discussion emphasis will be on the stress corrosion of titanium alloys in aqueous solutions; an attempt will be made to elucidate some of the critical variables in this process.

The primary concern in studying stress cracking in aqueous solutions is to prevent failures of titanium equipment in sea water applications. It should be noted at the outset that, to date, no in-service failures have been reported in this environment. Indeed it is even difficult to initiate cracks on unnotched specimens, in the laboratory in, for example, neutral sodium chloride solutions. For this reason most of the work in the literature has been concerned with crack propagation rather than initiation. Thus, in the discussion that follows, unless initiation is specifically alluded to, the term stress corrosion should be considered as applying to the propagation of existing cracks.

The most common specimen used in titanium stress corrosion testing is the cantilever beam specimen. This specimen is always notched and often fatigue cracked before use. The state of stress in a sharp notch is best expressed by a stress intensity parameter, K_I. This parameter takes into account the notch depth and overall specimen dimensions as well as the applied stress.[116] The susceptibility to stress corrosion in a certain environment is usually reported as K_I/K_{air} where K_{air} is the stress intensity required for fracture of the specimen in air. Invariably, the specimen dimensions are such that a state of plain strain develops. Thus most stress corrosion testing has been done in a very mechanically aggressive situation. One additional point on testing methods that should be emphasized is that since the state of stress is so strong a function of the specimen dimensions rigorous comparisons can only be made using identically shaped specimens.

Although cracks are hard to initiate in neutral aqueous solutions, when one does form it will propagate across the specimen at an extremely rapid rate. Beck[100] has measured crack velocities on the order of 1.5×10^{-2}cm/sec for the Ti-8Al-1Mo-1V alloy in 0.6M halide solutions. This rate is several orders of magnitude faster than crack velocities in most other systems.[101] Indeed, the most difficult feature to account for in postulating a mechanism for aqueous cracking in the titanium system in this very rapid cracking rate.

In room temperature aqueous solutions titanium cracks transgranularly[102-104] although intergranular cracking occurs in other environments.[104-106] The transgranular cleavage in aqueous solutions has been shown to occur on the $(10\bar{1}8)$ or $(10\bar{1}7)$ planes.[102] These planes are rotated 12 to 14 degrees from the basal plane. The addition of Cl^-, Br^- or I^- ions to aqueous solutions at room temperature will cause cracking but no other anions appear to be detrimental.[100] Additions of SO_4^{2-}, NO_3^-, or the halide, F^- inhibit the process while the cation appears unimportant.[100] It has not been established whether the cracks propagate continuously or discontinuously.

2. Metallurgical Variables

The following list of titanium alloys have been shown to exhibit at least some degree of susceptibility to stress corrosion cracking in salt water[107,108-110]: Ti-.3170, Ti-8Mn, Ti-2.5Al-1Mo-10Sn-5Zr, Ti-3Al-11Cr-13V, Ti-4Al-4Mn, Ti-5Al-2.5Sn, Ti-6Al-2.5Sn, Ti-6Al-4V, Ti-6Al-3Cb-2Sn, Ti-6Al-4V-1Sn, Ti-6Al-4V-2Co, Ti-6Al-6V-2.5Sn, Ti-7Al-2Cb-1Ta, Ti-7Al-3Cb (as received and beta annealed), Ti-7Al-3Mo, Ti-7Al-3Cb-2Sn, Ti-8Al-1Mo-1V, and Ti-8Al-3Cb-2Sn.

The following alloys appear to be insensitive to cracking in salt water: Ti-2Al-4Mo-4Zr, Ti-4Al-3Mo-1V, Ti-5Al-2Sn-2Mo-2V, Ti-6Al-2Mo, Ti-6Al-2Sn-1Mo-1V, Ti-6Al-2Sn-1Mo-3V, Ti-6Al-2Cb-1Ta-0.8Mo, Ti-6.5Al-5Zr-1V and Ti-7Al-2.5Mo (as received, beta annealed, and water-quenched; then 593°C aged for two hours). Note that the all-alpha alloys appear to be highly susceptible while some alpha-beta alloys are sensitive and some are not.

Susceptibility increases as the Al content increases.[88,90,108,110,111] In Ti-Al alloys the susceptibility was initiated at aluminum contents between five and six per cent. The addition of 2Cb-1Ta to the Ti-Al alloys raised this value to six-seven per cent Al. The addition of 0.5 to 1.0 per cent Mo to Ti-7Al-2Cb-1Ta produced excellent resistance, while additions of 0.13Si, 0.2Pd and 0.8Mn showed very little improvement in resistance.[111] The sensitivity with increased Al is thought to be because of the formation of Ti_3Al.[111] This compound tends to be formed by exposures in the temperature range 480-815°C depending on the aluminum content.

Tin is also detrimental, but to a lesser extent than aluminum: whereas zirconium, another alpha stabilizer does not appear to be harmful. Eutectoid beta stabilizers such as manganese or cobalt increase sensitivity.[112]

Seagle[111] found that Ti-O alloys showed a transition from resistant to susceptible between 0.2 and 0.4% oxygen. In this case adding 1% Mo did not help. Adding oxygen to the Ti-6Al-4V alloy produced detrimental effects. When the oxygen content of the alloy was 0.08% the resistance

was good but increasing it to 0.18% produced considerable susceptibility. In general, as the Al content of Ti-Al alloys increases, the amount of oxygen that can be tolerated decreases.

Light microscopy did not reveal any significant microstructural changes as the oxygen content was increased from 0.2 to 0.4%.[111] However, work by Amateau[113] relates the low temperature ductile-to-brittle transition behavior of Ti-0.25 oxygen to second order twinning within $(11\bar{2}2)$ twins.

The effect of heat treatment is very significant. Many alloys can easily be made susceptible or not susceptible by varying the heat treatment.[88,111,114] Howe[114] found that annealing a Ti-8Al-1Mo-1V alloy at 1065°C in vacuum for two hours followed by a helium cool in a cold-wall furnace produced no susceptibility to stress corrosion in 3.5% NaCl; whereas a one-hour, 1065°C anneal in argon with an air cool followed by aging at 650°C in argon for two hours and a water quench produced a very susceptible condition. Seagle[111] reported slow cooling from annealing temperature produced much more susceptibility than fast cooling for a Ti-7Al-2Cb-1Ta alloy. This is thought to be caused by the amount of time spent in the temperature range where Ti_3Al may form. Lane[115] found the same increase in susceptibility with slow cooling from the beta temperature range.

Reactive Metals[108] has plotted a time-temperature-stress corrosion relationship for Ti-8Al-Mo-1V similar to the familiar time-temperature transformation diagrams. This diagram shows that heat treatment above 843°C and below 482°C for two hours with an air cool will prevent susceptibility. The formation of Ti_3Al seems to be a diffusion controlled phenomenon. Long periods of time in a slightly sensitive temperature range will produce the same susceptibility as shorter times in a more highly sensitive temperature range.

3. Electrochemical Aspects

Crack propagation during exposure to salt water can be stopped by applying a cathodic potential to the specimen. Feige and Murphy[104] found that an applied voltage of -1000mV(SCE) would stop the crack propagation of a Ti-7Al-2Cb-1Ta alloy in sea water. The crack would begin to propagate again shortly after removal of the potential, but could be stopped again by re-applying it. Beck[100] found that cracks propagating in a Ti-8Al-1Mo-1V alloy in Br^-, Cl^- and I^- solutions were stopped when potentials of -1000 mV(SCE) or lower were applied. Leckie[117] found that an applied potential of -1500 mV(SCE) prevented a Ti-7Al-2Cb-1Ta specimen in 3% NaCl from breaking for a period of 200 hours. When the cathodic potential was removed the specimen still did not fail in 100 more hours. (The applied stress intensity in these tests was high enough that the specimen should have failed in a very short time).[117]

The susceptibility to cracking was also found to be lower within a range of anodic potentials. Beck[100] found that the load required to initiate cracks in Ti-8-1-1 specimens in .6M KCl or KBr increased over a range of anodic potentials. Feige and Murphy[104] also noted an increase in the load carrying capacity of the Ti-7Al-2Cb-1Ta alloy in sea water at an applied potential of roughly +800 mV(SCE). Chen[118] found an increase in applied load for failure at a potential of +250 mV(SCE) for Ti-8-1-1 specimens in 3.5% NaCl.

Experimentors do not agree on the potential at which maximum susceptibility occurs. The following potentials at which the susceptibility was a maximum were observed in neutral NaCl solutions: 0mV(SCE) for notched, 0.75 inch (19mm) thick, specimens in 3 point bending,[104] 0mV(SCE) for 1 inch (25.4mm) thick[117] and +300 mV(SCE) for 0.25 inch (6.35mm) thick[119] fatigue cracked cantilever beam specimens -500 mV(SCE) for 0.05 inch (1.3-2.1mm) thick notched* tensile specimens,[100] -642 mV(SCE) for 0.025 inch (.635mm) thick fatigue cracked tensile specimens,[118] and -742 mV(SCE) for 0.025 inch thick smooth bend specimens.[118] From this information it appears that the discrepancies are related to the specimen size. Thicker specimens show susceptibility at higher potentials than thinner specimens. While it is not clear why the thicker specimens should have a more noble susceptible potential than the thinner ones, it is not hard to understand why a difference exists. First, the state of stress which plays an extremely important role in stress corrosion is very likely different in the thick specimens than in the thin ones. The former are most likely in a state of plain strain while the latter may be in a state of plain stress which is much less aggressive. Secondly, the potential that is applied to the surface of a specimen is not the potential that exists at the tip of a propagating crack. The difference is due to the IR drop down the crack length. This IR drop depends on the dimensions of the crack which certainly vary with specimen size. Presumably, the applied potentials on the thinner specimens would reflect the potential at the crack tip more closely than those on the thicker ones. But even for the thin specimens the applied potential cannot be taken as an accurate measure of the tip potential.

Anodic breakdown characteristics of titanium alloys is thought to be related to the susceptibility to stress corrosion. Feige and Murphy[104] noted that environments in which stress corrosion occurred were uniquely the same environments in which anodic breakdown (accompanied by pitting) of pure titanium and titanium alloys occurred at impressed anodic potentials of less than 20 volts.

The effect of solution pH has been evaluated by many investigators. Williams[119] reported that varying the pH between 4.5 and 8 had little effect on stress corrosion in 3.5% NaCl for Ti-8Al-1Mo-1V and Ti-6Al-4V

---

*In these experiments some of the specimens were fatigue cracked and some were not. It did not appear to matter.

alloys. Above and below this range increased susceptibility was found. Haney[120] observed changes in the corrosion potential as a function of pH for the Ti-13V-11Cr-3Al alloy in 0.6N NaCl. However he was unable to detect a significant variance in cracking susceptibility with pH. Leckie[117] found the effect of pH to be negligible in his cantilever beam tests of the Ti-7Al-2Cb-1Ta alloy in 3% NaCl. From the above results it would appear that the hydrogen ion concentration is not a significant factor in the cracking process. However this is not necessarily the case since, similarly to the applied potential, the bulk solution pH does not reflect the pH at the crack tip. At the crack tip the solution is divorced from the bulk and significant changes in concentration can occur without any noticeable alterations in the bulk solution. An ingenious method for measuring the pH near the crack tip was developed by Brown et al.[121] The method consists of abruptly interrupting the process while a crack is propagating and freezing the entire specimen in liquid nitrogen. The specimen is subsequently broken open and the solution at the tip of the crack analyzed. Using this method, the pH at the crack tip in a Ti-8-1-1 alloy cracking in neutral NaCl was found to be about 1.7. This pH at the tip was insensitive to bulk values and remained under pH2 even when the bulk solution was made alkaline. Analysis of the tip solution also revealed the presence of Al^{3+} ions. Recently, Brown, using a different technique,[122] has been able to measure the potential near the crack tip while the crack is propagating. He measured this tip potential, for the Ti-8-1-1 alloy cracking in 3.5% NaCl, while the bulk specimen was being cathodically polarized by a galvanic connection to a Zn or Mg anode. He then froze the specimen and measured the pH at the tip corresponding to the observed tip potential. He found that under freely corroding conditions the potential at the tip was between -942 mV and -1142 mV(SCE) while the pH was 1.7. Connecting the Zn anode changed the tip potential to between -1142 mV and -1342 mV(SCE) and the pH to about 3.5. Connection to the Mg anode produced a tip potential between -1392 mV and -1642 mV(SCE) and a tip pH of about 3.8. These finding are very interesting. Assigning the corrosion potential at the crack tip a very active value is in qualitative agreement with estimates by other workers although this value, -1042 mV(SCE), is roughly 200 mV more negative than had been anticipated.[100,123] It is also quite interesting that the pH increases as the potential becomes more negative. The experimentors[122] qualitatively observed that the crack velocity decreased at the same time. Thus it appears that a low pH is not only observed inside stress cracks but is also necessary for their propagation.

Tiller and Schrieffer[176] have suggested an explanation for the negative potential at the crack tip. They proposed that the stress in the vicinity of the tip produces a change in the local volume per atom which leads to a redistribution of the free electrons in the metal. Their calculations indicate that the flow of electrons would be into the crack tip region which would make it cathodic with respect to the rest of the metal.

Other very important electrochemical aspects of the salt water cracking of titanium were determined by T. R. Beck at Boeing.[46,100] He found that the crack velocity increased as the applied potential

increased (noble direction). The increase was approximately linear from a potential of -800 mV(SCE) to +1000 mV(SCE). This increase in velocity at noble potentials may seem confusing in light of the observed anodic protection zones discussed above. Consider Ti-8-1-1 specimens in .6M KCl solutions. The load to initiate a crack was found to be higher at, say, +500 mV(SCE) than at -500 mV(SCE). However, once a crack was initiated its velocity was faster at +500 mV(SCE) than at -500 mV(SCE). The anodic current flowing from the crack was also found to increase linearly with potential.[46,100] These results apply to neutral halide solutions. In very concentrated HCl solutions (10-12N) the crack velocity was found to be independent of potential.[46] Even a large cathodic potential did not stop the propagation. In other experiments[46,100] Beck found that the crack velocity increased with the halide ion concentration. For concentrations above about 10^{-3} moles/liter the velocity varied as approximately the one-quarter to one-half power of the concentration.

4. Initial Sites for Stress Corrosion Cracking

In recent years much attention has been paid to relating the initial sites for stress corrosion cracking to the electrochemical attack of microstructural imperfections. It is when a metal is continually being deformed while in a corrosive environment that dissolution rates are accelerated the most. Pickering and Swann[124] cited three different mechanisms to account for this accelerated, localized attack at regions on an alloy surface which are in the process of plastic deformation: (a) protective surface films may be broken by growing surface slip steps which render the local surface unprotected, (b) the atoms around a surface slip step have fewer neighbors and hence will dissolve easier, and (c) dislocations emerging at the surface may produce a chemical fluctuation such as that caused by "dislocation pumping" of solute atoms to the surface.[124,125] This pumping effect occurs when the dislocations are moving slow enough so that the solute atoms can move along with them, i.e., the solute atoms can jump to a dislocation site on the moving dislocation. This is especially important in alloys which produce planar arrays of dislocations, because many more solute atoms can be brought to the surface, causing localized surface compositions quite different from the average composition. These localized in homogeneities could produce the necessary electrochemical reactions for stress corrosion cracking initiation. Swann[126] found that alloys forming planar arrays are in fact more subject to transgranular stress corrosion cracking than alloys that form cellular arrays of dislocations.

Whether the dislocations are distributed in a cellular arrangement or in a planar arrangement is generally dependent on the stacking fault energy. With high stacking fault energy cross slip of dislocations is easy and the arrangement is cellular. But when the stacking fault energy is low cross slip is difficult and the dislocations tend to stay on their slip planes and form planar arrays. At room temperature, pure alpha titanium deforms by slip on $(10\bar{1}0)$, $[11\bar{2}0]$, systems and by twinning on $(10\bar{1}2)$, $(11\bar{2}2)$ and $(11\bar{2}x)$, where x = 1,2, and 4.[113] This high

number of deformation modes suggests that cross slip is easy in pure titanium. Blackburn,[127] however, has reported for Ti-Al binary alloys that slip is confined to the slip system $(10\bar{1}0)$, $[11\bar{2}0]$, and that the dislocations lie in coplanar arrays. A transition from cellular to coplanar arrays occurs at the same aluminum content at which the alloy becomes susceptible to stress corrosion (about 5% Al).[102]

In order for electrochemical dissolution to occur at dislocations there must be a potential difference between the dislocation and the matrix. Tromans and Nutting[128] have claculated the potential difference between a dislocation with no solute atoms around it and the matrix. They obtained a value of approximately 0.0085 volts. If their calculations are correct then potential differences high enough to cause dissolution would likely arise only from segregation of solute atoms to the dislocations. In this same light, preliminary tests at Reactive Metals, Inc.[111] indicate that Ti_3Al (Ti-15.8% Al) is about 0.2 volts more anodic than the matrix phase (Ti-3.5% Al).

5. Proposed Mechanisms

Many attempts have been made to develop a unifying mechanism to account for all stress corrosion failures. But each time a trend developed in which a particular mechanism appeared applicable, an exception was always found. Even for each particular metal the mechanism appears to vary from environment to environment. For example, planar arrays of dislocations have been considered to produce transgranular cracking in titanium alloys. However, in N_2O_4 titanium fails intergranularly regardless of the dislocation structure.[106] In this section, the most prominent theories for stress corrosion of titanium alloys in aqueous solutions will be outlined and compared. Further discussion can be found in Chapter VI where an attempt is made to correlate the results of the present investigation and the electrochemical information developed in Chapter I to the existing theories. The theories apply to occurrences at the tip of an existing crack and thus to the propagation process.

There are two opposing schools of thought under which the theories can be grouped. One school believes that the cracking proceeds by preferential anodic dissolution. The second believes that cracks are propagated mechanically, by cleavage. Considering the dissolution theories first, one prominent theory is the film rupture model. This model was discussed by Feige and Murphy[90] and is supported by the work of Beck.[100] In this theory the thin protective film is ruptured at the crack tip. The crack walls remain passive (they are not deformed) and act as cathodes. Now, at the tip competing processes occur, passivation and dissolution. Propagation occurs when the localized dissolution process creates a stress concentration which causes further plastic yielding. If passivation occurs before this stress concentration is built up then propagation should stop. The high current density necessary for this model must come from the large cathodic to anodic area developed by the extended passive walls related to the small active

region at the tip. The key reactions for chloride solutions would be:

(21) $H^+ + e^- \rightarrow H$

(22) $Ti + 3Cl^- \rightarrow TiCl_3 + 3e^-$

(23) $2TiCl_3 + 3H_2O \rightarrow Ti_2O_3 + 6H^+ + 6Cl^-$

The first reaction would occur on the passive crack walls while reactions (22) and (23) would occur at the tip. The hydrolysis reaction is particularly important because it produces both hydrogen ions and chloride ions which enhance the dissolution. This model predicts transgranular cracking because the film rupture by step-step emergency would occur in a grain rather than at a grain boundary.

Another anodic dissolution mechanism is called the "mechanochemical" theory. It is advocated by T. P. Hoar,[129] and is based on the premise that dynamically straining metal is more reactive than nondeforming metal. Accelerated dissolution is localized at the crack tip due to the rapid deformation occurring there. The basis for this theory comes from the experiments of Hoar and Scully on austenitic stainless steel wires in boiling magnesium chloride solutions.[130] They found that when these wires were rapidly strained in the solution large increases in anodic current were measured, (from a current of 0.013 mA/cm^2 for static metal to a current of 3.0 mA/cm^2 for a metal being strained at a rate of 107%/min). A calculation of the thermodynamic potential difference between cold-worked and annealed metal arising from differences in stored strain energy results in a maximum difference of only a few millivolts.[129] The observed (three orders of magnitude) change in the current then, must come from kinetic changes rather than thermodynamic differences. In the kinetic equation for an electrochemical reaction (see Appendix) there are two terms which could by significantly changed by dynamic straining. One is the activation energy for the process $\Delta G_a^\dagger$ and the other is the concentration of reactant, C_m. An increase in current may arise from an increase in C_m, a decrease in $\Delta G_a^\dagger$, or both. The maximum change in $\Delta G_a^\dagger$, or both. The maximum change in $\Delta G_a^\dagger$ was estimated to be the difference in stored energy and would be about 100 cal/mole.[129] Even in the exponential term this change results in an increase in current of only about 20% at room temperature. Therefore, the increase in kinetics is thought to be due mainly to an increase in C_m. This concentration increase arises from the dynamic surface activity due to the rapid emergence of dislocations.

It is not necessary that film rupture and lattice disarray theories be mutually exclusive. The latter theory merely gives a basis for an expected increase in the dissolution rate at a crack tip. This increase could easily be coupled with a small anode, large cathode effect to produce quite a large change in current density.

Another cracking theory is the "Stress Sorption" model. This model, proposed by Uhlig,[131] contends that crack propagation results from the specific adsorption of a "damaging ion" at the tip of the crack. This adsorption causes a reduction in the bond strength of the metal atoms resulting in cleavage. This theory is really not an anodic dissolution theory in that it involves a brittle mechanical failure and not electrochemical dissolution. It is listed with the dissolution models because in aqueous solutions the "damaging ion" would be the halogen ion and the rate of cracking would be related to the availability of the halogen ions at the crack tip, similar to the film-rupture theory. It has, in fact, been suggested[100] that the cracking velocity in NaCl solutions is proportional to the rate of transport of chloride ions to the crack tip. (If this is true the cracking should be a continuous process.) The stress sorption theory is perhaps the only theory that can easily account for the very rapid cracking rate of titanium alloys. This is because it involves a brittle cleavage type fracture which can occur at a rate as high as the speed of sound.[101] As has been pointed out elsewhere,[101] the main difficulty with the stress sorption theory is that of designing a critical experiment to determine its validity. Also, it is somewhat difficult to understand why the adsorption of certain ions, e.g. Cl^- ions, should reduce the bond strength and cause cracking while the adsorption of other ions, e.g. SO_4^{2-}, inhibits the process.

Although they are quite different in their theoretical basis, these three anodic dissolution models are in many cases difficult to distinguish experimentally. Therefore in subsequent discussions they will often be grouped under the general heading of dissolution mechanism. However, attempts will be made, whenever possible, to relate appropriate observations to each of them individually.

The foremost theory to be considered under the heading of mechanical theories is the hydrogen embrittlement theory. This theory postulates, simply, that the hydrogen atoms, which are produced by proton reduction at the crack tip, enter the lattice and embrittle the metal. The mechanism by which the absorbed hydrogen embrittles involves the precipitation of hydrides similarly to the slow strain rate embrittlement which is common in hydrogen containing titanium alloys.[132,133] The actual details of the internal embrittlement mechanism have been considered elsewhere[134-138] and will not be discussed here. The crucial question in determining the applicability of this model to aqueous stress corrosion is not whether hydrogen in sufficient amounts can embrittle the metal. There is no doubt that it can. The question is whether the hydrogen can be absorbed fast enough to account for the high crack velocity.

In connection with the mechanism of hydrogen embrittlement recent work by Nelson, Williams, and Tetelman[177] is noteworthy. They studied the gaseous hydrogen embrittlement of high strength steel in a partially dissociated hydrogen environment. They found that the presence of atomic hydrogen increased the crack growth rate by several orders of magnitude. Further, they found that the activation energy for this

atomic-molecular crack growth was nearly identical to that for the heat of solution of hydrogen in the metal lattice. These findings suggested that the slow step in the embrittlement reaction involves the dissociation of molecular hydrogen and that "the hydrogen-metal interaction resulting in embrittlement takes place just below the first atomic layer of the crack surface." The same situation holds for titanium alloys, the rapid crack velocity could be explained without the need for lattice diffusion of the hydrogen.

One final theory which should be mentioned is also a mechanical fracture theory. It was first proposed by Forty[139] and involves the discontinuous process of repeated fracture and re-formation of a brittle surface layer. The rate of crack propagation is determined by the rate of film growth. This theory does not have strong experimental support in the aqueous titanium cracking system although it has been suggested that the fracture of a brittle hydride surface layer could be involved in the cracking process.[46] (Brittle oxide films have been rejected on the basis that they could not form fast enough to keep up with the propagating crack.)[46] The brittle film theory does, however, have excellent experimental support in other systems.[101]

Proposed mechanisms for the stress corrosion of titanium alloys in aqueous solutions must account for the following salient observations of the cracking process:

1. The very rapid propagation rate.

2. The specificity of anions that cause cracking.

3. The transgranular, cleavage type fractures which occur on a rather odd fracture plane.

4. The existence of cathodic and anodic protection zones.

5. The effect of applied potential on the crack velocity and on the measured current.

6. The low pH and very negative corrosion potential in the crack tip region.

As would be expected, none of the above theories can explain all the experimental observations. Both the dissolution theories and the hydrogen embrittlement theory have difficulty accounting for the very high crack velocity (1.5×10^{-2} cm/sec). To achieve a rate of that magnitude by pure anodic dissolution, a current density of about 600 amp/cm^2 would be required. This extremely excessive current is the main reason why an electrochemical anodic dissolution mechanism appears doubtful. However, Beck[46] has pointed out that current densities this high are often used in electrochemical machining. The bulk diffusion of hydrogen in alpha titanium is also too slow to account for this

velocity. In this light, it has been suggested that a high hydrogen content may initiate a cleavage crack which may then travel until it is arrested by a physical barrier, perhaps a grain boundary.[140] This could produce discontinuous cracking at a rate much faster than the hydrogen diffusion rate. Cleavage processes have been observed in Ti-Al alloys even in the absence of a stress corrosion environment.[102] Scully[140] has pointed out that if hydrogen acts only as an initiator, then crack velocities should be determined mainly by the physical and mechanical properties of the metal. This could explain the observed large variance in velocity from alloy to alloy.[140] As was pointed out previously, a stress sorption mechanism controlled by the transport of Cl^- ions to the crack tip could produce continuous cracking at a very rapid rate.

The specificity of anions tends to support the dissolution theories which require direct involvement of the halide ions. However the presence of chlorides would likely increase the rate of hydrogen absorption. This fact is well established in ferrous alloy systems.[141] Also the hydrolysis reaction of the halide salt may serve as a source of hydrogen ions.

The fracture characteristics are strong support for the hydrogen embrittlement theory. The general appearance of the fracture surfaces is indicative of a brittle mechanical failure. Cleavage produced, river-bottom, markings are in evidence. The fractures show no indication that a prior dissolution reaction had occurred, especially not a reaction of the magnitude necessary for a dissolution mechanism. The hydrogen embrittlement model can also explain the unusual fracture planes. This has been done in a paper by Mauney and Starke.[142] They demonstrated that hydride precipitation on the normal slip planes would promote slip on another slip system which would lead to fracture on the observed $(10\bar{1}7)$ and $(10\bar{1}8)$ planes. The situation is complicated however by the fact that a stress sorption theory would also produce brittle type fractures and by the fact that susceptible alloys show the same odd fracture plane when broken in air as when broken in a stress corrosion environment.[102]

The existence of a cathodic protection zone is, of course, support for the dissolution theories. In fact, this observation has classically been considered pro f that the cracking process is anodic. However, recent experiments such as the ones by Brown,[122] discussed above, which show that the hydrogen ion activity decreases as the potential decreases have cast doubt on this practice. Another possible explanation for the cathodic protection zone which is consistent with the hydrogen embrittlement theory is the rapid formation of surface hydrides at very negative potentials. Hydrides appear to have a lower hydrogen over voltage than bare titanium and may act as preferential sites for hydrogen reduction. This could prevent the hydrogen from being discharged at the crack tip and thus lower the amount of hydrogen absorbed. The effect of surface hydrides on the cracking process will be discussed in more detail later. On the other hand, anodic protection zones which support the hydrogen theory are harder to explain on the basis of a dissolution mechanism, at least no plausible explanations have been put forth in the literature.

The strongest support for the dissolution mechanisms comes from the observed linear increase in both crack velocity and anodic current as the potential is shifted in the noble direction.[46,100] Increases in the potential would increase the rate of anodic reactions at the tip and the rate of transport of chloride ions to the crack tip.

The low pH and very negative corrosion potential at the crack tip are consistent with both dissolution and hydrogen embrittlement mechanisms. This fact points out a major difficulty in trying to distinguish between the two mechanisms. They are inter-connected. The reason is that the hydrogen embrittlement theory requires protons for reduction. These must be produced by the hydrolysis reaction which depends on the anodic dissolution reaction. Therefore, any effect which slows down the anodic reaction can be argued as ultimately lowering the proton concentration. On the other hand, any effect which increases the rate of dissolution also increases the concentration of hydrogen ions. A good example of this anomaly is the observation by Brown[122] that decreasing the potential at the crack tip slows down the cracking rate but also increases the pH. The crucial question, which is presently unanswered, is whether the cracking rate decreased because the anodic reaction decreased or because the proton concentration decreased as a result of the decrease in anodic kinetics.

There is however one critical experimental observation which is yet to be made but which could elucidate the problem dramatically. That is whether the microscopic crack propagation is discontinuous (hydrogen embrittlement) or continuous (mass transport controlled anodic process).

III. THE STRAINING ELECTRODE

Since a large portion of the data gathered in this investigation involves a straining electrode, some background in this area should be presented. The main purpose of this work, however, is the study of stress corrosion cracking. Therefore, the review of the literature on the straining electrode will be kept brief. The reader is referred to the work of Murata[74] for a comprehensive review of the subject.

The straining electrode has been used mainly as a tool for general observations although a few attempts have been made to treat the subject quantitatively.[74,159] The biggest problem is that it is impossible to determine, with certainty, the actual area from which the current is flowing during dynamic straining. The technique became experimentally popular because of the work by Hoar and his colleagues.[129,130,160] Hoar has advanced a theory[129] for stress corrosion cracking based on the premise that dynamically straining metal is more reactive than static metal. (see Chapter II, section 5)

1. Elastic Strain

The effect of elastic strain on the rate of electrochemical reactions is generally not large. An estimate of the expected change in electrode potential from the increase in internal energy during elastic straining is often made and the change is negligibly small. Yang, Horne and Pound[161] calculated the change in the reversible potential of a pure electrode during elastic strain using only thermodynamic considerations. Again the effect was found to be extremely small - a stress of 1000 psi was calculated to produce a potential shift of 10^{-4} to 10^{-5} mV. Impurity atoms increase the change. Interstitial impurities such as hydrogen produce the largest effect, but it is still quite small. The exact magnitude depends on the partial molar volume of the impurity but it is on the order of 0.01-0.1 mV/1000 psi. When considering differences between substitutional and interstitial solutes Yang et al.[161] came to an interesting conclusion. The chemical potential of a substitutional solute or a pure solid increases with the application of a nonhydrostatic stress whereas the chemical potential of an interstitial solute may increase or decrease depending on the sign of the applied stress. Compression increases it; tension decreases it.

Nobe et al.[162] measured transient changes in E_{corr} during elastic straining of copper in $CuSO_4$ and NaCl and zinc in $ZnSO_4$. These transients were short lived and died out in a few seconds. Their magnitude was typically about 0.01 mV.

These observations indicate that the change in electrode potential during elastic straining is not a factor in stress corrosion cracking, certainly not in terms of the "mechano-chemical" effect. There is no information available in the literature about changes in current flow during elastic straining at constant potential.

2. Cold Work

When a metal is cold worked its internal energy increases. From a thermodynamic point of view this should increase the reactivity. An estimate of the magnitude of this effect can easily be made. This has been done[129] and, as in the case of elastically stressed metals, it is very small.

The internal energy of a cold worked metal is stored mainly in the dislocation structure. The dislocation density may increase by a factor as high as 10^4 to 10^6 when a metal is severely cold worked. The preferential dissolution of dislocations has received a good deal of attention in recent years.[74,124-126,128,163] As far as static dislocations in a cold worked metal are concerned, the increase in reactivity is not large enough to be important unless the segregation of solute atoms to the dislocations is significant. Moving dislocations can exert considerably more influence by producing dissolution sites on the surface as they emerge. This is especially true if the dislocations form planar arrays (see Chapter II, section 4).

Finley and Meyers[164] studied the effect of cold work on the anodic polarization of iron in 1N sulfuric acid. They found that cold working shifted the potential for complete passivation in the noble direction. This shift was also found by France for low carbon steel in 0.6M NH_4NO_3.[165]

In the same paper, France also summarized the results of numerous workers on the effect of cold work on corrosion rates. He found the results to be very inconsistent, one worker would report increased corrosion rates after plastic deformation and another decreased rates. The discrepancies were related to the lack of adequate control of the experimental variables.

Tomashov and Ivanov[166] studied the effect of cold work on the corrosion of titanium in sulfuric and hydrochloric acid solutions. They found that the corrosion rate of the rolled surface decreased with increasing plastic deformation (from 20% to 95% reduction). However, they found increased corrosion on the edges of the sheet specimens, the edge perpendicular to the rolling direction having a greater rate than the edge parallel to it. They explained the phenomenon by crystallographic texturing (the basal plane tends to be parallel to the rolling plane) and by a higher density of grain boundaries in the edges.

3. Dynamic Straining

Only when metals are strained dynamically does the effect of strain on dissolution rates become large enough to be a consideration in stress corrosion cracking. The largest effect was found by Hoar and Scully[130] for austenitic stainless steel in boiling magnesium chloride solutions. They found that the current increased over 200 fold when the metal was strained at very rapid strain rates. If the stainless steel is film free in this environment, as Hoar and Scully assumed, then this change

represents a very large increase in dissolution kinetics. However, Slater,[167] using the same experimental conditions, was unable to reproduce this high dissolution current. In addition, his experiments as well as those of other workers[168] showed evidence of film formation in the boiling $MgCl_2$ solution. With a film present the increase in current with straining can often be explained by rupture of the film without the need for a large change in dissolution kinetics.[167]

Despic, Raicheff and Bockris[169] ran a series of straining experiments taking special care to avoid the formation of surface films. They compared the current response to straining of bcc metals (Fe and Mo) to fcc metals (Ni and Cu) at potentials slightly above the steady state corrosion potential. A definite increase in current was observed when the metals were strained, the magnitude of the change being greater for the bcc than for the fcc metals. The response was largest for Fe and smallest for Ni. They explained this difference on the basis of enhanced dissolution on the less tightly packed (higher index) planes which are exposed during slip of the bcc metals. Since fcc metals slip on closely packed planes no enhanced dissolution occurs. The actual magnitude of the current increases observed by Despic et al.[169] was quite small for the fcc metals (about 2 fold) and thus their results do not confirm the large increase in dissolution kinetics observed by Hoar and Scully for austenitic stainless steel. However, part of the difference could be due to the fact that the latter workers used much larger strain rates.

Windfelt[170,171] studied the effect of continuous straining on the dissolution processes by measuring potential transients. He measured the potential changes at open circuit and under galvanostatic conditions. The systems studies were Fe and Ni in acid chloride solutions and Cu in acid cupric sulphate solutions. The corrosion potential shifted in the active direction during straining. The magnitude of the shift increased with increasing strain rate and in the order of metals Cu < Fe < Ni, the largest shift being about 40 mV for Ni at a strain rate of 180%/min. In the galvanostatic tests the shifts were qualitatively identical and their magnitude decreased with increasing anodic current. Assuming a film free surface Windfelt was able to explain his observations in terms of changes in the density of kink sites. It is typical of literature on the straining electrode that Windfelt found the straining response to be the largest for Ni and smallest for Cu whereas Despic et al. found the effect to be largest for Fe and smallest for Ni with Cu in between.

Giddings et al.[172] measured the change in open circuit potential of several metals when subjected to a sudden plastic strain in distilled water. Potential shifts were in the active direction and were quite large. The effect was largest for Al (-800 mV) and smallest for Ag (-39 mV). The metals tested in order of decreasing effect were Al > Zn > Ni > Fe > Cu > Ag. The authors related the transients to the rupture of surface films. Thus metals having very low positions on the electromotive series and very protective films produce the largest changes.

Recently, Hoar and Galveli[173] studied the anodic behavior of oxide covered mild steel during yielding in nitrate solutions. They observed appreciable current increases and interpreted them on the basis of enhanced dissolution at sites of film rupture. By assuming that the current was flowing only from new area exposed by the film rupture (calculated directly from the elongation of the wire) they were able to magnify the measured current density of 100 A/cm^2 into a projected value of 2 A/cm^2. This projection is supported by the fact that the observed current transients were a linear function of strain and almost independent of strain rate.

IV. EXPERIMENTAL PROCEDURE

1. Material

The material used in this investigation was Ti-8Al-1Mo-1V alloy in the form of wire 0.020 inches (0.58 mm) in diameter. The wire was obtained from Astro Metallurgical Corporation, Wooster, Ohio. It was cold drawn by them from 3/8 inch (10 mm) diameter rod via a series of 12% reductions with three to four 30 minute anneals at 788°C in argon. It was received in the cold drawn condition after being descaled in salt and pickled in HNO_3-HF. The chemical composition is shown in Table 3. The microstructure and surface appearance of as received wire are shown in Figures 4 and 5.

Table 3. The Chemical Analysis of the Ti-8-1-1 Wire used in this Investigation

Alloying Element	Per cent
C	0.016
Fe	0.065
Al	8.04
V	0.98
Mo	1.12
O	0.09
N	0.008
H	0.0008
Ti	bal.

Before use the wire was vacuum annealed at 760°C for 8 hours followed by a furnace cool. The vacuum was 10^{-7} mm Hg. The microstructure and surface appearance of the annealed wire are shown in Figures 6 and 7.

2. Solutions

The electrolyte used throughout this investigation was 5N HCl. It was made using double distilled water and reagent grade hydrochloric acid.

The specimens were pickled before use. The pickle solution was 33%HNO_3 + 1.5% HF and the balance water. This solution has a tendency to age so fresh solutions were used throughout the investigation.

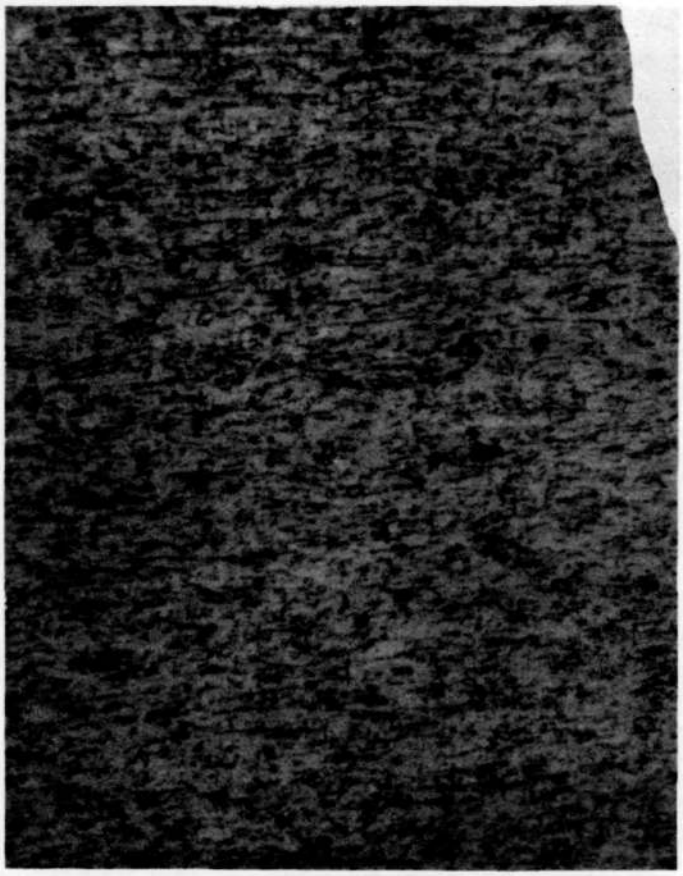

Figure 4 - The Microstructure of the As-Received Ti-8-1-1 Wire. 500X

Figure 5 - Scanning Electron Micrograph of the Surface Appearance of the As-Received Ti-8-1-1 Wire. 2000X

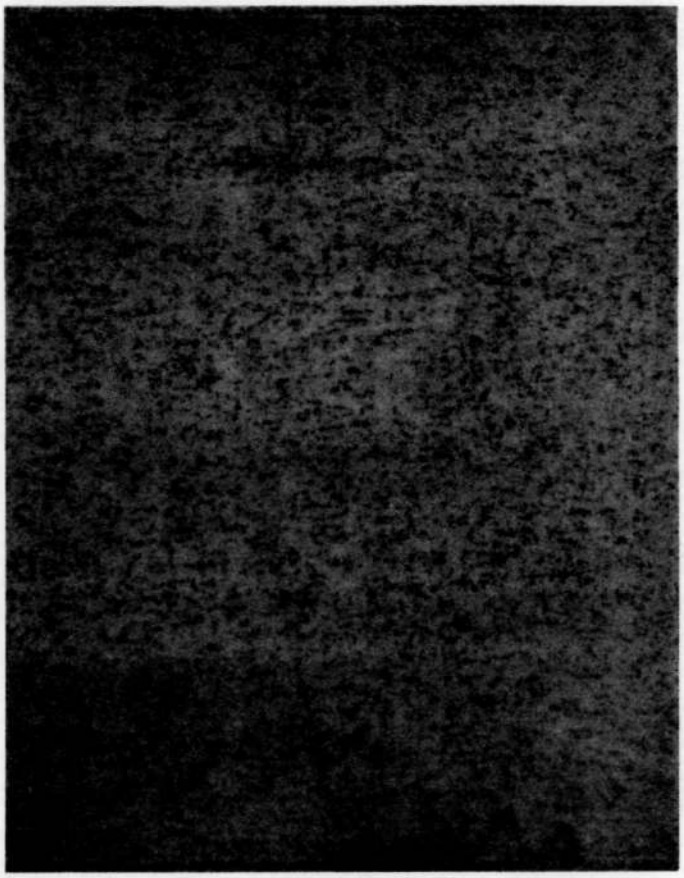

Figure 6 - The Microstructure of the Ti-8-1-1 Wire after a Vacuum Anneal at 760°C for 8 hr and a Furnace Cool. 500X

Figure 7 - Scanning Electron Micrograph of Surface Appearance and the Ti-8-1-1 Wire after a Vacuum Anneal at 760°C for 8 hr and a Furnace Cool. 2000X

3. Experimental Apparatus

All electrochemical measurements were carried out in a polarization cell which was mounted in the test stand of an Instron Tensile Testing Machine. This was done so that a static test could be interrupted at any time by dynamic straining. In addition, the Instron test stand proved to be an effective shield against external stray currents.

Figure 8 shows the polarization cell. It consists basically of the familiar 1000 ml multinecked polarization flask with an extra large top neck to accommodate 1 3/4 inch (45 mm) O.D. heavy wall Pyrex tubing. A male ground glass taper joint matching the top neck of the flask was attached to the outside diameter of the thick wall tubing. It was wrapped with Teflon tape during testing to avoid sticking. Two smaller side necks were used for a Luggin probe and an inlet for inert gas purging. A third side neck, not shown, was used for temperature measurement or, in some tests, to accommodate a salt bridge which was connected to a remote counter electrode. The normal counter electrode consisted of two 1/4 inch (63.5 mm) in diameter graphite rods which were mounted to the inside of the thick walled tubing with GE Silicone Sealant. They were sleeved tightly with heat shrinkable PVC tubing leaving a 3 cm length exposed to the solution. Electrical connections were made using platinum wire. The heavy walled tubing had windows cut, one on each side, to allow free flow of the solution near the sample.

The wire sample was mounted in the thick wall tubing externally and then the whole assembly placed in the polarization cell. The connections can be seen in Figure 8. The wire was held at the top by a Starrett No. 240A pin vise through a piece of PVC. A solid connection to the PVC was afforded by a stainless steel bolt. Care was taken to avoid sharp bends in the wire specimen. A stainless steel rod was connected to the pin vise and extended through a PVC separator. A sleeve on top of the PVC was tightened to hold the wire straight when it was not being strained. Teflon washers were used between the PVC pieces and the glass tubing. During testing in the solution the stainless steel bolt was coated with silicone sealant and the pin vise and stainless steel rod were coated with microstop.

The entire polarization cell was mounted under the moving crosshead of the Instron test stand. The stainless steel rod extended through the moving crosshead and was connected to the upper stationary crosshead. Downward movement of the crosshead resulted in compression of the thick walled tubing and extension of the wire specimen. Figure 9 shows the cell positioned under the crosshead.

When tests were run at very negative potentials chlorine gas was evolved on the graphite counter electrodes. To avoid this contamination a remote counter electrode was used. This consisted of a bridge assembly extending from the cell to an external container in which another graphite electrode was placed. The ends of the bridge were fitted with pieces of fine fritted glass to avoid transport of the chlorine gas to the

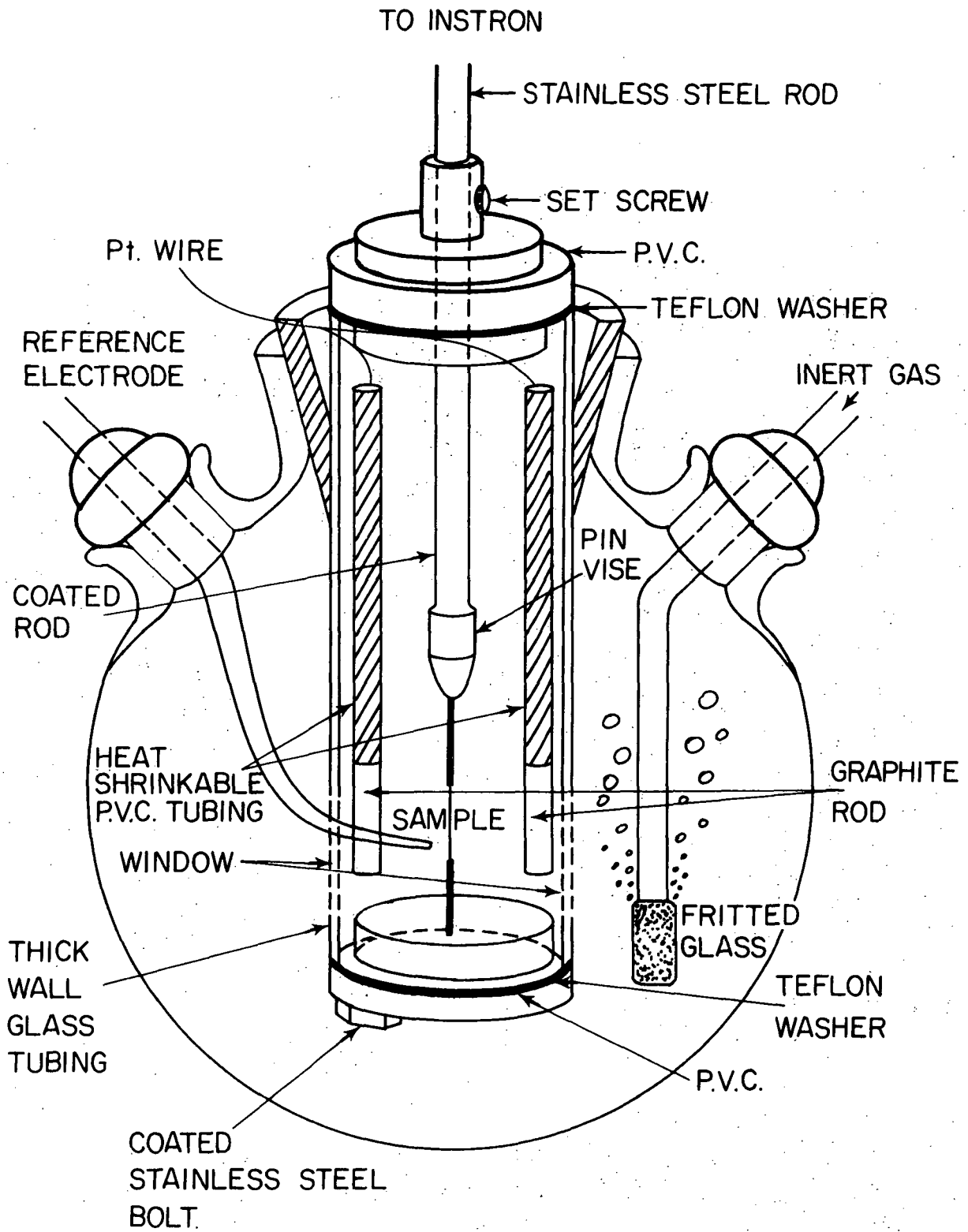

Figure 8 - The Polarization Cell

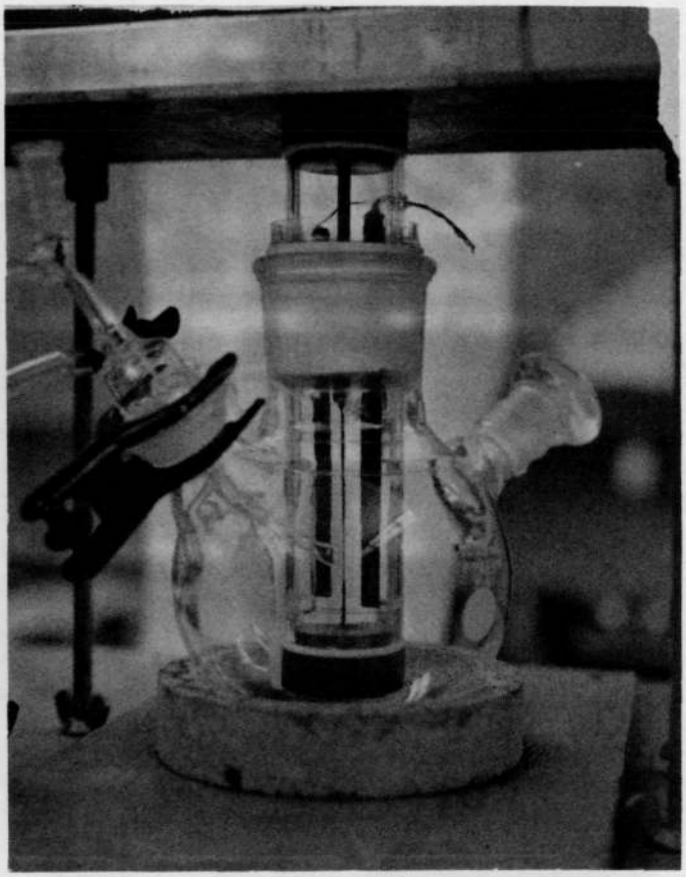

Figure 9 - The Polarization Cell as Positioned under the Cross-head of the Instron Tensile Machine

specimen. The diameters of the bridge and the graphite electrode were made as large as possible to prevent an excessive IR drop during testing. Figure 10 is a picture of the polarization cell with the remote electrode assembly attached.

Potential measurements were made with a saturated calomel reference electrode. Polarization of the specimen was carried out using a Wenking Model 68 TS 10 potentiostat with a Wenking MP 165 motor potentiometer. Measurements were recorded on an Esterline Angus Model E1101S recorder.

Most of the tests were run in solutions deaerated with nitrogen or argon. In order to avoid delays while the oxygen was being purged from the polarization cell a deaeration system was set up by which enough solution for several tests could be deaerated beforehand and continually purged during the tests. The deaerated solution was contained in a 6000 ml flask from which it could be pumped into the polarization cell prior to each test. A four way glass stopcock allowed the large flask and the polarization cell to be purged at the same time. The inert gas was high purity grade, 99.995 per cent pure, argon or nitrogen. It was further purified before use by passing it through ascarite and drierite, then through copper turnings heated to a temperature of 500°C.

4. Specimen Preparation

In order to obtain a consistent surface for study the wires were pickled before testing. They were immersed in the nitric-hydrofloric acid solution for 30 seconds, then thoroughly rinsed with distilled water. The pickling left a small amount of a black powdery residue on the surface (probably a hydride) which was rubbed off with tissue. The wires were then mounted in the PVC and connected to the pin vises. Next they were rinsed with acetone and coated with microstop leaving a 2 cm length uncoated. When the microstop was dry a thin coating of silicone sealant, diluted with toulene, was put over the microstop. The stainless steel bolts and the pin vises were coated with silicone sealant and microstop, respectively. The specimens were then put in a polyethelene box, covered loosely, and left overnight. Since the silicone sealant cures by reaction with water, the bottom of the box was kept wet with distilled water.

5. Procedure

Since the silicone sealant required several hours to cure, specimens were prepared in the evening for tests the next day. The base solution for the next day's runs was also purged with inert gas overnight. To begin a test, the polarization cell was purged, while empty, with inert gas, then about 800 ml of solution was pumped into it. A coated specimen already connected to the thick walled tubing was then introduced into the solution. The cell was put into place in the test stand and the Luggin probe positioned. The solution used in the probe was drawn into it directly from the test cell. Inert gas was bubbled through the test solution and the base solution throughout a run. After each test the

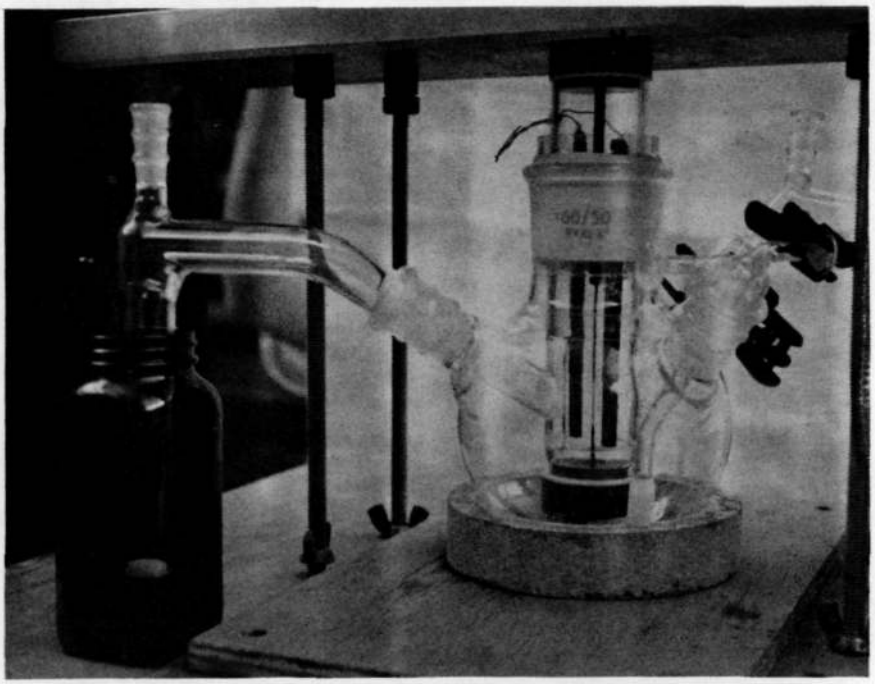

Figure 10 - The Polarization Cell
Showing the Remote
Electrode Assembly

used solution was discarded and the test cell and thick wall tubing rinsed with distilled water. Fresh solution was also introduced into the probe for each test.

Since the wires were left in the air overnight they were covered with an oxide film. Therefore when connections to the potentiostat were made at the beginning of each test the open circuit potential was between -200 mV and +50 mV(SCE). The corrosion potential was monitored while the specimen activated naturally. When the corrosion potential reached its quasi-steady state value of -680 mV(SCE) the test was begun. All tests were run at room temperature.

V. RESULTS AND DISCUSSION

The primary purpose of this investigation was to study the stress corrosion cracking of titanium alloys in aqueous solutions. The emphasis was placed on the propagation stage of the cracking process. The environment used, deaerated 5N HCl, was chosen to simulate conditions at the tip of a crack. The 5N HCl solution has a lower pH than has been observed in cracks but use of the strong acid was necessary in order to obtain a surface for study which was not covered by a passive film. The experiments were designed to study (1) the basic electrochemical behavior of titanium in 5N HCl under static conditions and (2) the response of the metal to dynamic straining in the solution.

As the investigation progressed it became obvious from certain experimental results and from work reported in the literature that surface films could be present on the metal even in the "active" condition and that these oxides and/or hydrides, if present, would be extremely influential in determining the electrochemical properties of titanium in the acid solution. A foremost consideration should be the identification of the surface films. These determinations have been made as indicated in Chapter I. However due to limitations in the analysis process these identifications were made on relatively thick films such as the oxides existing on passive titanium or the thick hydrides formed by cathodic charging. Information about the very thin films on titanium in say, the "active" condition is not easily obtained. And yet these films, which may be only a few angstroms thick, can exert a profound influence on the electrochemical behavior - particularly as related to stress corrosion cracking. Consequently, the results of this investigation were analyzed whenever possible in terms of the surface films and an attempt was made to relate the experimental observations to the existence and properties of these films.

1. Static Response

a. Anodic Region

The anodic polarization behavior of titanium in HCl solutions is well documented in the literature[2,7,35,49] and is discussed in Chapter I. However, only one experimentor[35] measured the curves using the Ti-8-1-1 alloy. Therefore, the measurements were repeated here as a check. Figure 11 shows anodic polarization curves at various scan rates. These tests were run in 5N HCl + 0.6N NaCl solutions. Other curves, run without the added sodium chloride, were identical. The potential range was scanned continuously at the given rates beginning at the "active" corrosion potential and moving in the noble direction. The curves shown are in good agreement with published results. The very low current at the peak of the curve ($\sim$150 $\mu A/cm^2$) is indicative of the extent to which the anodic processes are inhibited on titanium surfaces. As indicated previously, this value is over three orders of magnitude lower than the corresponding current for iron. The tendency for the current in the passive

range to increase slightly as the potential is increased has been observed by other workers.[3] As Figure 11 shows, the scan rate affects the magnitude of the current flowing, particularly in the passive region, but does not affect the potential at which passivation begins. The time dependence of the formation and dissolution of the passive film can be seen on Figure 12 which shows the current behavior during a back scan. The large hysteresis demonstrates that the passive oxides are dissolved very slowly. Figure 13 compares an aerated solution with the normal deaerated environment. As the figure shows, the only change is in the height of the active peak. Thus the presence of oxygen in the solution inhibits the dissolution reaction even more. Before discussing the probable explanations for this observed polarization behavior some information about the behavior of the open circuit or corrosion potential in the solution would be helpful.

A great deal can be learned about an electrochemical system by noting changes in the open circuit potential under different conditions. The open circuit potential is the potential at which the sum of the currents from all the cathodic reactions which are occurring equals the sum from all the anodic reactions. Thus the value of the corrosion potential can be useful in determining the possible reactions that are going on at the surface. When an oxide-coated wire is put into the 5N HCl solution E_{corr} is initially about -100 mV(SCE). However, the oxide film is not stable in the acid and, as it dissolves, the corrosion potential gradually shifts in the active direction. This is illustrated in Figure 14(b). After this shift in the corrosion potential is complete the specimen is said to be in the "active" condition. This curve was measured on a specimen which was passivated at a potential of +200 mV for 1 hour before monitoring the corrosion potential. The same curve was obtained after polarization at +500 mV(SCE) and after a polarization scan to a potential of +750 mV. The natural activation of the air formed film also produced the same curve. It can be seen that the curve shows no horizontal plateau which would indicate the reduction of an oxide of definite, stoichiometric composition. The knee of the curve, commonly called the Flade potential, E_F, is roughly -270 mV(SCE). (In the ideal case, for a stoichiometric oxide this potential would be the horizontal part of the curve and would represent the potential below which the oxide is not stable and dissolves.)

Curve (a) of Figure 14 was measured after polarization at a potential of -200 mV(SCE). Comparison of the two curves shows that they obviously represent different oxides. The Flade potential for the oxide in curve (a) is about -370 mV(SCE). Reference back to Figure 11 shows that -370 mV is just after the peak of the curve. Thus the formation of this oxide apparently accounts for the intial stages of passivation. The probable reaction would be (Table 1, Chapter I)

$$(24)\quad 3Ti_2O_3 + H_2O \rightleftarrows 2Ti_3O_5 + 2H^+ + 2e^-$$

$$E^o = -422 \text{ to } -732 \text{ mV(SCE)}$$

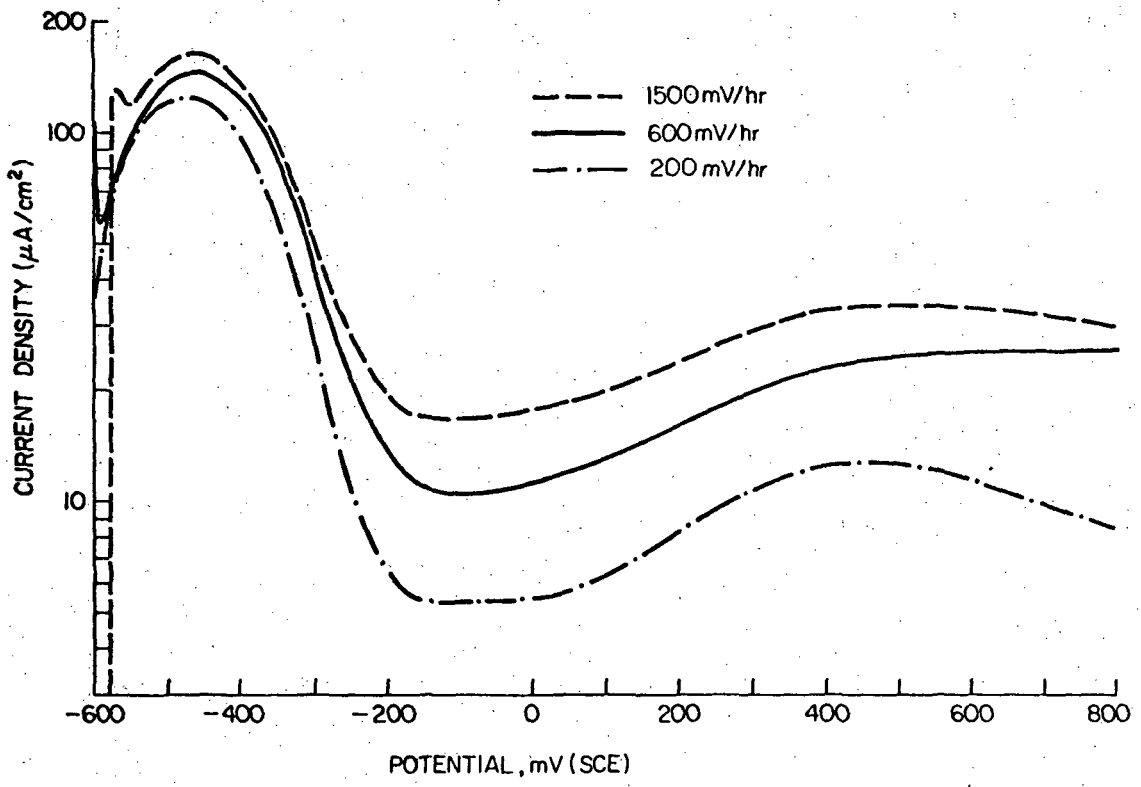

Figure 11 - The Effect of Scan Rate on the Anodic Polarization Curves

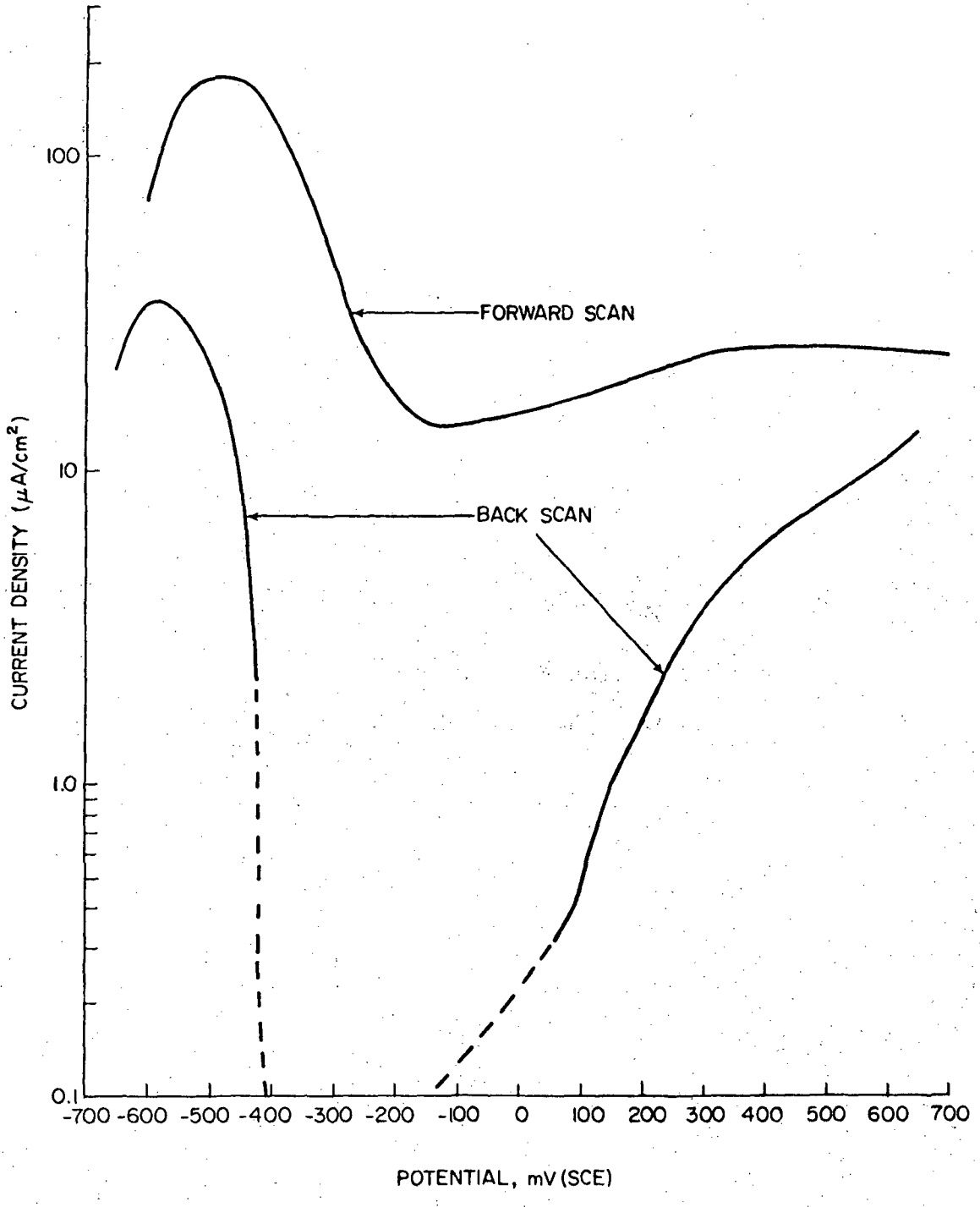

Figure 12 - The Hystresis of the Current during a Back Scan in the Anodic Region

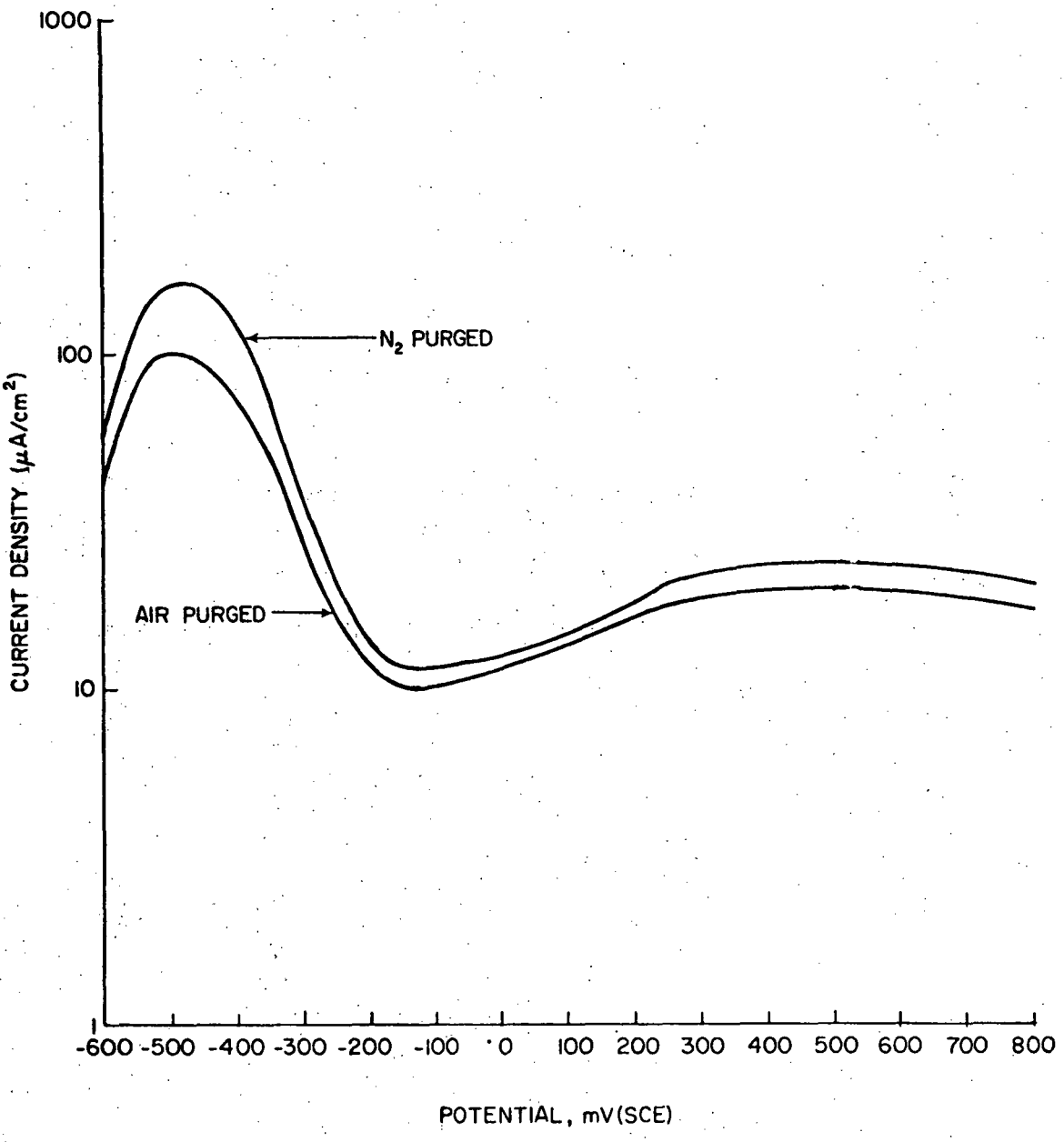

Figure 13 - Comparison of Anodic Polarization Behavior for Aerated versus De-aerated Solutions.

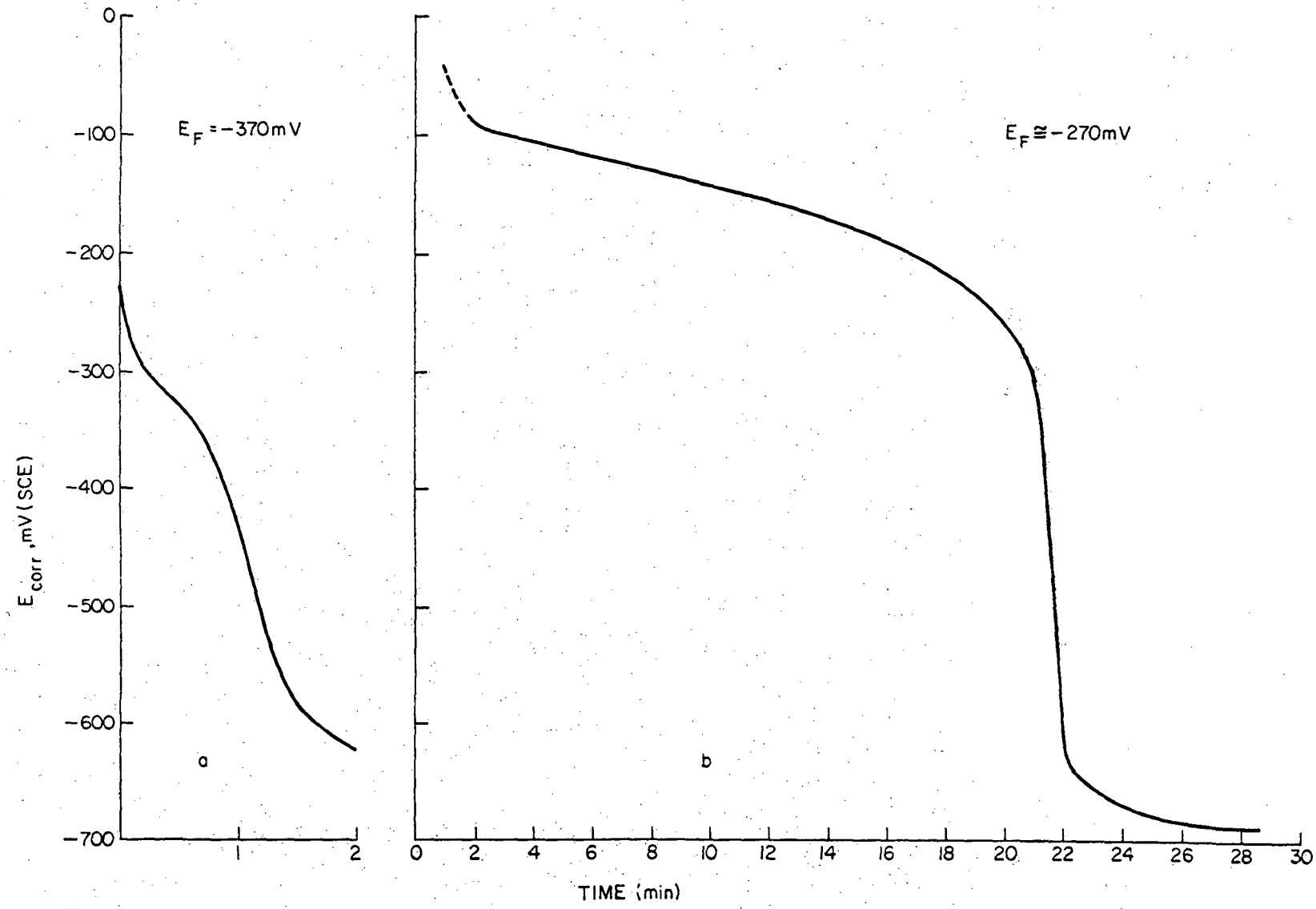

Figure 14 - Potential Decay Curves after Polarization (a) at -200 mV(SCE) for 2 hours; (b) at +200 mV(SCE) for 1 hour.

(The range of standard electrode potential values indicates that there is some uncertainty in the free energy data.) This reaction requires that an oxide be present during the dissolution process before passivation. There is, in fact, strong evidence that this is the case as was discussed in Chapter I. Although the oxide Ti_3O_5 is not thermodynamically stable with respect to Ti_2O_3 and TiO_2, it has been observed on the surface of titanium in sulfuric acid.[8]

From Table 2 in Chapter I the passive oxide in this solution would be expected to be $Ti_2O_3 \cdot 3\text{-}4\ TiO_2$. This is a nonstoichiometric oxide which explains the sloped potential decay curve. Since it is a mixture of two oxides there would be no definite potential at which it will be formed. The final stages of passivation are probably accounted for by the formation of TiO_2 from Ti_2O_3 and Ti_3O_5. From Table 1 there is also some uncertainty about the potential at which Ti_2O_3 can be oxidized to TiO_2. The given potential range is [-792 mV to -352 mV(SCE)]. The reaction would be

$$(25)\quad Ti_2O_3 + H_2O \rightarrow 2TiO_2 + 2H^+ + 2e^-$$

Reactions 24 and 25 can be combined to give a standard potential for the formation of TiO_2 from Ti_3O_5. This yields

$$(26)\quad Ti_3O_5 + H_2O \rightarrow 3TiO_2 + 2H^+ + 2e^-$$

$$E^o = -307\ mV(SCE)$$

In making this calculation E^o for reaction 24 was taken as -442 mV and E^o for reaction 25 as -352 mV since these values seem to be most appropriate to account for the observed data. The pH of the 5N HCl solution is approximately -0.7. A pH of this value would shift the reversible potentials of each of the above reactions 41 mV in the noble direction. Including this correction the final reversible potentials for the reactions are $Ti_2O_3 \rightarrow Ti_3O_5$, $E_{rev} = -401$ mV(SCE); $Ti_3O_5 \rightarrow TiO_2$, $E_{rev} = -266$ mV(SCE) and $Ti_2O_3 \rightarrow TiO_2$, $E_{rev} = -311$ mV(SCE). Thus, the explanation for the observed polarization curves and potential decay curves includes the formation of Ti_3O_5 at the initial stages of passivation followed by the formation of TiO_2 as passivation becomes complete.

As may be obvious to the reader there is an apparent inconsistency in the above explanation of the passivation behavior. From the potential decay curve, Figure 14(b), and the thermodynamic calculations the final oxide should be formed above a potential of about -270 mV(SCE) and yet a 2 hour exposure at -200 mV does not produce it. The explanation for this apparent anomaly is related to the kinetics of the reactions. Although a reaction may be possible at a certain potential it may not occur at a significant rate until a sizeable driving force (overpotential) has been applied. Thus, as the potential is increased TiO_2 is apparently not formed until a potential between -200 and +200 mV(SCE) is reached. Also the Ti_3O_5 which is formed is apparently completely oxidized to TiO_2 at potentials of +200 mV(SCE) and above because its inflection is not observed in the potential decay curve of the final oxide.

It should be pointed out here that sloping potential decay curves such as those in Figure 14 can also be explained on the basis of a gradual reduction of a monolayer of adsorbed oxygen.[72] In other words the adsorption theory of passivity could apply. Kossyi et al.[72] ran experiments using pure titanium in 3N HCl solutions to which a small amount of HF had been added. They were able to conclude that the adsorption theory did not apply to their passive films which were formed at potentials of 1250 - 1500 mV(SCE). Their results should apply for the final passive film i. e. Figure 14(b). However they may not be applicable to the film formed at -200 mV, and so adsorption processes cannot be ruled out in that case.

In the section on passivity in Chapter I it was pointed out that the current flowing in the passive range is used not only for film formation but also for metal dissolution. For this reason the amount of charge passed cannot be used to calculate the thickness of the film. This fact is emphasized by the present results. The film formed at -200 mV for 2 hours is much thinner than the film formed at +200 for 1 hour as is obvious from the difference in the length of time required to dissolve them (Figure 14). Yet the amount of charge passed during passivation at -200 mV was calculated to be much larger than that passed at +200 mV.

It is pertinent at this point to discuss the reactions occurring on the wire surface at the "active" corrosion potential. This is the quasi-steady state potential that is obtained after the natural dissolution of the passive film. There is strong evidence that surface hydrides may play an important role in the reactions that produce this "active" corrosion potential (-680 mV(SCE) for Ti-8-1-1 wires in 5N HCl).

In Chapter I, the formation of surface hydrides on titanium immersed in non-oxidizing acids was discussed in some detail. It was determined that hydrides will form spontaneously in acid solutions and grow to a considerable thickness.[7] A study of analytically measured corrosion rates showed that the dissolution behavior of a hydride coated specimen was exactly the same as a supposedly uncoated specimen.[42] Anodic polarization curves run on pure hydride were identical to curves run on a titanium specimen.[41] From these results it was concluded that apparently a thin hydride layer is present at all times when titanium is "active" in a non-oxidizing acid. The passivation and dissolution processes then occur on top of the hydride layer. The composition of the hydride varies with the acid concentration. In 5N HCl the composition should be TiH.[7] The reaction to form it would be

$$(27) \quad Ti + H^+ + e^- \rightarrow TiH$$

Once a hydride layer has formed there are many reactions which can occur on it. (In contrast to the passive oxide, titanium hydride has high electrical conductivity[7] and thus can easily support electrochemical

reactions.) From Table 1 the likely anodic ones in 5N HCl are

(3) $TiH \rightarrow Ti^{3+} + 1/2\ H_2 + 3e^-$ $E_{rev} = -1350$ mV(SCE)

(28) $TiH + H_2O \rightarrow TiO + 3H^+ + 3e^-$ $E_{rev} = -851$ mV(SCE)

(29) $2TiH + 3H_2O \rightarrow Ti_2O_3 + 8H^+ + 8e^-$ $E_{rev} = -971$ mV(SCE)

Here the pH is again assumed to be -0.7 and the Ti^{3+} concentration is taken as 10^{-6} moles/liter. Since the dissolution reaction (equation 3) is quite inhibited as can be seen from the low anodic peak in Figure 11, it is quite likely that reactions 28 or 29 occur at least to some extent. The active corrosion potential, then, is probably composed of inhibited hydride dissolution (reaction 3) and hydrogen ion reduction (reaction 7).

It was mentioned above that this "active" corrosion potential is a quasi-steady state value. If a specimen is left in the acid for a long time E_{corr} slowly shifts in the noble direction. After 7 hours it reaches a value of -570 mV(SCE) and appears to be steady. This shift would normally be considered to be due to an increase in the kinetics of the hydrogen reduction reaction but it could also be due to a decrease in the kinetics of the anodic reaction. The latter is quite possible since the corrosion rates of titanium have been observed to decrease with exposure time by other workers.[7]

If an "active" specimen is held at -850 mV(SCE) for 6 hours, then the current is switched off, the same corrosion potential is obtained (-570 mV). However in this case the potential then shifts back in the active direction slightly reaching a value of -600 mV in about one-half hour.

Long exposures also cause a change in the appearance of a specimen. It loses its shiny appearance and becomes a dull gray color.

b. Cathodic Region

A more important potential range than the anodic region, from the standpoint of stress corrosion, is the range of potentials below the corrosion potential. In this region corrosion processes are still occurring but they are overshadowed by large cathodic currents. Figure 15 shows a cathodic polarization curve for the Ti-8-1-1 wire in deaerated 5N HCl. The potentials were scanned starting at the corrosion potential at a rate of 600 mV/hr. The most striking feature about the figure is the extremely large current which flows compared to that in the anodic regions. Current densities of well over 100,000 $\mu A/cm^2$ are typical at very negative potentials. The mid portion of the curve is linear through almost three orders of magnitude of current. The slope in this region (Tafel slope) was measured to be 0.1 volts per decade of current.

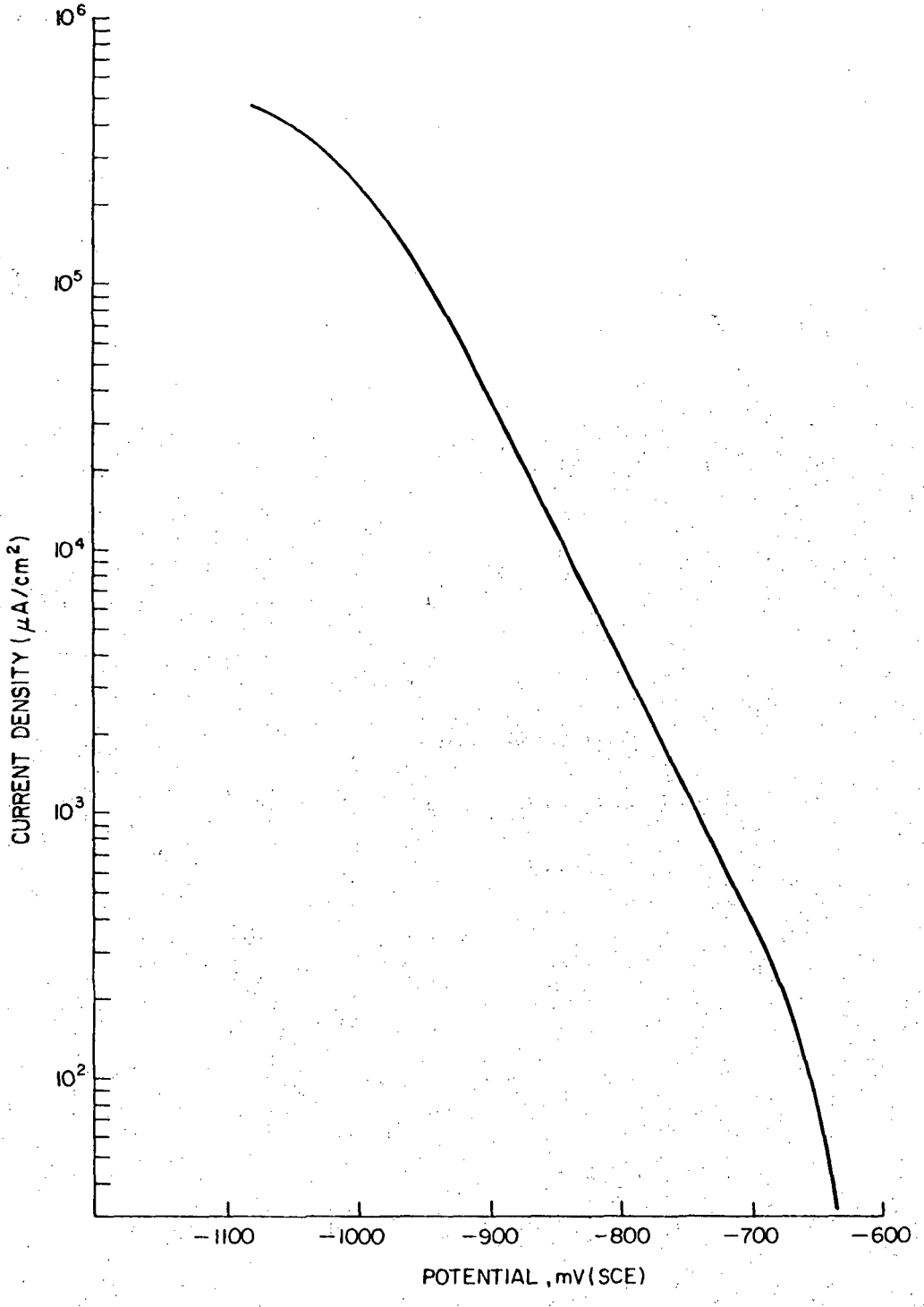

Figure 15 - Cathodic Polarization Curve at a Scan Rate of 600 mV/hr

The consequences of having Tafel behavior are quite significant. The net current that is measured on the polarization curve is the algebraic sum of the currents from all the anodic and cathodic reactions that are occurring on the surface. Each reaction current is represented by an equation of the form

$$(30) \quad i = A\, e^{B\eta}$$

where A and B are constants and η is the overpotential which equals the potential difference between the applied potential and the reversible potential for the given reaction. (See the Appendix for details about the terms in this equation.) The measured current then, is the sum of a number of exponential terms. A plot of the log of this net current versus potential can be straight only if there is but one term involved. This means that one reaction is occurring at a rate much faster than all the others and that the measured current is essentially due only to it. In a deaerated solution hydrogen ion reduction and hydride formation and growth are the only cathodic reactions that would be expected on "active" titanium over the range of potentials where the plot is linear (see Table 1). The growth of a hydride involves diffusion processes and would be much slower than proton reduction. Further, the fact that the measured current is accompanied by the copious evolution of bubbles on the surface leaves little doubt that the polarization curve represents, singlely, the hydorgen reduction reaction.

At very negative potentials the polarization curve deviates from linearity. This is due to the reaction rate becoming limited by transport processes. In other words, the slow step in the process has become the transport of the protons to the surface.

The fact that the measured current on the polarization curve is only due to the hydrogen reaction does not mean that other reactions are not occurring. It only means their rates are small compared to that of proton reduction. For example, at -1000 mV(SCE) the rate of the hydrogen reaction is 225,000 $\mu A/cm^2$ (Figure 15). At this potential an anodic dissolution rate of say 1000 $\mu A/cm^2$ would not even be noticed and yet that rate is very large relative to the anodic polarization curves. Another point that should be mentioned is that chemical reactions could be occuring on the wire surface. Since they do not affect the measured current their rates cannot be monitored directly.

Figure 16 is another cathodic polarization curve. This curve was measured at the same scan rate as Figure 15 with air bubbling through the solution. The Tafel slope here is again 0.1 volt which indicates that the current from the oxygen reduction reaction is small relative to that of hydrogen ion reduction.

The curves in Figure 17 were run at a scan rate of 1500 mV/hr in a deaerated solution. The Tafel slopes are again the same within experimental error. This is not surprising since changes in the scan rate would not be expected to affect an activation controlled electrochemical

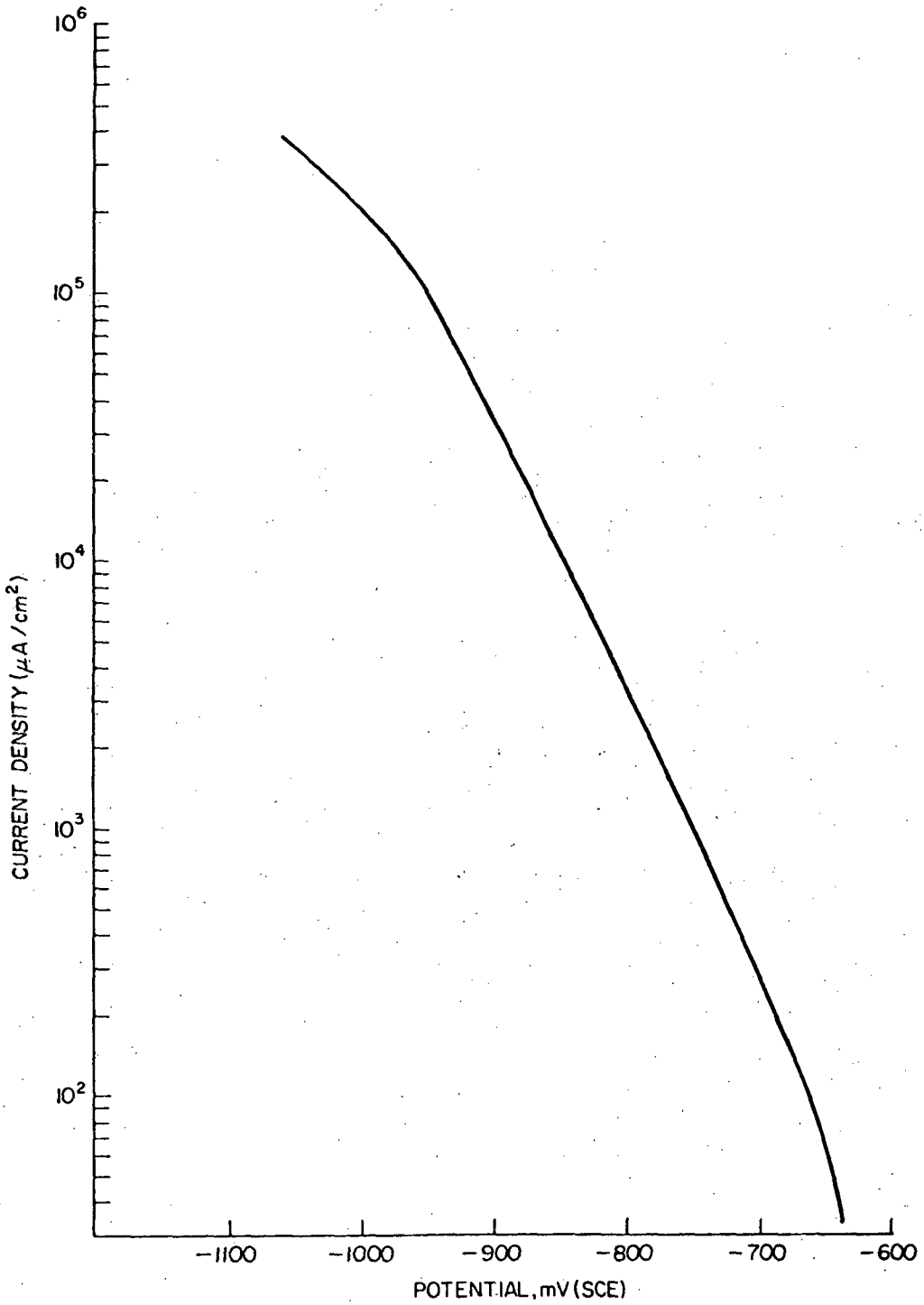

Figure 16 - Cathodic Polarization Curve at a Scan Rate of 600 mV/hr with an Aerated Solution

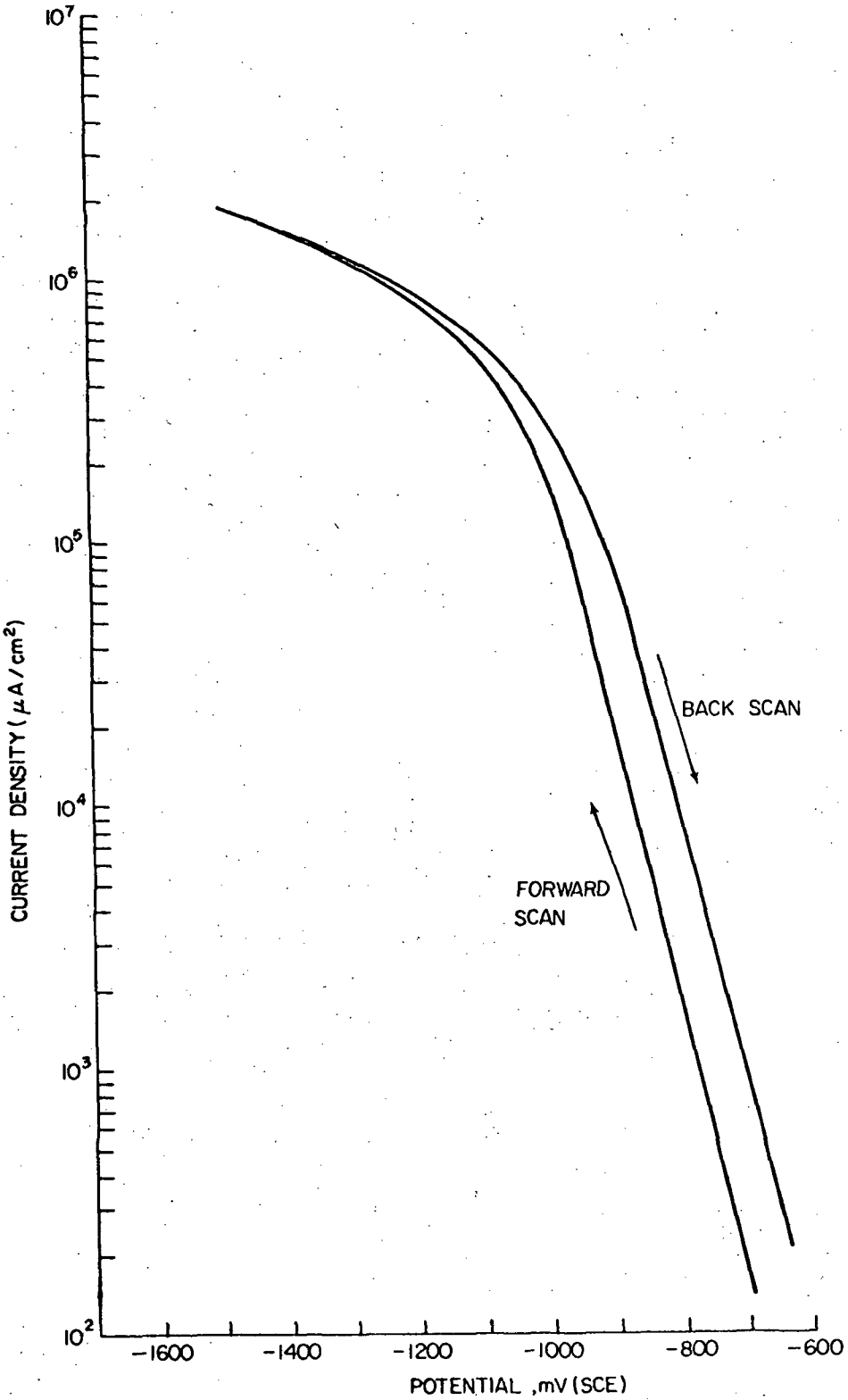

Figure 17 - Cathodic Polarization Curve at a Scan Rate of 1500 mV/hr Showing the Hystereses During a Back Scan.

process. The difference in behavior on the back scan is very noteworthy. It can be seen that at a given potential the current on the back scan is significantly higher than the current on the forward scan. This indicates that the metal surface has changed in such a way that the hydrogen reaction can occur much faster. This effect has been observed by other workers[37,40] and has been attributed to the formation of a surface hydride. Extrapolation of the Tafel portion of the curves back to the reversible potential for hydrogen ion reduction (-201 mV in 5N HCl) will yield a value of the exchange current for the reaction. The values from this extrapolation for the curves on Figure 17 are

$$(31)\quad i_{o_{H_2}\ \text{forward}} = 4 \times 10^{-3}\ \mu A/cm^2$$

$$(32)\quad i_{o_{H_2}\ \text{back}} = 35 \times 10^{-3}\ \mu A/cm^2$$

The reaction rates are 9 times faster on the back scan. This type of increase has been taken to imply that the rate of proton reduction is intrinsically faster on a hydride surface. In other words, that the mechanism is different on the hydride. But the effect could also be due to an increase in reaction area due to a roughening of the surface from the absorption of hydrogen and from dissolution. Experimental evidence indicates that the latter reason must be at least partially responsible for the increase. The important facts are: (1) Hydrides would be expected to form quite rapidly in the strong acid, especially with the application of cathodic polarization. As discussed in Chapter I a thin hydride layer, say 20 Å thick, would require less than a second to form at a cathodic current density of 5000 $\mu A/cm^2$. Therefore a surface hydride is most certainly formed before the forward scan is complete. If the reaction mechanism changes when it forms then the Tafel slope should change. No such change is observed on Figure 17. In fact, the Tafel slope is still the same on the back scan. (2) The visual observation of the surface after the test of Figure 17 shows that the surface has a dull, grey appearance and looks much rougher. Thus the increase in current could be explained by a roughening of the surface of a hydride which is already present at the beginning of the test.

The appearance of a surface layer which causes a change in the reaction mechanism is illustrated in Figure 18. This experiment was run using a platinum counter electrode. Platinum will dissolve in concentrated hydrochloric acid if a high positive potential is applied to it. In the experiment, when the potential of the titanium wire reached about -850 mV(SCE) the potential of the platinum electrode was pushed up to its dissolution value. The platinum ions which formed were then rapidly plated out on the titanium due to the negative potential there. Hydrogen reduction on a platinum surface occurs by a different mechanism and is much faster than on titanium. This accounts for the change in slope and the sharp increase in current.

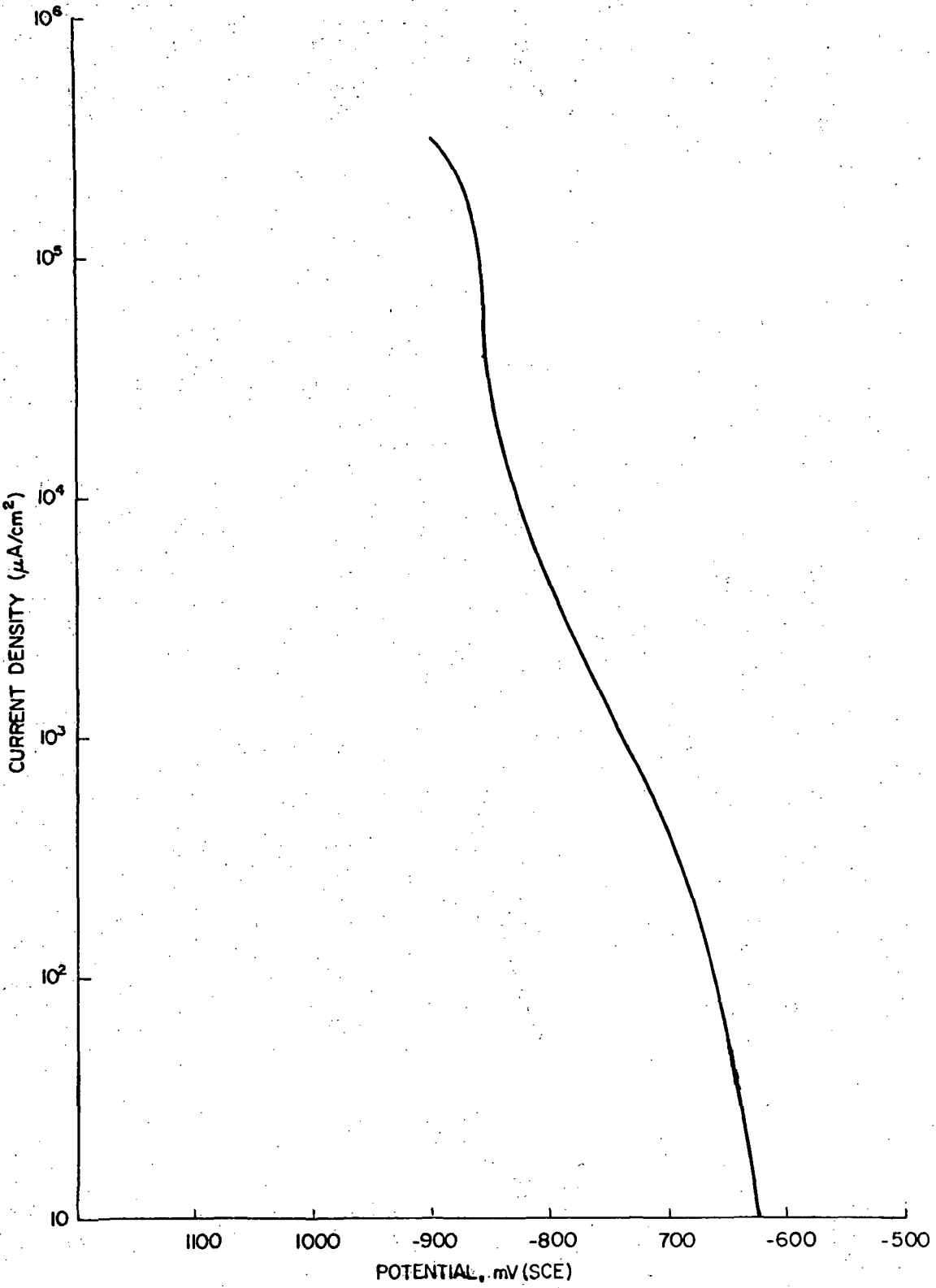

Figure 18 - Cathodic Polarization Curve Using a Platinum Counter Electrode

2. Cathodic Embrittlement

When Ti-8-1-1 wires are exposed to 5N HCl solutions at potentials from the corrosion potential downward (active direction) their surface appearance changes.

The surface of the wires becomes darker as the exposure time increases. After a long exposure under open circuit conditions (2 days) agitation of the immersed wire results in the loosening of a black powdery substance from the surface. Specimens removed from the solution and stored in air appear to retain their darkened surface appearance indefinitely. The time required for the metal surface to darken is a function of potential. The more negative the applied potential the faster the surface darkens.

Concurrently with the darkening of the metal surface embrittlement of the wires occurs. Since the exposure of the wire specimens to the 5N HCl solution was conducted in the straining cell connected to the Instron machine, static tests could be interrupted at any time by dynamic straining without any change in electrochemical conditions. A common procedure then, was to expose a specimen at a particular potential for a specified length of time, then strain, keeping the potential constant. Evidence of embrittlement was a flat fracture surface (easily distinguished from the normal ductile tearing type fractures which are accompanied by necking), low ductility as measured by per cent elongation, and the presence of cracks on the wire surface.

As the applied potential was moved in the active direction a striking decrease in the exposure time necessary to embrittle was observed. A 30 minute exposure at -1500 mV(SCE) produced a more embrittled condition (the wire surface was covered with cracks and the specimen broke before it reached the yield) than a 6 hour exposure at -850 mV(SCE) (only a few surface cracks were observed and the elongation was 2%). Tests run under open circuit conditions and at -740 mV(SCE), and -1000 mV(SCE) confirmed this trend. Visible hydrogen evolution from the wire surface occurred at all applied potentials. (No visible hydrogen bubbles were seen under open circuit conditions.) The rate of hydrogen bubbling increased as the applied potential was made more active. This was accompanied by an increase in the cathodic current. The most logical explanation of the phenomenon is that part of the hydrogen produced by the reduction of protons entered the lattice and embrittled the wire. It could be argued, however, that the embrittlement was the result of an anodic dissolution process which occurred during exposure. Anodic reactions are certainly possible at the potentials of interest and are likely occurring. An experiment was run in the present investigation, however, which, it is believed, leaves no doubt that the embrittlement is due to hydrogen. In this experiment two identical wires were exposed to 5N HCl, under open circuit conditions, for 3 days. The wires were then removed from the solutions. The surface of both specimens was darkened as described above. One of the specimens was then bent manually

and found to break in a brittle fashion with very little ductility. The other specimen was placed in an envelop and left in the air at room temperature for 15 days. It was then bent in the same manner as the first specimen and found to have recovered nearly all of its initial ductility. The surface of the wire was still dark but the embrittlement had disappeared. It would appear virtually impossible for corrosion damage to reverse itself during aging in air whereas absorbed hydrogen could certainly diffuse out of the specimen.

A detailed look at the processes occurring during embrittlement may help in understanding the nature of the phenomenon, particularly the role of cathodic overvoltage in increasing the rate of embrittlement.

When a cathodic potential, say -850 mV(SCE) is applied to the titanium wire in 5N HCl solutions, three events are known to occur. They are the absorption of hydrogen into the metal, hydrogen evolution on the metal surface, and hydride formation on the metal surface. The latter reaction should occur quite rapidly and therefore the other reactions can be assumed to be occurring on a hydride surface. As discussed in Chapter I, the mechanism of the hydrogen evolution reaction should be the same on a hydride surface as on the base metal. Therefore the evolution reaction should consist of the following steps (see Chapter I, section 8):

$$(8)\quad Ti + H^+ + e^- \leftrightharpoons Ti\text{-}H_{ads} \quad \text{(discharge)}$$

$$(9)\quad Ti\text{-}H_{ads} + H^+ + e^- \rightleftarrows Ti + H_2\uparrow \quad \text{(desorption)}$$

with the desorption reaction being rate controlling.

The sequence of events for hydrogen embrittlement are as follows:

$$(8)\quad Ti + H^+ + e^- \leftrightharpoons Ti\text{-}H_{ads}$$

$$(33)\quad Ti\text{-}H_{ads} \rightleftarrows Ti\text{-}H_{abs}$$

$$(34)\quad (H_{abs})_{surface} \rightleftarrows (H_{abs})_{interior}$$

The discharge reaction again occurs first. The adsorbed hydrogen is then absorbed into the metal (reaction 33) and diffused into the lattice (reaction 34).

Considering the two sequences, gas evolution, and embrittlement together, it is clear that the relative rates of reactions 9 and 33 are critical. If embrittlement is to occur then the adsorbed hydrogen must be absorbed before it is reacted with a proton to evolve gas. Reaction 34 is not critical for static electrodes because it can be safely assumed that once hydrogen is absorbed into the metal it will diffuse into the lattice. However the rate that it diffuses, which is controlled by the

concentration gradient and thus by reaction 33, is critical in determining the role of hydrogen in the propagation of a stress corrosion crack.

Reactions 8 and 9 are electrochemical and their rates can be described by a general kinetic expression. To simplify the discussion a net cathodic current is taken as positive

$$(35) \quad i_{net} = i_c - i_a = \vec{i} - \overleftarrow{i}$$

For the discharge reaction (reaction 8)

$$i_8 = \vec{i}_8 - \overleftarrow{i}_8$$

$$(36) \quad i_8 = (1-\theta)\, C_{H^+}\, \vec{k}_8\, e^{-\beta F\eta_8/RT} - (\theta)\, \overleftarrow{k}_8\, e^{(1-\beta)F\eta_8/RT}$$

where θ = fraction of surface covered by adsorbed hydrogen

C_{H^+} = concentration of protons in solution near the metal interface, moles/cm^2

η = overpotential, i.e. departure of the applied potential from equilibrium, volts

$\vec{k}_8$ = the electrochemical rate constant for reaction 8 in the forward (cathodic) direction.

(See the Appendix for a more complete description of the terms in the equation.) Similarly for the desorption reaction (reaction 9)

$$i_9 = \vec{i}_9 - \overleftarrow{i}_9$$

$$(37) \quad i_9 = \theta\, C_{H^+}\, k_9\, e^{-\beta F\eta_9/RT} - (1-\theta)\, P_{H_2}\, \overleftarrow{k}_9\, e^{(1-\beta)F\eta_9/RT}$$

The composite hydrogen evolution reaction i.e., $2H^+ + 2e^- \rightleftarrows H_2$ is in equilibrium at a certain reversible electrode potential $E_{rev}^{H_2}$. But at equilibrium the rate of reaction 8 in the forward direction must equal the rate of reaction 9 in the forward direction since they are consecutive reactions and must go at equal rates under any steady state condition. Therefore the respective rates in the back direction must also be equal because the total forward rate must equal the total back rate. Hence both reaction 8 and reaction 9 are in equilibrium at the reversible electrode potential $E_{rev}^{H_2}$. For a 5N HCl solution of pH = -0.7, $E_{rev}^{H_2}$ = -200 mV(SCE). The overpotential can be expressed by the following equation:

$$(38) \quad \eta = E - E_{rev}^{H_2}$$

where E = the applied electrode potential. So at -850 mV(SCE), $\eta_8 = \eta_9 = -650$ mV.

The total current that is measured at any applied potential is the sum of the individual currents for the separate reactions. Here, the total current is

$$(39) \quad i_T = (\vec{i}_8 + \vec{i}_9) - (\overleftarrow{i}_8 + \overleftarrow{i}_9)$$

where the individual currents are given by equations 36 and 37. But if $\eta = -650$ mV is put into the equations it becomes obvious that the rates of the back reactions are negligible compared to the rates of the forward reactions. Hence

$$i_T = \vec{i}_8 + \vec{i}_9$$

$$(40) \quad i_T = (1-\theta)\ C_{H^+}\ \vec{k}_8\ e^{-\beta F \eta_8/RT} + \theta\ C_{H^+}\ \vec{k}_9\ e^{-\beta F \eta_8/RT}$$

Now, as time passes from the initial application of the potential, say -850 mV for example, each reaction (discharge and desorption) will go at its own rate. However, since the reactions are consecutive they must depend on each other. For example, if the discharge reaction proceeds more rapidly than the desorption reaction, a condition will soon be reached where all the adsorption sites are full. Then the rate of reaction 8 must slow down to await more sites. This in fact is the condition which exists on Ti as mentioned previously. Therefore a steady state condition should be reached where $i_8 = i_9$. This steady state should result in a large θ and thus a rapid embrittlement rate by reaction 33.

Writing out the terms for the steady state condition produces a very interesting result.

$$i_8 = i_9$$

$$(1-\theta)\ C_{H^+}\ \vec{k}_8 \exp \frac{-\beta F \eta_8}{RT} = \theta\ C_{H^+}\ \vec{k}_9 \exp \frac{-\beta F \eta_8}{RT}$$

rearranging

$$(41) \quad \frac{\theta}{1-\theta} = \frac{\vec{k}_1}{\vec{k}_2}$$

The ratio of the covered surface to the uncovered surface is a constant and not a function of overpotential. An increase in overpotential would increase the rates of both discharge and desorption and thus the rate of hydrogen evolution but it would not change the concentration of hydrogen on the surface and thus would not change the diffusion rate of hydrogen.

This result is very important because it indicates that the large increase in the rate of embrittlement with overpotential cannot be accounted for by a change in the amount of adsorbed hydrogen.

For simplicity, the above analysis was carried out assuming Langmuir type adsorption. This adsorption model assumes that there is no interaction between adsorbed species. A more rigorous model is the Temkin adsorption isotherm which considers interaction between adsorbed particles. Substitution of this isotherm in the above development results in a slightly more complicated equation for the fractional coverage (equation 41) but does not introduce an overpotential dependence.

The most logical explanation of the overpotential dependence of the embrittlement is that it is related to changes in the surface oxide. As was indicated previously there is strong evidence that oxides are present on titanium even during "active" dissolution. The presence of an oxide film would lower the hydrogen evolution rate because of the low electronic conductivity of the oxide. It would also act as a diffusion barrier for the nascent hydrogen and thus lower the rate of embrittlement. In 5N HCl the passive oxide, $Ti_2O_3 \cdot 3\text{-}4\ TiO_2$, is not stable at the potentials where embrittlement occurs. The oxide present at these potentials would be a lower oxide, likely TiO or Ti_2O_3. The thickness of the oxide would vary with the applied potential, becoming thinner as the potential is made more negative until finally it is reduced completely. These oxides (Ti_2O_3 and TiO) are not reduced to titanium metal until a potential of about -1500 mV(SCE) is reached. However, they are reduced to the hydride (TiH) at much more noble potentials, -892 mV(SCE) for TiO and -1012 mV(SCE) for Ti_2O_3 (see Table 1).

The effect of oxide films in reducing the hydrogen evolution rate and slowing down the embrittlement was demonstrated very graphically in another experiment. In this test one specimen was switched to a potential of -850 mV(SCE) directly from the active corrosion potential (-680 mV) and held for 6 hours. Another specimen was first polarized at +500 mV(SCE) for 2 hours to form a thick passive film. Then it was switched directly to -850 mV from the passive potential and held for 6 hours. The cathodic current flowing to each specimen while at -850 mV is plotted in Figure 19. The specimen without the passive oxide supports a much higher hydrogen evolution current. Also the rate of bubble formation on the surface was different enough to be visably lower on the passivated specimen. After the 6 hour period each specimen was strained to failure while still at -850 mV at a strain rate of 10%/min. The unpassivated specimen was embrittled; it had numerous surface cracks and only 2% elongation. The passivated specimen was not embrittled; it had an elongation of 8.2% and no surface cracks.

These results clearly demonstrate the effectiveness of the passive oxide in reducing the rate of hydrogen embrittlement. However they pose another question. Why didn't the oxide dissolve during the long 6 hour exposure at -850 mV(SCE)? If a specimen is left at open circuit in the

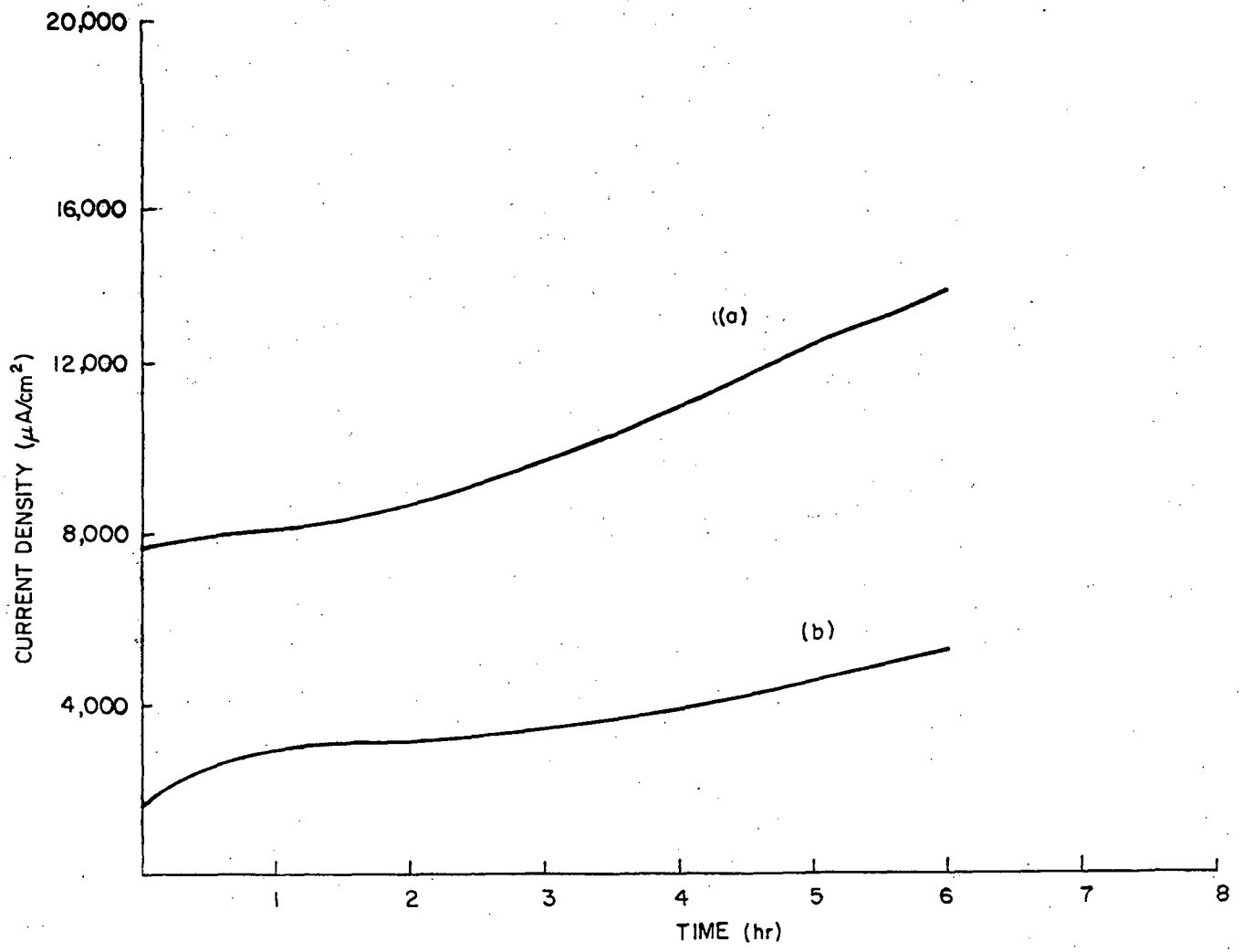

Figure 19 - Current versus Time Behavior for Specimens held at -850 mV(SCE): (a) Specimen Switched to -850 mV Directly from the Active Corrosion Potential; (b) Specimen Switched to -850 mV following a 2-hour Polarization at +500 mV(SCE).

5N HCl after a 2 hour polarization at +500 mV the passive film will dissolve naturally in less than one hour. Since the films are formed electrochemically, an applied potential of -850 mV would be expected to hasten the process. To help clarify the situation SEM pictures of the surface of the two wires which produced the behavior of Figure 19 were taken. Figure 20 shows the embrittled wire and Figure 21 the passivated one. The surface appearance of the two wires is clearly quite similar. Since a hydride is certainly present on the surface of the embrittled wire, this suggests that a hydride formed on top of the oxide and protected it from dissolving. The reaction of an oxide directly to a hydride is not unreasonable and could occur at -850 mV(SCE) (see Table 1, reactions s - z).

When a specimen with an air-formed film was put at -850 mV directly from its passive corrosion potential (-100 mV(SCE)) no passivating effect was found and the specimen supported a large cathodic current similar to the top curve of Figure 19. This could be because the air-formed film was thinner than the solution-formed film and dissolved too quickly. Air-formed films have been found to be quite thin (Chapter I, section 4). Or this could be verification of the observation by other workers (Table 2) that the air-formed film is not the same as the solution-formed film.

Figure 22 shows a SEM picture of the fracture surface of the unpassivated specimen which produced the upper curve of Figure 19. Two different fracture modes are in evidence. Around the outer edge of the wire the fracture is very flat corresponding to a brittle fracture mode while in the center the fracture shows ductile characteristics. A fairly clean demarcation line can be seen between these two regions. The distance from the outer edge of the specimen to the point where the fracture becomes ductile is thus an effective embrittlement distance. It represents the distance over which the hydrogen was able to embrittle during the 6 hour test. By knowing the actual diameter of the wire and measuring the distances across the picture the embrittlement distance, x, was found to be 6.98×10^{-3}cm. Using the equation $x^2 = 2Dt$ to give a rough calculation of what the effective diffusion distance should be, it was discovered that if hydrogen diffused only in the alpha phase ($D = 2 \times 10^{-11}$)[153] it should not have penetrated nearly so far. In fact the distance from alpha diffusion was almost 2 orders of magnitude too low. This calculation gives only a very rough estimate of the penetration distance because it does not take into account the concentration gradient which actually determines the diffusion rate. However it does indicate that the hydrogen was embrittling to a much greater distance than would be expected.

To check this effect, a more detailed calculation was made using the solution of Ficks Second Law for a semi-infinite circular cylinder. A graphical solution of the diffusion equation can be found in Crank[154] assuming diffusion in the radial direction only. The boundary conditions for the solution are a constant surface concentration and an initially uniform internal concentration. In making this calculation the

Figure 20 - Scanning Electron Micrograph of the Surface Appearance of the Unpassivated Wire which Produced the Upper Curve of Figure 19; Strained at 10%/min. 2000X

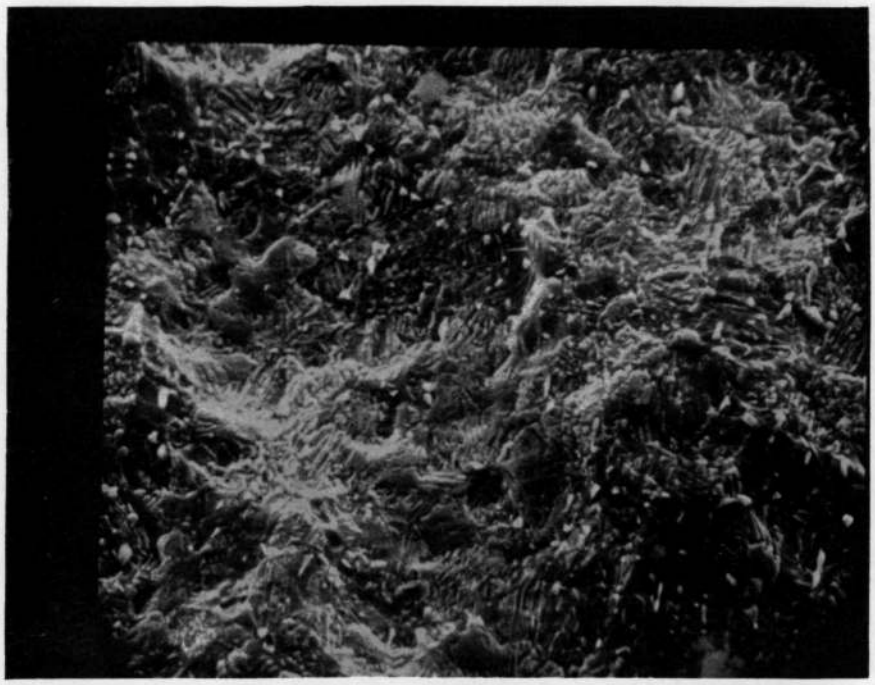

Figure 21 - Scanning Electron Micrograph of the Surface Appearance of the Passivated Wire which Produced the Lower Curve of Figure 19; Strained at 10%/min. 2000X

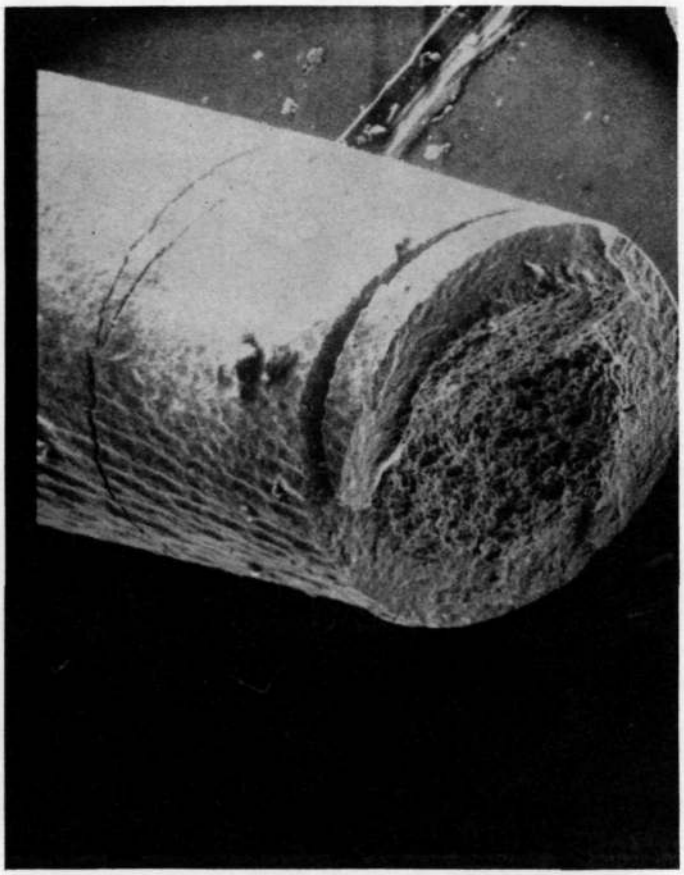

Figure 22 - Scanning Electron Micrograph of Fracture Surface of the Unpassivated Wire which produced the Upper Curve of Figure 19; Strained at 10%/min. 100X

concentration gradient was maximized so that the penetration distance would represent the largest possible diffusion distance. The conditions imposed were as follows: (1) The initial concentration of hydrogen was given in the wire specifications as 8 ppm or 3.61×10^{-5} moles/cm^3. (2) The surface concentration was taken as the largest possible hydrogen concentration. This would be when all the tetrahedral holes are filled with hydrogen, and corresponds to the composition of the highest hydride, TiH_2. The value is 0.188 moles/cm^3. (3) The final internal concentration at the point where the fracture mode changed was taken as 200 ppm or 9.02×10^{-4} moles/cm^3. This value was given by Boyd[137] as a minimum amount of hydrogen needed to embrittle the metal via precipitation of hydrides. The penetration distance corresponding to these boundary values was determined from the graphical solution of Ficks Second Law (see Crank[154]) using the dimensionless parameter Dt/a^2 where D is the diffusivity, 2×10^{-11}cm^2/sec; t is the diffusion time, 6 hours; and a is the radius of the wire, 2.51×10^{-2}cm. Using these values the penetration distance was definitely found to be less than the measured distance of embrittlement. This calculation leaves no doubt that the distance over which brittle fracture occurred cannot be accounted for by diffusion of hydrogen only in the alpha phase.

This conclusion is emphasized by the fact that the concentration gradient was maximized. A surface concentration of 0.188 mole/cm^3 would be about 50,000 ppm - a tremendous concentration. Further, the minimum concentration for embrittlement of 200 ppm was obtained for strain induced precipitation of hydrides at low strain rates.[137] Since the wires were strained at a fairly rapid strain rate (10%/min), this concentration should undoubtedly be higher.

There are three possible explanations for the large embrittled distance. One is that the hydrogen diffused in part through the regions of beta phase and along the grain boundaries. Since the grain size in the Ti-8-1-1 wires was so small (see Figure 6) this could significantly increase the penetration distance. Another is that the hydrogen induced brittle fracture near the surface, and the cleavage cracks, thus produced, then propagated further into the metal. Finally, it is possible that the value for the diffusivity is in error. The experiments to determine diffusivity, described in a paper by Wasilewski and Kehl,[153] were run between 500 and 824°C. The extrapolation to room temperature could introduce an error. Also, a careful reading of their paper shows a lack of agreement between their experimental points and a theoretical curve at high hydrogen concentrations. The authors[153] were aware of this discrepancy and pointed out that the diffusivity could increase markedly at high solute concentrations, above 5 at.% (1100 ppm).

3. Straining Response

Since the tip of a propagating stress corrosion crack is in a state of dynamic yielding, the straining electrode experiments were undertaken to simulate this condition. Experiments of this nature have been conducted to study the cracking of Fe-Cr-Ni alloys[130,167,168] but very

little information is available for titanium alloys - none in aqueous solutions. The purpose of the experiments was to study the electrochemical changes which occur when a static, steady-state, situation is interrupted by dynamic straining, and to relate these changes to the surface films and ultimately to stress corrosion cracking.

Before the electrochemical response to straining is considered in detail a brief description of the mechanical behavior of the Ti-8-1-1 wires is pertinent.

a. Mechanical Behavior

Figure 23 shows the load elongation curve for Ti-8-1-1 wire specimens fractured in air at a strain rate of 10%/min. The curve exhibits a yield point followed by a very low rate of work hardening during plastic deformation. When specimens are strained in the solution the yield point is less pronounced as shown in Figure 24. Sharp yielding at a definite stress level should produce a large amount of dislocation activity in a very short period of time. Therefore, a large area of fresh surface should be abruptly produced at the yield. This effect produces a fluctuation in the current versus time curves as will be seen later. Straining in the solution reduces the amount of plastic elongation somewhat from 10-11% in the air to an average of 8-9% in the solution.

Increasing the strain rate to 100%/min raises the yield load slightly but does not alter the general shape of the load-elongation curves for either air or solution straining.

Figure 24 represents the mechanical behavior of specimens strained in the anodic potential range. In this range gross changes of the metal surface do not occur. However, as discussed previously, the surface undergoes pronounced changes when held at a cathodic potential. These changes result in a lower yield point. This is illustrated in Figure 25 which is for a specimen held at -1000 mV(SCE) for one-half hour.

In determining the electrochemical straining response the main experimental variables were strain rate and applied potential. The straining response was assessed by monitoring the current change, as a measure of the reaction rates, at constant applied potential and by monitoring changes in the corrosion potential under open circuit conditions. The general procedure was to switch to the potential of interest from the "active" corrosion potential and, if possible, allow a steady state condition to be reached. The specimen was then strained at a given strain rate until an elongation of four per cent, measured from the yield point, was obtained. Dynamic straining was then stopped and the current response was allowed to decay while the specimen was still loaded. After a time the load was released and further current changes were measured.

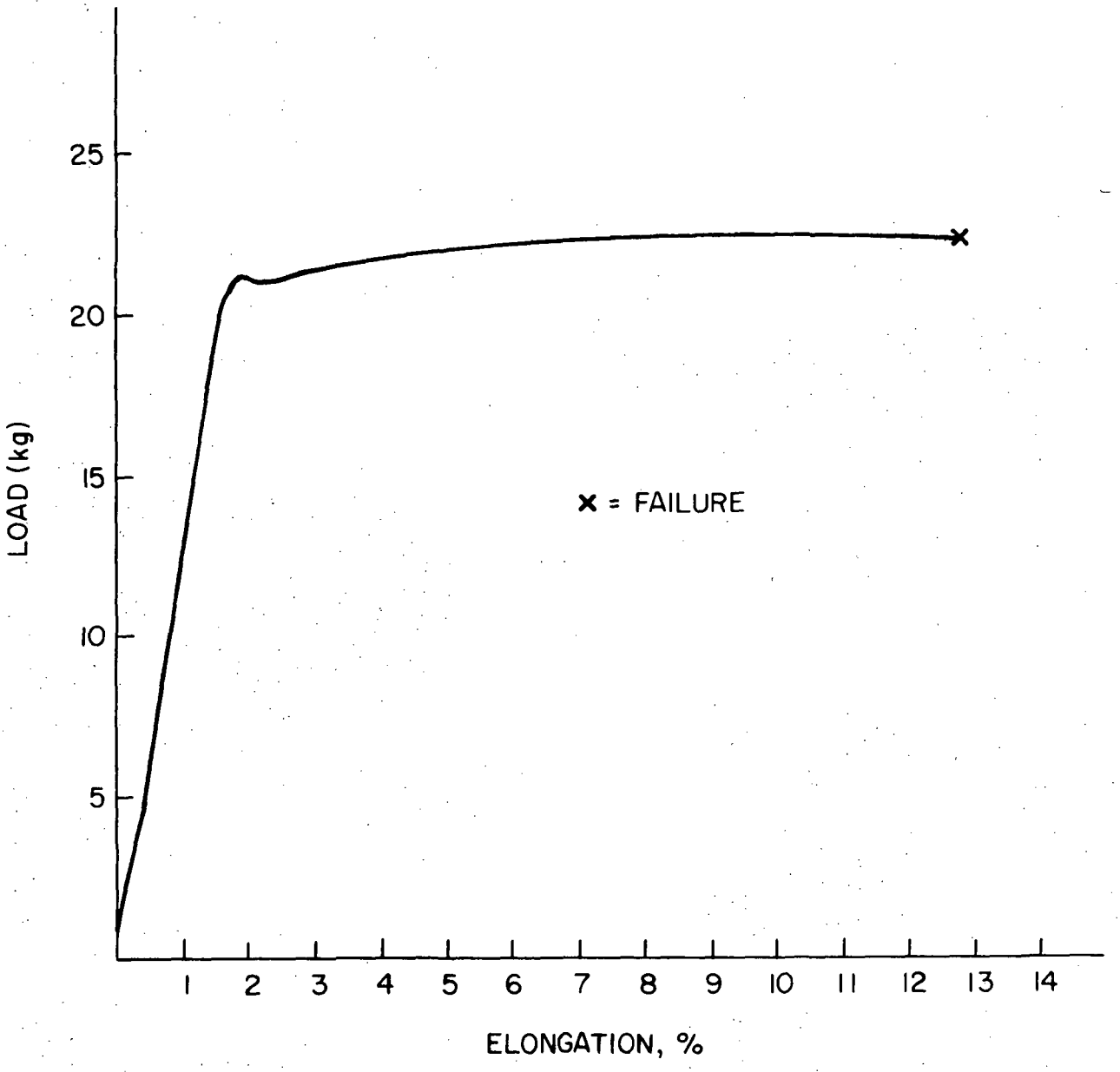

Figure 23 - Load versus Elongation Curve for a Specimen Fractured in Air at a Strain Rate of 10%/min.

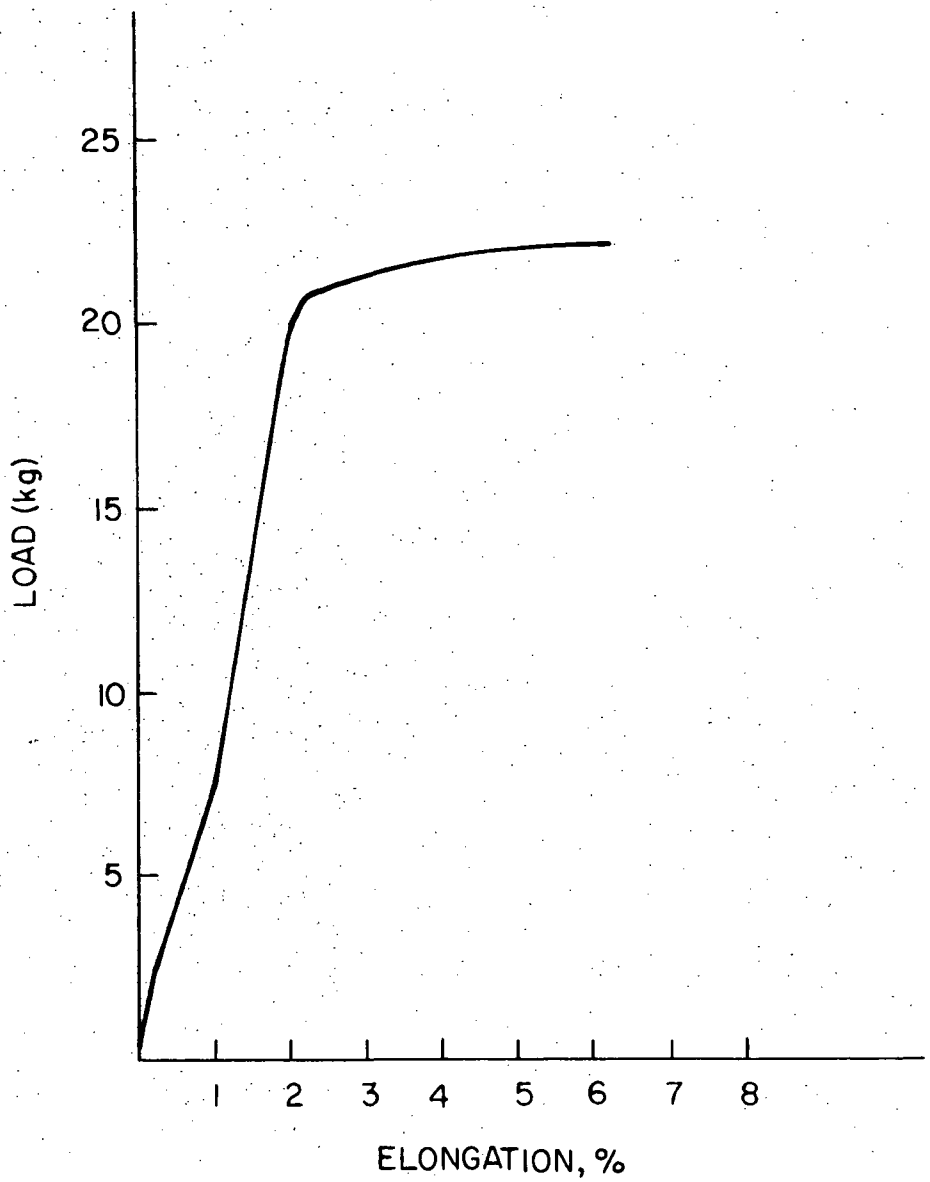

Figure 24 - Load versus Elongation Curve for a Specimen Fractured in Solution with an Applied Anodic Potential; Strained at 10%/min.

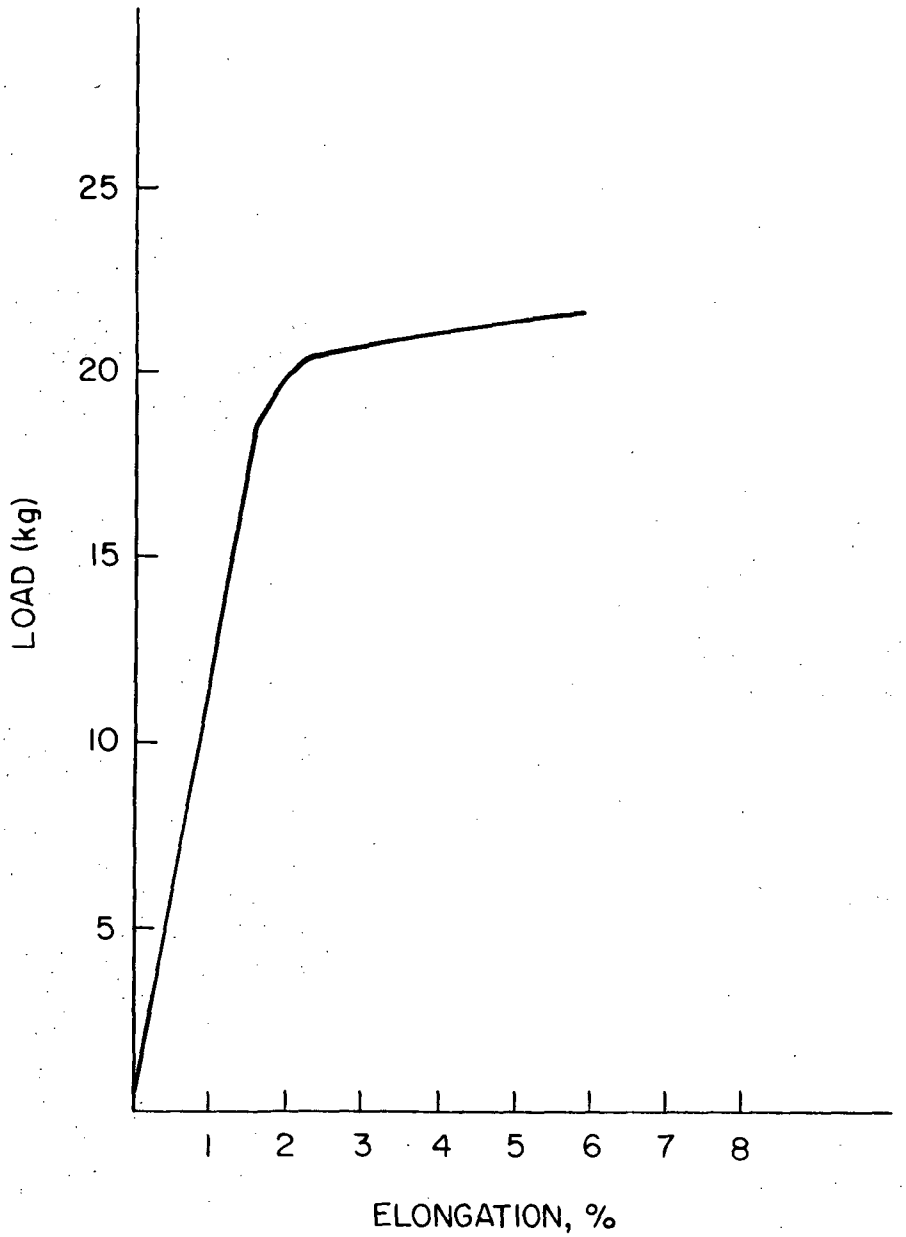

Figure 25 - Load versus Elongation Curve for a Specimen Held at -1000 mV(SCE) for One-Half Hour, Then Strained at 10%/Min.

b. Anodic Region

Initial experiments were run in the anodic region. This region is taken to include all potentials noble to the "active" corrosion potential. These results should be analyzed with reference to the anodic polarization curves (Figures 11-13).

Figure 26 shows the current response to straining at a potential of +200 mV(SCE). The specimen was held for two hours at the potential before straining. The strain rate was 10%/min. At +200 mV the metal is quite passive and the base current density before straining, i_s, is quite small (3.8 $\mu A/cm^2$). The straining starts at the axis and the Δ i values represent the change in current density, i.e., the observed current density minus the static base current density. The current begins to increase slightly before the yield and increases sharply at the yield. This figure was traced exactly from the experimentally recorded current versus time curve to show the serrated current behavior which is characteristic of the straining response in the anodic region. The decrease in current at the beginning of plastic flow is related to the initial yielding as discussed above. As such, it disappears if the specimen is unloaded and strained again.

As the straining continues the current increases again but tends to reach a saturation value and level out. The saturation of the current can be understood by considering the straining process to be composed of single slip events each of which produce a unit area of fresh surface. At a given strain rate the number of these slip events per unit time can be assumed to be constant. This situation was considered in detail by Murata[74] and is illustrated in Figure 27. As each unit area of fresh surface is exposed an anodic current spike of magnitude ΔI° occurs due to the increase in the dissolution rate. As time passes this unit area becomes passivated and the dissolution current decays. The total current is the sum of the currents from each of the slip events. As the figure shows each slip event adds to the total current until a situation is reached where the first unit area is completely passivated. From that point on a steady state exists and the current saturates at a value ΔI_m.

When the straining is stopped the current density decays smoothly and takes a relatively long time to reach steady state. This corresponds to the formation of the reasonably thick passive film which is stable at this potential.

Release of the load produces a discontinuous change in the current. This occurs in all the straining tests regardless of the potential. At potentials of -700 mV(SCE) and above the current discontinuity is in the anodic direction and is followed by a smooth decay curve. The discontinuity shown in Figure 26 is a typical example. At these potentials the perturbation is thought to be due to the rupture of portions of the newly formed film by putting it into compression when the specimen is unloaded. This hypothesis is supported by the fact that the discontinuity is larger when the load is released suddenly.

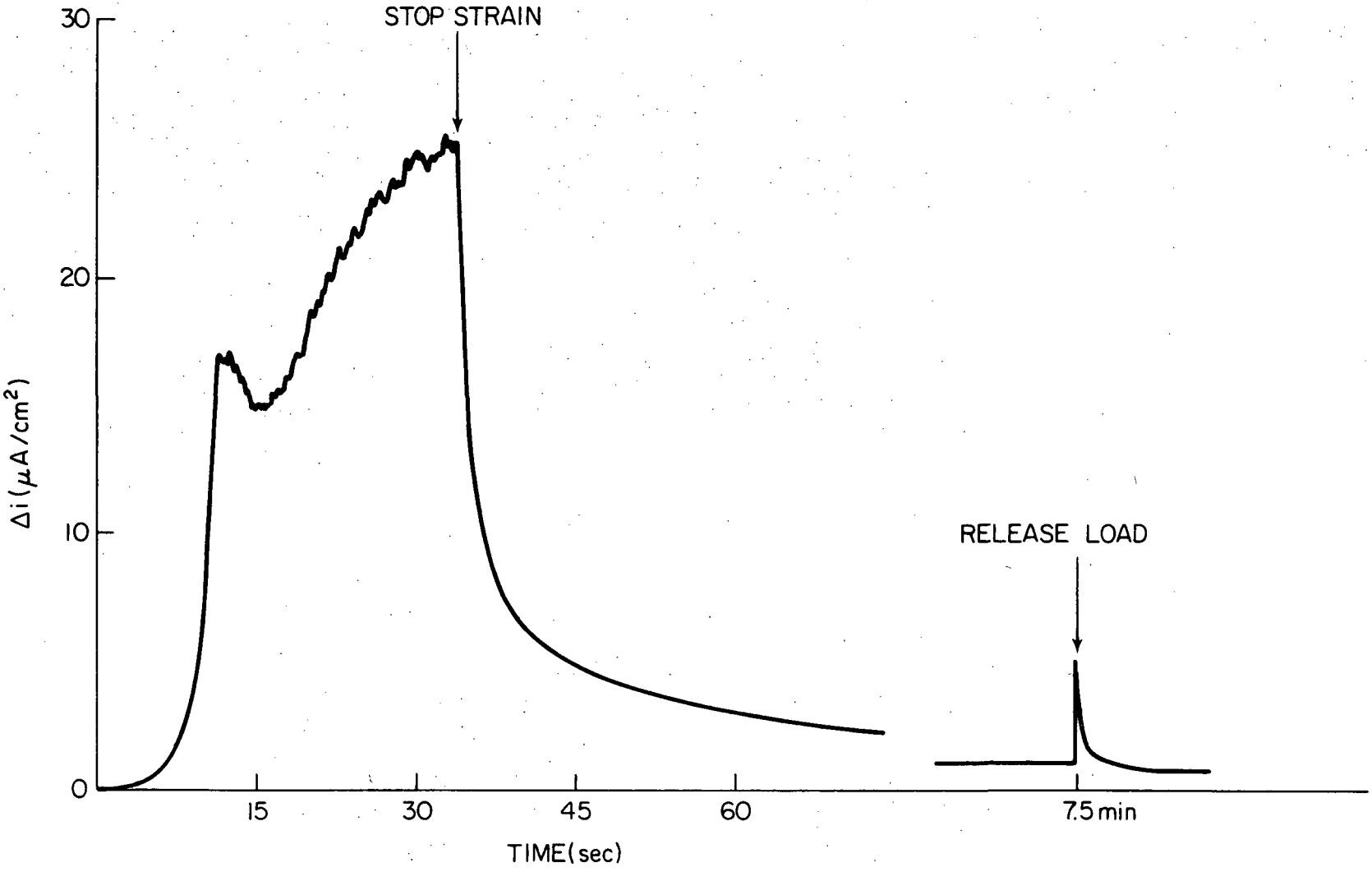

Figure 26 - Current Response to Straining at a Potential of +200 mV(SCE) at a Strain Rate of 10%/min; Base Current Density is 3.8 μA/cm²

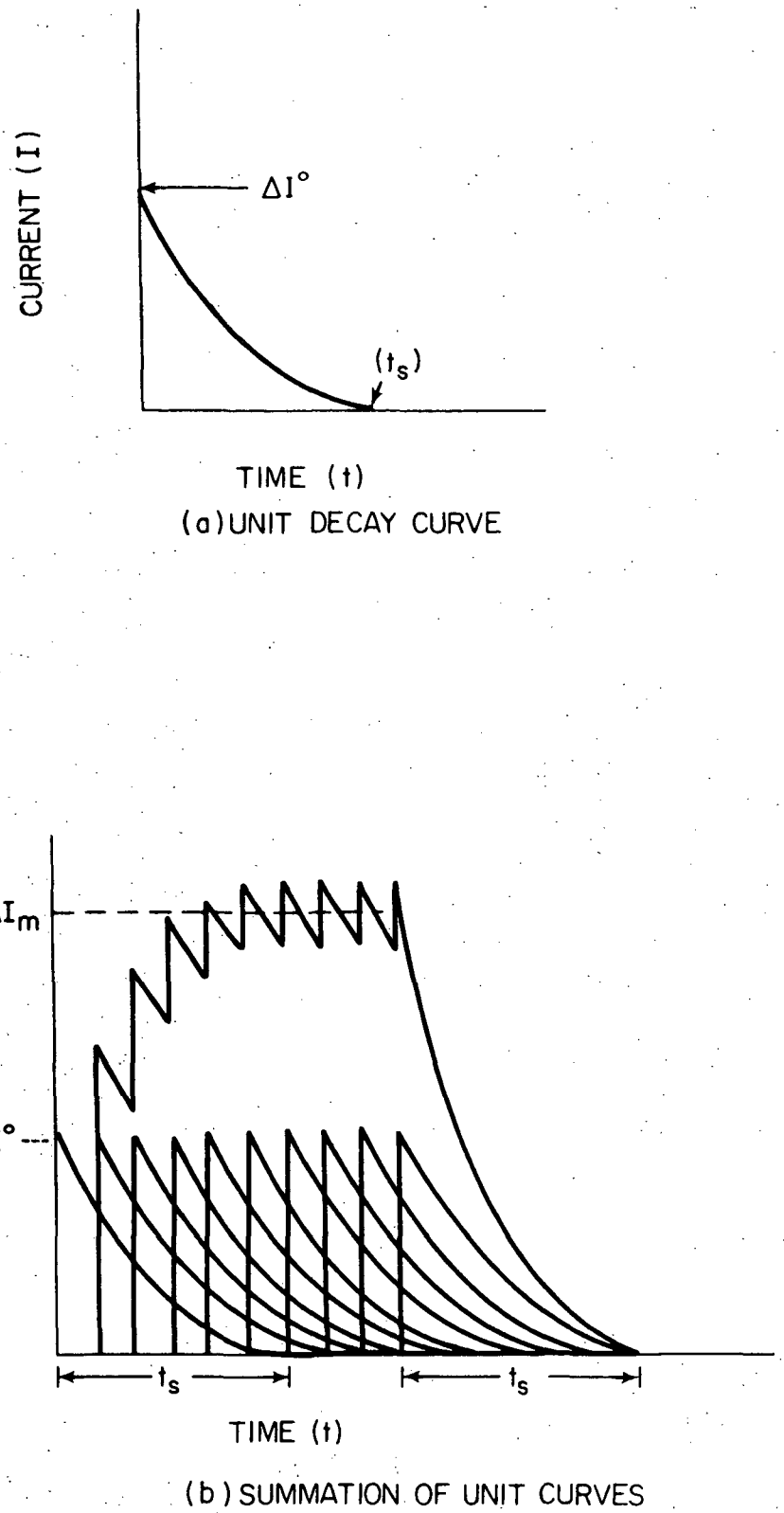

Figure 27 - Schematic Representation of the Change in Current during Straining: (a) Response of a Unit Area; (b) Summation of the Unit Responses. (Ref. 74)

Figures 28, 29, and 30 show the straining response at other potentials in the anodic region. These figures were plotted from the recorded data and thus do not show the serrated straining behavior although it is present in all three cases. Figure 28 shows the response to straining at a potential just at the start of the passive region, -200 mV(SCE). The final passive oxide is not present here and the base current density is larger, about 11 $\mu A/cm^2$. The general characteristics of the response during straining are quite similar to the +200 mV test with a slightly lower saturation current. However when the straining is stopped, the current decays more rapidly to a minimum value then increases again. The same tendency for the current to go through a minimum during repassivation occurs after the load is released (assuming that the film was ruptured again).

Straining tests were also run in the "active" region. Figure 29 shows the response at -470 mV(SCE) which is at the peak of the anodic polarization curve and Figure 30 shows the behavior at -600 mV(SCE) which is just above the "active" corrosion potential. As the figures show, the straining response is essentially the same as in the "active" region. A smooth decay occurs in both cases after straining is stopped. Release of load produces an anodic discontinuity followed by another smooth decay at both potentials. The same tendency for these decay curves to go through a minimum which was seen at -200 mV also occurs at -470 mV and -600 mV. At first glance it appears that in the active region especially at -470 mV the current does not decay back nearly so far when straining is stopped as is does in the passive region. This illusion occurs in the plotted graph because the base current is much larger in the active region than the passive region. For example the current density at the minimum of the decay curve in Figure 29 is about 11% above the base current while the current at the minimum of the decay curve in Figure 26 is about 25% higher than the base current.

The similarity of the straining curves in the "active" and passive regions is strong evidence that there is an oxide film on the surface of the titanium even in the "active" region. It could be argued, however, that the increase in current during straining is due only to an increase in the dissolution kinetics and that the decrease after straining is stopped is from the decay of this transient. But this effect, while it undoubtedly occurs especially at high strain rates, should die out very fast, in less than a second, and thus cannot account for the relatively slow decays which were observed.

The magnitude of the current response to straining in the active region was a marked function of strain rate. Figure 31 is a plot of the current increment versus strain for wires strained at +200 mV at different strain rates. (Due to the scale of the graph, the current relaxation which occurs at the yield cannot be shown for the smaller strain rates.) Even though the total plastic strain is the same in each case the current change is much larger at faster strain rates. This increase is related to the relative rates of passivation and of production of fresh surface.

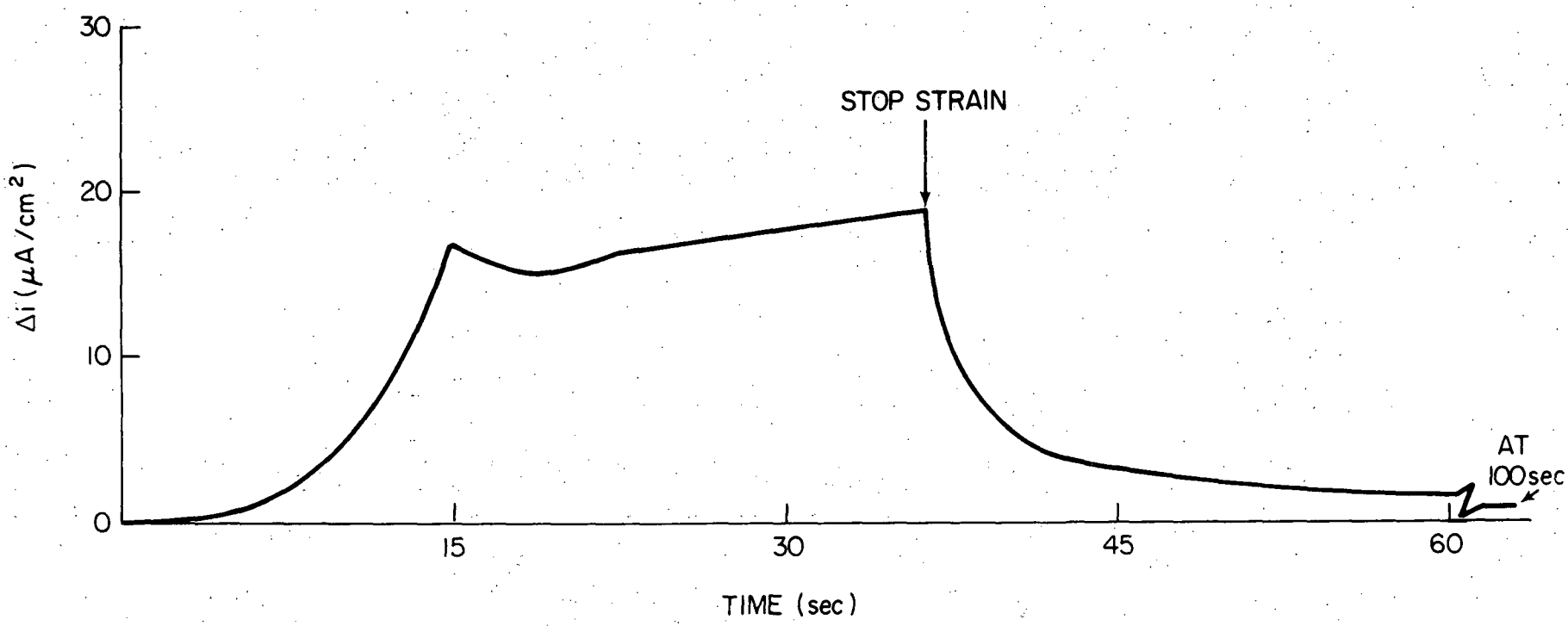

Figure 28 - Current Response to Straining at a Potential of -200 mV(SCE) at a Strain Rate of 10%/min; Base Current Density is 11 $\mu A/cm^2$

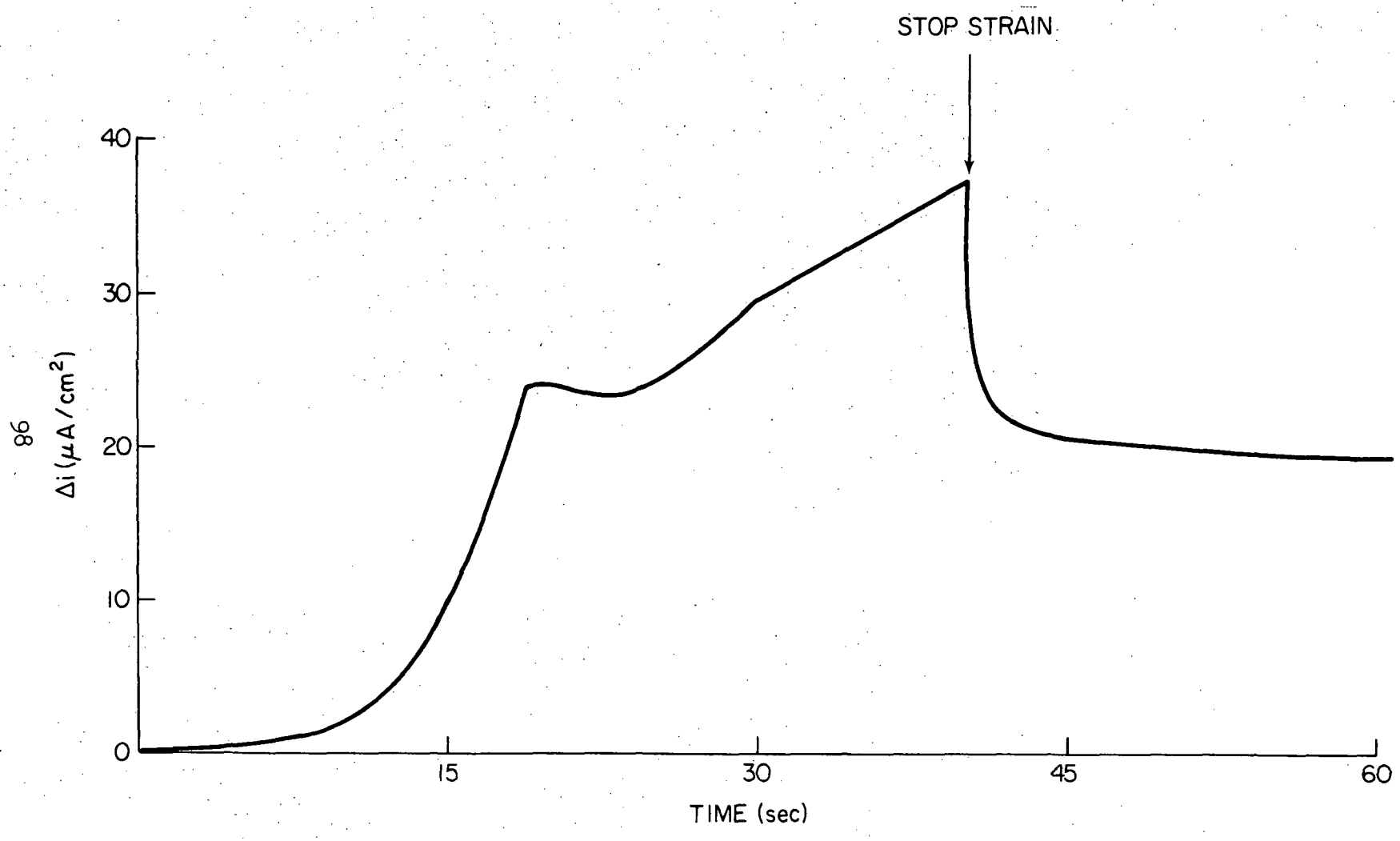

Figure 29 - Current Response to Straining at a Potential of -470 mV(SCE) at a Strain Rate of 10%/min; Base Current Density is 176 μA/cm²

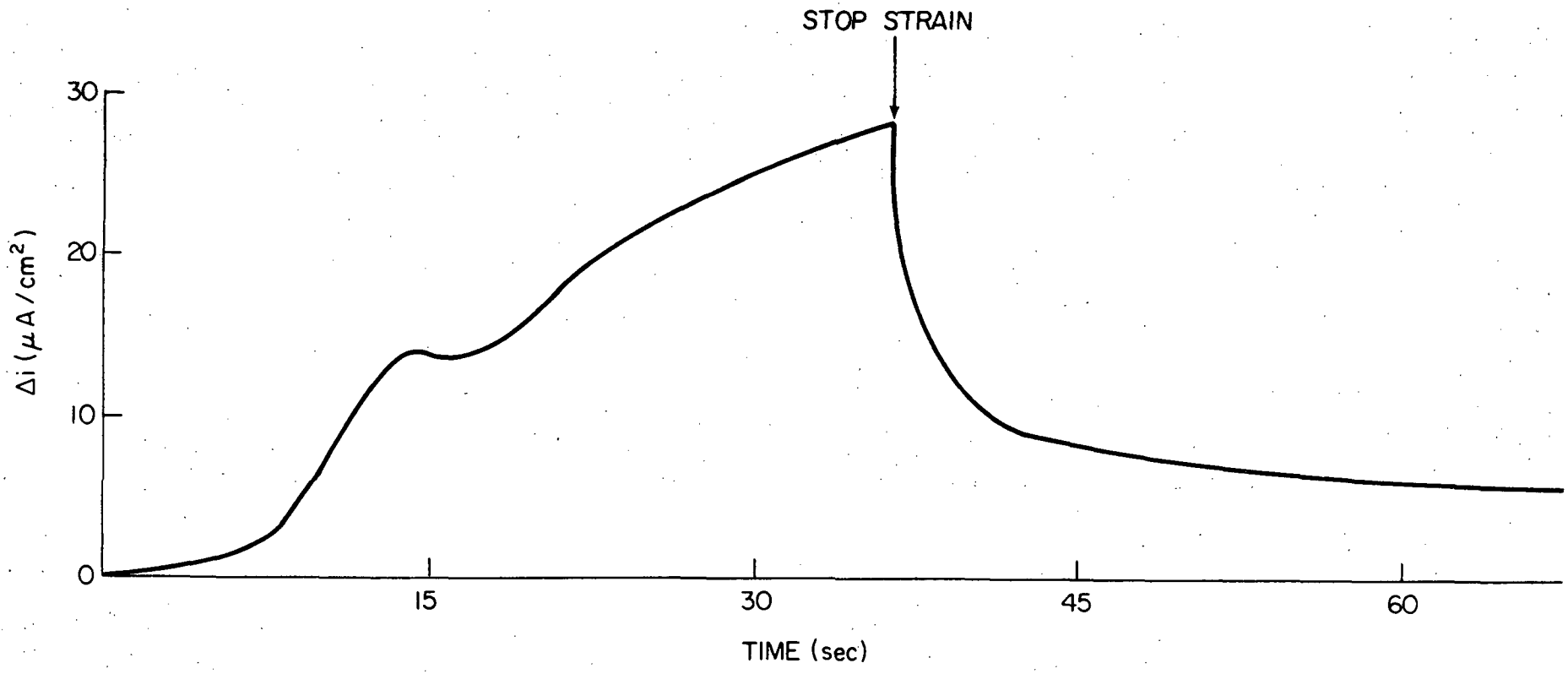

Figure 30 - Current Response to Straining at a Potential of -600 mV(SCE) at a Strain Rate of 10%/min; Base Current Density is 80 $\mu A/cm^2$

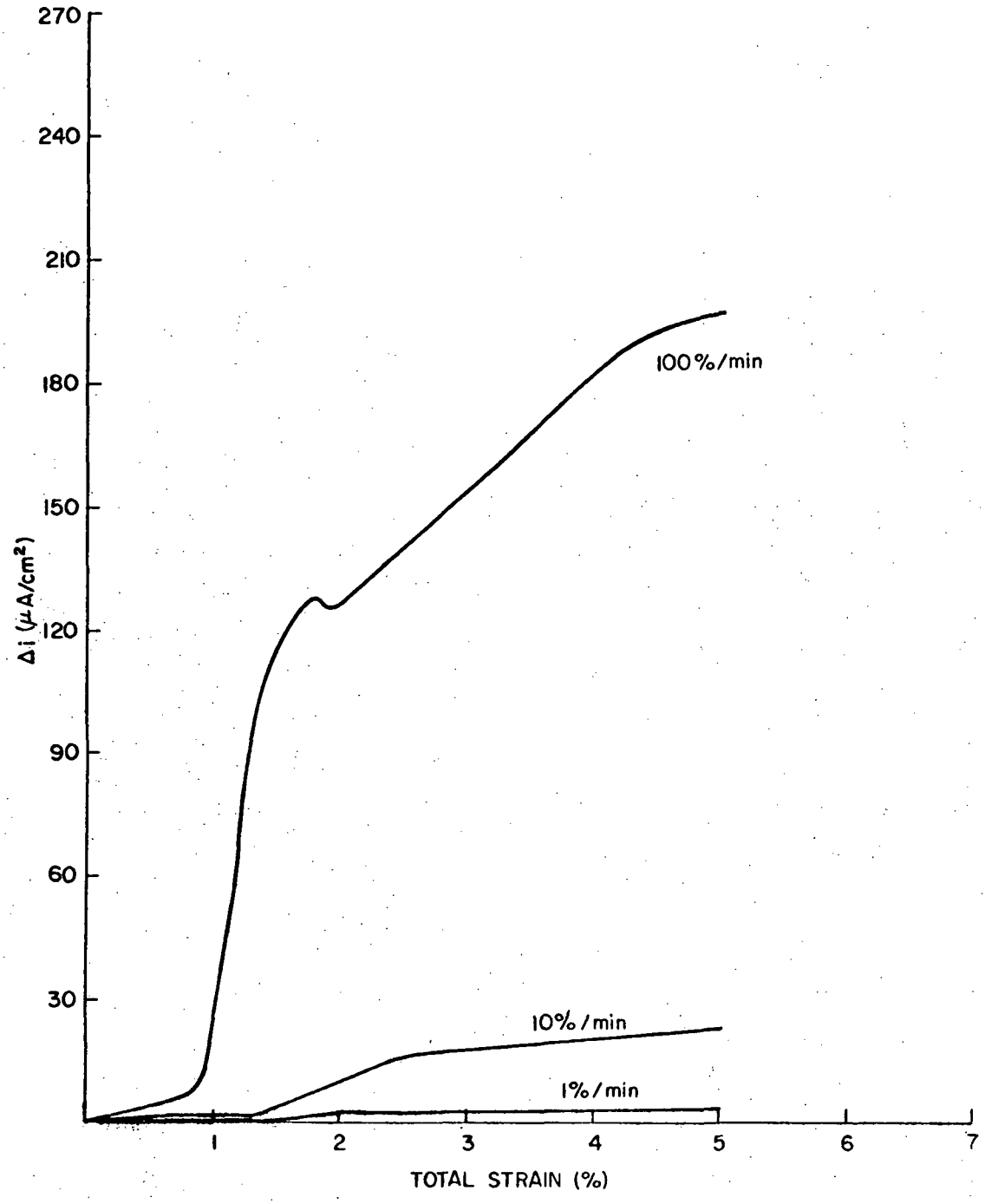

Figure 31 - Current Response to Straining at a Potential of +200 mV(SCE) as a Function of Strain Rate

The latter rate will increase with strain rate while the former should remain constant. Thus at high strain rates more surface is produced per unit time and the current is higher. It is important to note, however, that even at a strain rate of 100%/min the current transient has a tendency to reach a limiting value. This gives an indication of how very fast the rate of passivation is on a titanium surface.

Changes in the active corrosion potential were also monitored during straining. It was found that straining shifts the potential in the negative (less noble) direction. The more rapid the strain rate the greater the change. At a strain rate of 100%/min the change is about 30 mV. The shape of the potential versus time curve while straining is similar to the current versus time curves for straining in the passive region (Figure 26). In other words, there is a sharp decrease in E_{corr} at the yield which is usually followed by a relaxation. Then, as the straining continues the potential decreases again but tends to reach a saturation value and level out. When the straining is stopped the potential decays back (noble direction) to its original value before straining. When the load is released there is a potential discontinuity in the negative direction. If the straining is continued to fracture the potential shifts sharply in the negative direction as the wire breaks.

A shift in the corrosion potential is evidence that straining produces a change in the actual reactions that are occurring. If the current densities of the original anodic and cathodic reactions that make up E_{corr} remained the same and only the area increased there would be no change in the corrosion potential during straining. A negative potential shift implies faster anodic reactions. This would be expected when a film covered electrode is strained because fresh uncoated surface is exposed to the solution and dissolution rates are much faster on a fresh surface. However as time passed the new surface would become passivated. Thus, saturation of the potential shift would be expected similarly to the saturation of a current response. The discontinuity in E_{corr} in the active direction when the specimen is unloaded can be explained by the rupturing of the newly formed film by putting it into compression. Thus the response of the corrosion potential to straining also lends support to the hypothesis that the titanium is covered by a film even in the "active" condition.

With the available information it is not possible to determine whether or not a hydride was formed on the fresh surface during straining at open circuit. The formation of a hydride is a cathodic reaction and would cause a noble potential shift. However the amount of current expended in forming a thin hydride layer would not be large and it could easily be overshadowed by the anodic dissolution current.

c. Cathodic Region

Determination of the straining responses of titanium in the cathodic region is very important from the standpoint of stress corrosion cracking because it is in this potential range that the susceptibility is the

highest. Of particular interest are the changes which may occur in the various anodic processes. Reference back to Table 1 shows that a myriad of anodic reactions can occur at potentials below the "active" corrosion potential especially when a fresh surface is exposed to the solution. Unfortunately an accurate determination of these anodic responses is very difficult to make due to the rapid rate at which the hydrogen reduction occurs at these potentials. This cathodic current is so large (see Figure 15) that anodic responses are often completely masked.

Even an accurate measurement of the response to straining of the hydrogen reduction reaction itself is difficult due to complications from the surface changes which occur when a cathodic potential is applied. Hydrides form and thicken, hydrogen is absorbed into the metal, and the surface becomes darker and rougher in appearance. These surface changes occur continuously with time after the application of a cathodic potential. As a result, a steady state situation, from which a quantitative measurement of straining response can be made, is never obtained. The cathodic current increases from the time the potential is applied until the wire becomes too embrittled to strain. Also the magnitude of the measured static current varies noticeably between specimens. This is not surprising since the degree of roughening of the surface due to corrosion and hydrogen absorption would not be expected to be consistent from specimen to specimen.

Another factor which could contribute significantly to the current differences is the uneven growth of the surface hydrides. The rate of growth of surface hydrides during cathodic charging was studied by Tomashov et al.[83,152] in sulfuric acid solutions. They found that while the hydrides grew uniformly on pure titanium they grew very unevenly on a Ti-4.35 Al alloy with large differences in thickness from specimen to specimen.

Even though the magnitude of the current is not completely predictible from test to test the general shape of the current time curves during straining is reproduceable and definite trends in the current response as a function of potential and strain rate were observed.

Figure 32 shows schematically the current response to straining at -700 mV(SCE). This potential is just negative of the "active" corrosion potential. The cathodic current density flowing at this potential is reasonably small, about 130 $\mu A/cm^2$. The current levels off as straining begins which indicates an anodic response in the elastic range. As the metal yields the current begins to increase cathodically again. It continues to increase as the metal plastically deforms. When the straining is stopped the current decays smoothly in the cathodic direction. This decay is over in a few seconds and the current continues to increase cathodically as it did before straining. The same anodic discontinuity which occurred in the anodic region is again seen when the load is released.

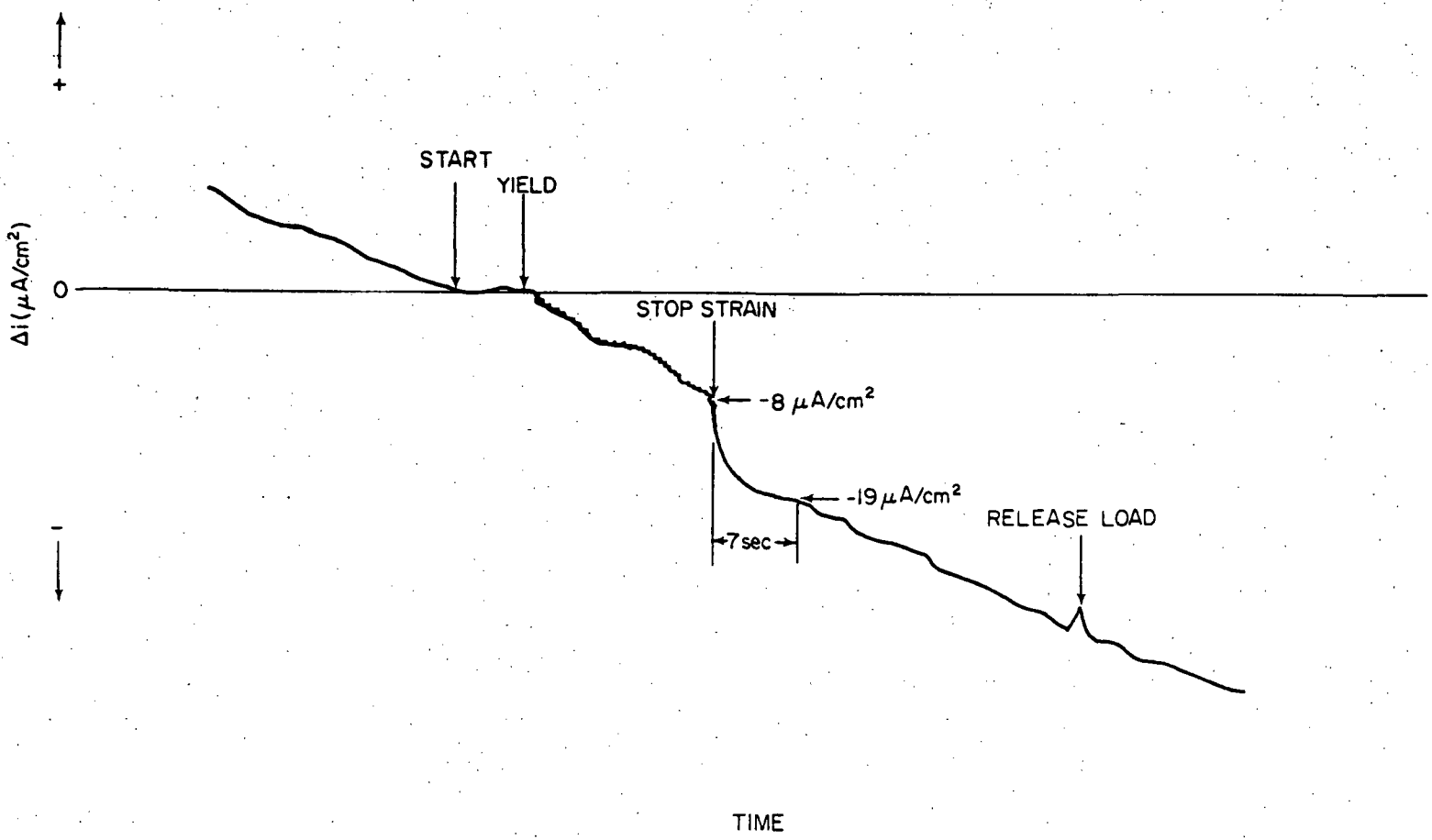

Figure 32 - Schematic Current Response to Straining at a Potential of -700 mV(SCE) at a Strain Rate of 10%/min; Base Current Density is -130 $\mu A/cm^2$

The decay in the cathodic direction when straining is stopped may appear strange but is the result of the fact that the applied potential is near the corrosion potential and thus the measured straining response contains both anodic and cathodic parts. This is illustrated in Figure 33. The measured current is the algebraic sum of the anodic and cathodic currents. The anodic response is a transient one and dies out when the straining is stopped due to repassivation. The cathodic response on the other hand is probably mostly due to the increase in area of the specimen. These factors produce the observed decay. The observance of a similar decay for nickel wires strained in sulfuric acid at a potential just below E_{corr} was explained analogously by Murata.[74]

Figure 34 is another schematic diagram showing the response to straining at -850 mV(SCE). At this potential a much larger cathodic current is flowing, about -2500 $\mu A/cm^2$. The current response during straining is similar to that at -700 mV. There is a slight decrease (anodic response) in the elastic range followed by a steady cathodic increase during plastic deformation. When the straining is stopped, there is a slight decay in the anodic direction. This is due to a relaxation of a cathodic transient. The fact that it is so small indicates that most of the current response is due to the increase in the area of the specimen. The absence of a cathodic decay like that seen at -700 mV means that the anodic responses are too small, relative to the large cathodic current, to be detected. Anodic reactions are still occurring as is evidenced by the anodic response in the elastic region. At this potential release of the load produces a discontinuity in the cathodic direction. The reason for the change in direction of this discontinuity is not clear.

Tests at -850 mV were run at strain rates of 10, 30, 50 and 100%/min. Faster strain rates produced noticeably larger cathodic responses. At 100%/min Δi_c was about 900 $\mu A/cm^2$. The anodic response in the elastic range increased slightly as the strain rate increased, from an average of 12 $\mu A/cm^2$ at 10%/min to 25$\mu A/cm^2$ at 100%/min.

Figure 34 is typical of the straining response at potentials between -800 mV and -900 mV(SCE). However when a potential of -1000 mV(SCE) is applied the response is markedly different. Instead of the expected current change in the cathodic direction the response is entirely anodic. Figure 35 is a copy of the recorded current response as a function of time for a specimen strained at this potential. As the figure shows there is an anodic response in the elastic region which continues after yielding. This implies that an anodic reaction is occurring on the freshly produced surface. The magnitude of this current is quite large compared to normal anodic currents (see Figure 11). The only reasonable explanation for this odd behavior is that the oxide film does not reform when it is ruptured at this potential. From Table 1, an oxide film could form directly from the fresh surface. However, oxidation of a hydride layer would be very difficult at -1000 mV (reactions s - z, Table 1). Therefore if a hydride layer formed first on a freshly exposed surface, then an oxide would not likely form on top of it. This is very

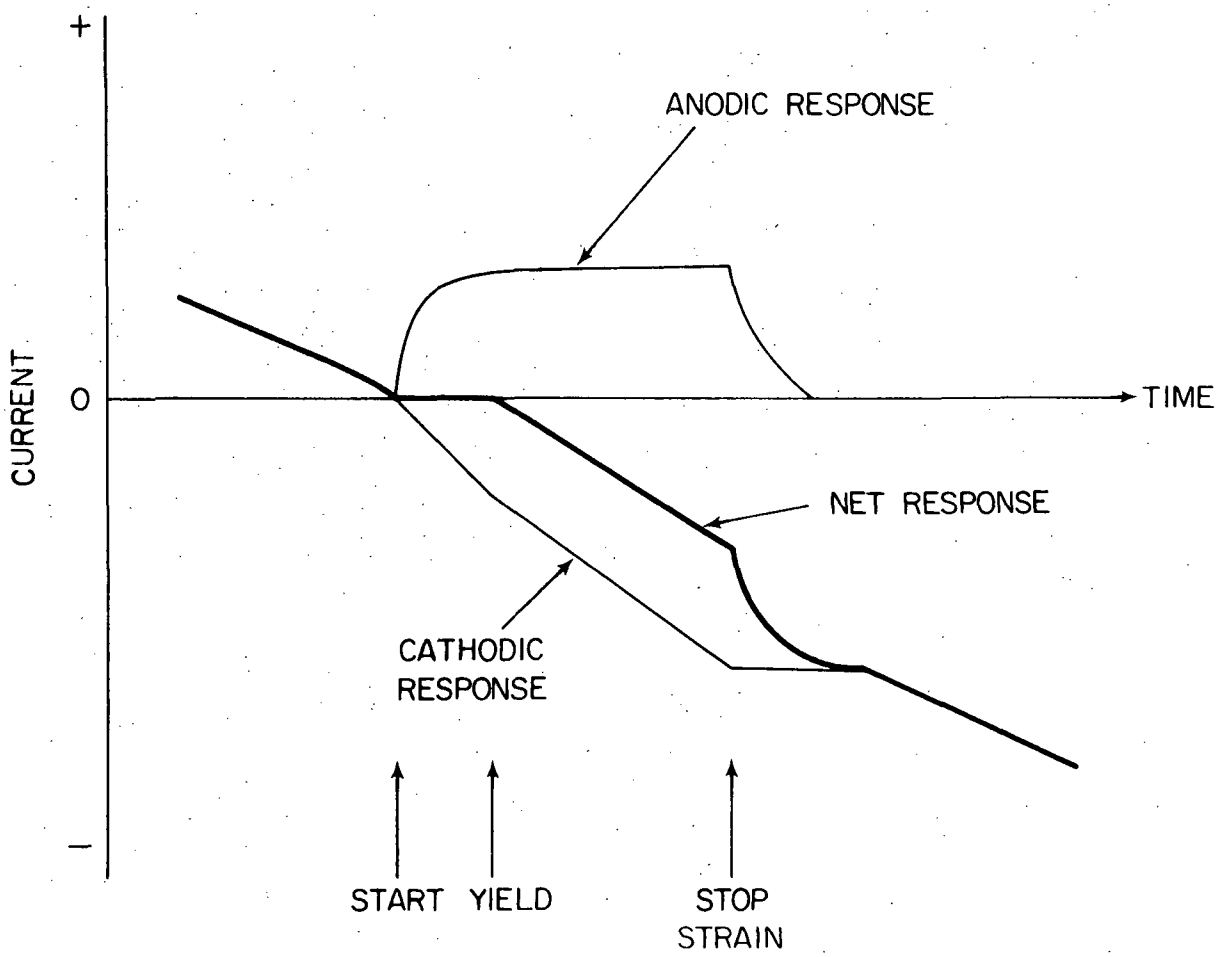

Figure 33 - Explanation of Observed Current Response at -700 mV(SCE)

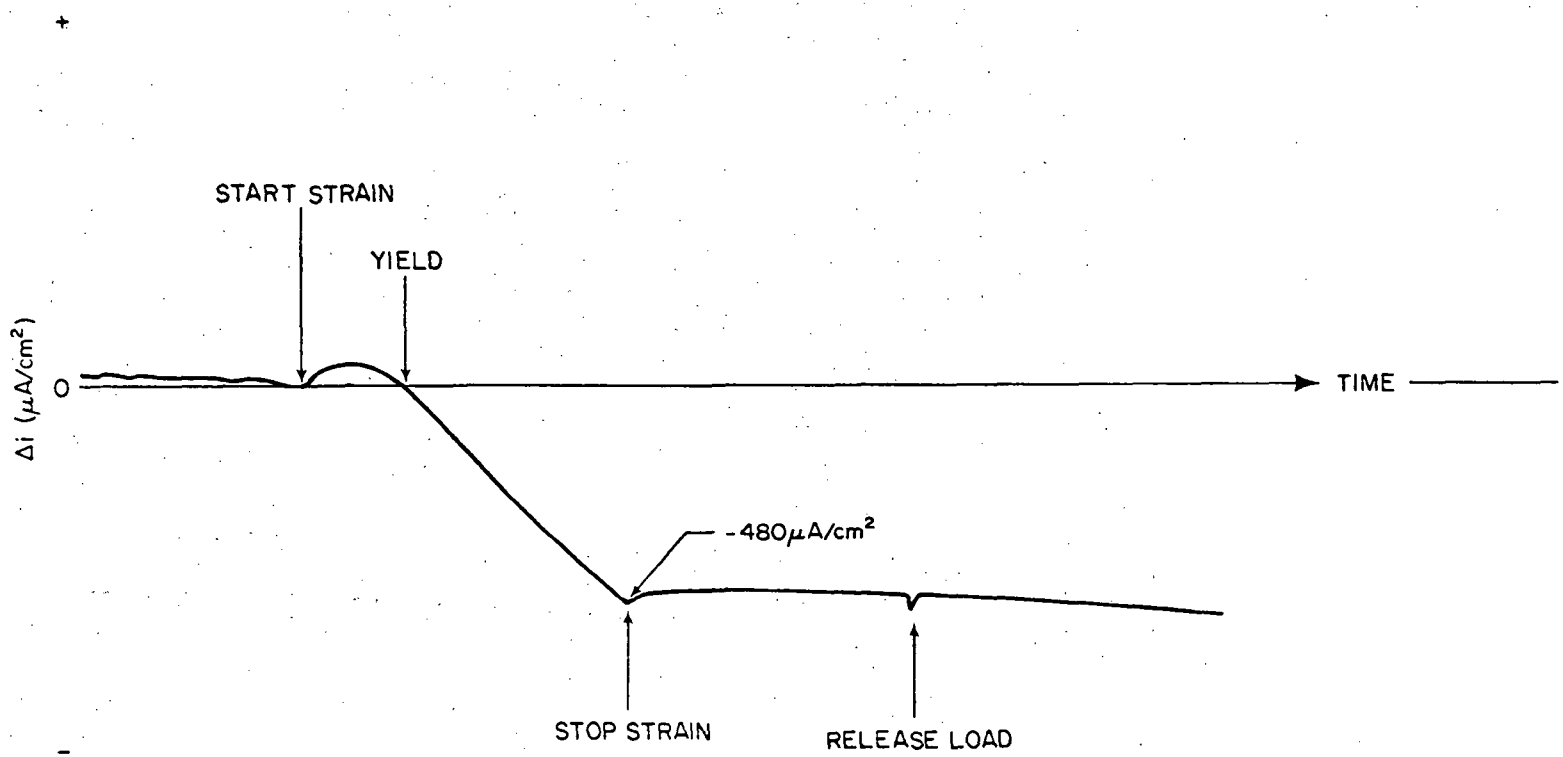

Figure 34 - Schematic Current Response to Straining at a Potential of -850 mV(SCE) at a Strain Rate of 10%/min; Base Current Density is -2500 μA/cm²

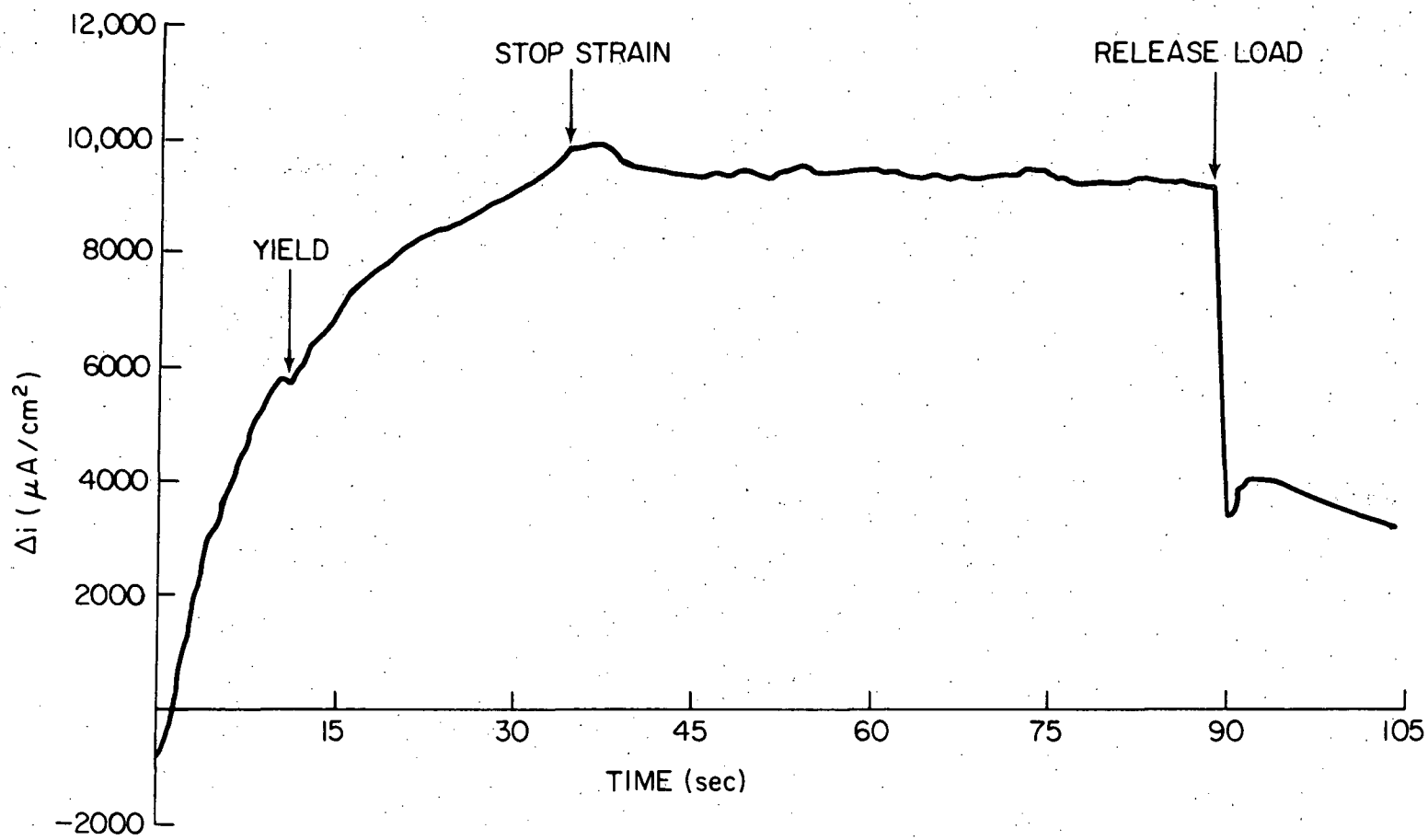

Figure 35 - Actual Current Response to Straining for a Specimen Strained at 10%/min at a Potential of -1000 mV(SCE); Base Current Density is -225,000 μA/cm²

possible since hydride formation would be extremely fast under these conditions. The hypothesis that fresh surfaces are not repassivated is supported by the current behavior after straining is stopped. A smooth current decay which is always associated with repassivation is not observed. (Occasionally the current will drift in the cathodic direction after straining is stopped but the characteristic repassivation decay such as that seen in Figures 26, 28, 29, 30 and 32 is never observed.) Also, numerous other workers[83,99,157] have measured increased dissolution rates at cathodic potentials and have associated the phenomenon with the reduction of surface oxides.

When the load is released the current shifts abruptly back in the cathodic direction. This discontinuous shift is clearly a mechanical effect rather than a chemical one. Its magnitude is exactly equal to the current change in the elastic region. This implies that the elastic response was mechanical in nature. The cause of this behavior is not clear but a plausible explanation is that when the wire is strained, cracks form in the surface layer at stresses in the elastic range. These cracks would be sites for anodic dissolution. When the yield is reached plastic deformation is likely to occur at localized areas on the metal surface, particularly since the thickness of the hydride film is uneven. Therefore, during the four per cent plastic strain many areas of the surface may not undergo extensive deformation. When the load is released the metal contracts and tends to close up the cracks in the surface layer on these areas.

As was mentioned previously, the current flow in the cathodic region, both static and dynamic, varies from specimen to specimen. Therefore the exact response depicted in Figure 35 is not always observed. At a strain rate of 10%/min, the anodic response in the elastic region is occasionally followed by a cathodic response after yielding. Also the magnitude of the anodic responses varies from specimen to specimen. However unlike at -850 mV a net cathodic response never occurs. Further, if the strain rate is increased to 100%/min then the response is always totally anodic (as in Figure 35) and cathodic shifts after yielding are not observed.

Straining at the faster strain rate does not significantly alter the magnitude of the currents but it does increase the size of the discontinuity which occurs at the yield.

Since embrittlement of the titanium wires occurs after exposure for about 45 minutes at -1000 mV(SCE), an effort was made to determine if the straining response varied as the embrittlement progressed. Specimens were strained after being held at -1000 mV for varying times up to 45 minutes. Analysis of the results showed no noticeable trends in the straining response as a function of time.

During the course of the straining experiments in the cathodic range many specimens were broken while being strained in the 5N HCl solution. Most of the fractures occurred after short exposure times in the

solution and thus were ductile. However, surprisingly, not one of these ductile failures occurred in the solution. Failures always occurred under the microstop-silicone sealant coating. If the exposure time before straining was long enough for the wires to become embrittled then, of course, the fracture occurred in the solution. On the other hand, in the anodic region the failures were always ductile and appeared to occur randomly on the wire, some in the solution, some under the coating. Apparently the surface hydride layer was mechanically stronger than the base metal and forced the failure to occur under the coating.

VI. MECHANISMS

1. Initiation

Crack initiation has long been an elusive factor in the stress corrosion cracking of titanium alloys in aqueous solutions. If crack propagation is defined as beginning when an actual crack exists in the metal, then initiation would be the process of creating the crack from the initial oxide-coated surface. Plausible mechanisms for the propagation of an existing crack are easily formulated because the crack is separated from the bulk electrolyte. Therefore concentration changes can occur and stress risers are present. But the initiation process must occur in a neutral salt solution where the passive film is very adherent and protective. Further, this film is reformed so rapidly when it is ruptured that it is very difficult to develop any concentration changes, even at localized slip steps. This is why very few workers have been able to initiate cracks in unnotched titanium specimens.

The results of the present investigation indicate that surface hydrides may play a critical role in the initiation process. Hydrides can be formed from the surface oxides or they can form when the film is ruptured. Their postulated role in initiating cracks comes from the fact that they form unevenly on Ti-Al alloys and tend to be preferred sites for the hydrogen evolution reaction. If hydrides form preferentially on certain grains or on, say, alpha grains rather than beta grains, a small galvanic cell could be set up. Since the cathodic hydrogen reaction would occur on the hydride the anodic counterpart could be concentrated elsewhere. Owen[143] observed this type of localized reaction for Ti-6Al-4V specimens in 5N HCl. Figure 36 shows a scanning electron micrograph of a specimen held at -742 mV(SCE) for 4 hours. The holes, which developed at beta phase regions, could be formed from localized attack or they could simply be surface areas that remained uncoated by the hydride. In either case they are tiny crevices in which the concentration changes and stress risers necessary for crack propagation can develop. (The blocky particles which appear in the figure were suggested to be particles of diamond polishing compound.)[143]

The fact that hydrides form evenly on pure titanium could explain why initiation is much more difficult on the pure metal than on the alloy.

The observed potential dependence of crack initiation can also be explained by a hydride mechanism. Crack initiation is most rapid between potentials of about -1000 mV(SCE) and 0 mV(SCE). At noble potentials initiation would be prevented because hydrides do not form. At very negative potentials the driving force for hydride formation would be so large that the whole surface may be covered and localization thus prevented.

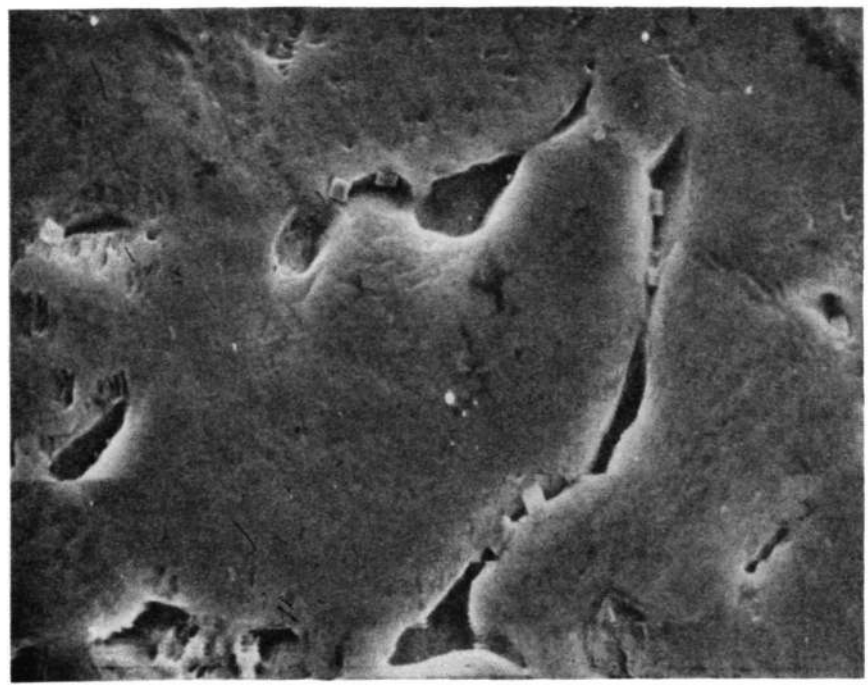

Figure 36 - Scanning Electron Micrograph of Ti-6-4 Alloy Surface after 4 hours at a Potential of -742 mV(SCE) in 5N HCl. (Ref. 143)

It must, of course, be remembered that the localized situation of Figure 36 was developed in a strong acid solution in which the passive oxide is not stable and therefore is not directly applicable to neutral solutions. However, hydrides can be formed in neutral solutions by cathodic charging.[7] Over a period of time this could lead to a localized situation. Consider for example a passivated Ti-8-1-1 specimen in neutral 3.5% NaCl. Assume surface hydrides form unevenly on the oxide surface. This is illustrated schematically in Figure 37. The result of this situation is that the hydrogen evolution reaction would again occur preferentially on the hydride. The anodic reactions, which would be mainly oxide formation and growth, would occur on the oxide surface. But a product of the oxide reactions is protons (Table 1, reactions h-p). Thus the solution at the surface between the hydrides would become more acidic. Rupture of the film at these points would then result in slower repassivation. Also if the hydrides are mechanically stronger than the oxide the surface may tend to be ruptured preferentially at points not covered by hydrides.

2. Propagation

The major disagreement in mechanistic considerations of the propagation of stress corrosion cracks in titanium in aqueous NaCl is whether the damaging specie is the chloride ion or the hydrogen ion. It is impossible, with the information presently available in the literature, to conclusively prove or disprove either theory. However, it is hoped that the information developed in the present investigation may be helpful in this endeavor.

First, the results of the straining electrode experiments produce no support for the existence of a large mechano-chemical effect. The largest anodic current change that was measured during straining was about 10 mA/cm^2. Even if this current is assumed to be flowing entirely from the new surface produced by straining it yields a current density of only 0.5 A/cm^2. In order to project larger current densities very localized dissolution would have to be occurring. Examination of specimens subsequent to straining revealed no localized attack. It could be argued that the small currents in the present tests were due to rapid repassivation of the freshly exposed surface and that consequently bare titanium was never allowed time to react at its intrinsic rate. This is probably true but the environmental conditions during the straining tests were purposely made as aggressive if not more aggressive than those at the crack tip (low pH and low O_2 content). Therefore if passivation occurred instantly, even at the very high strain rates of some of the tests, then it should also occur at the crack tip.

The current density necessary to propagate a crack by anodic dissolution is about 600 A/cm^2 for the velocities observed in aqueous cracking of titanium. If a crack propagated through a specimen via this huge current then the fracture surface should show gross evidence of a prior corrosion reaction. But tests reported in the literature indicate that the fracture surfaces show only evidence of brittle fracture with no extensive corrosion damage.

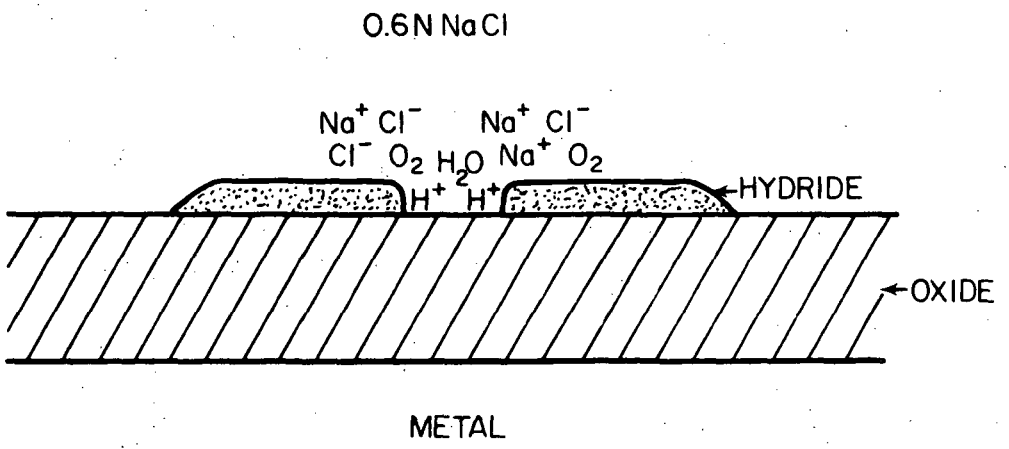

REACTIONS ON HYDRIDES

$$2H^+ + 2e^- \longrightarrow H_2$$

$$Ti + H^+ + e^- \longrightarrow TiH$$

REACTIONS ON OXIDE

$$xTi + yH_2O \longrightarrow Ti_xO_y + 2yH^+ + 2ye^-$$

$$2TiO + H_2O \longrightarrow Ti_2O_3 + 2H^+ + 2e^-$$

$$Ti_2O_3 + H_2O \longrightarrow 2TiO_2 + 2H^+ + 2e^-$$

Figure 37 - Illustration of Proposed Initiation Mechanisms for Stress Corrosion of Titanium Alloys in Aqueous Solutions.

Thus, the absence of high current densities during straining in the present investigation and the observations of the fracture surface made by other workers make it very unlikely that cracks are propagated by a pure anodic dissolution process. This is not to say that anodic dissolution processes do not occur at the crack tip. In fact, there is strong evidence that they are an important part of the total cracking process. Also, these observations do not rule out the other "chloride ion" theory, stress-sorption. This theory does not require a large anodic current and could produce the cleavage type fractures.

The very rapid crack velocity can be explained easily by the stress-sorption theory because it requires no solid state diffusion but only adsorption of Cl^- ions at the crack tip - a process which should be quite fast. The fast cracking can also be explained, with some difficulty, by the hydrogen embrittlement theory if the propagation is assumed to be a discontinuous process. The rationale is that a high hydrogen content in the metal at the crack tip may initiate a rapid burst of mechanical cleavage followed by an arrest while the hydrogen accumulates again, then another burst, etc.

It is also possible that hydrogen may be diffusing faster than would be anticipated from the published value of the diffusivity. As indicated previously (Chapter V section 2) the diffusivity could increase at high solute concentrations. In this connection, in a very recent paper, Gray[155] described a method of measuring hydrogen concentration profiles near the surface using ion-probe mass-spectrometric techniques. He was studying hot salt cracking of the Ti-8-1-1 alloy using stressed (creep) specimens at a temperature of 427°C. He measured a concentration of 4500 ppm at a depth of 0.1μ for a profile taken near the fracture surface. The concentration of hydrogen in the base metal was 90-126 ppm. The results of the present investigation also indicated, although rather qualitatively, that the effective distance over which hydrogen may embrittle a metal is larger than can be accounted for by the published diffusivity.

To compare the stress-sorption and hydrogen embrittlement theories from the point of view of the electrochemical aspects of the cracking process it is helpful to discuss an actual, actively propagating, crack. First, consider a crack in a Ti-8-1-1 alloy propagating in sea water under open circuit conditions. Brown[122] has measured the pH at the crack tip to be 1.7 for this situation. An obvious question which arises immediately is how did the hydrogen concentration become so high at the crack tip. The protons could not have diffused into the crack from the bulk because their concentration in the bulk is very low. Therefore the protons must be produced by a reaction at the crack tip. Protons could be produced by the formation of an oxide or by the dissolution of titanium to a titanium chloride followed by a hydrolysis reaction. Specifically,

$$(42) \quad xTi + yH_2O \rightarrow Ti_xO_y + 2yH^+ + 2ye$$

or

$$(22)\quad Ti + 3Cl^- \rightarrow TiCl_3 + 3e^-$$

and

$$(23)\quad 2TiCl_3 + 3H_2O \rightarrow Ti_2O_3 + 6H^+ + 6Cl^-$$

The first reaction is for the formation of an oxide from the base metal. This can be applied to a propagating crack when fresh metal is exposed. It is also important to note that protons are produced when a lower oxide is oxidized to a higher one. Thus the availability of bare metal is not necessary for the hydrogen ion concentration to increase. The formation of higher oxides as a proton source is probably most important during the initiation stage when the conditions for cracking are being developed in a crevice. The second reaction is the dissolution of titanium to the trichloride. This is followed by the reaction of the trichloride with water to form protons and more chloride ions. It is easy then, to account for the increase in the proton concentration at the crack tip.

In the stress-sorption theory the crack is propagating by the specific adsorption of Cl^- ions at the tip. The cracking rate then depends on the availability of Cl^- ions. Initially they must diffuse into the crack from the bulk solution although once an active dissolution process is set up at the tip then the chloride ions can be recycled via reactions (22) and (23). Since the supply of Cl^- ions should be continuous the crack should propagate continuously.

In the hydrogen embrittlement theory the crack is propagated by the entry of nascent hydrogen into the metal at the crack tip. The hydrogen concentration must build up to a level such that it can initiate a cleavage crack. As discussed above this cleavage crack may then propagate a distance into the metal before being arrested. The nascent hydrogen is produced by the hydrogen reduction reaction which was discussed in detail previously. The reaction will be written here as simply

$$(21)\quad H^+ + e^- \rightarrow H$$

The exposure of fresh metal to the solution as the crack propagates will induce electrochemical reactions to occur. Reactions (42) and (22) are anodic and since they require bare surface they will occur at the crack tip. But the cathodic reaction (reaction 21) must also occur <u>at the crack tip</u>. This is because the electrochemical reactions will always occur at the fastest possible rate, i.e., they will occur via a reaction path which allows them to go the fastest. Under open circuit conditions the rate of the anodic reactions must be equal to the rate of the cathodic reactions. In other words the anodic reactions of passivation and/or dissolution, which want to go at a very rapid rate, must be supported by an equally fast cathodic reaction. Further, each titanium

atom that takes part in an anodic reaction requires a minimum of two and probably three or four electrons to be transferred. This means that reaction (21) must occur two to four times for each titanium atom that reacts. But as was seen in the present investigation the hydrogen reduction reaction occurs very slowly on an oxide coated surface. Therefore if the reduction reaction occurs on the passive crack wall, its slow rate will severely limit the rate of the anodic reactions. The often expressed concept that since the anodic reactions occur at the crack tip the cathodic reactions must occur at discrete distance away on the crack walls is unfounded. From the definition of an electrochemical corrosion reaction electrons must flow through the metal from the node to the cathode. But on a microscopic scale this simply means that the electrons which are given up by a titanium atom that is being oxidized must flow to another titanium atom, near which a proton is available, to be reduced. Further, the surface is in a state of dynamic activity and specific anodic and cathodic sites may change many times in a short period of time. Thus both adsorption of Cl^- ions and absorption of hydrogen atoms should occur at the crack tip. The question of which of these species promotes the actual cracking perhaps must be resolved by other experimental observations.

Observed changes in the cracking process with changes in the applied potential can be extremely informative. Yet they must be analyzed carefully because the applied potential at the surface of a specimen does not necessarily reflect the potential at the tip of a crack. For Ti-8-1-1 alloys cracking in sea water the crack velocity and anodic current are observed to increase linearly with applied external potential. The potential at the crack tip of a specimen cracking at open circuit has been measured by Brown[122] to be between -942 mV and -1142 mV(SCE). It is possible that the tip potential may remain at about -1040 mV(SCE) even when a more noble potential is applied at the surface. This could be true if the resistance or the current in the crack were high, producing a large IR drop. Also, if the electrochemical reactions at the crack tip were rapid enough, they would tend to hold the potential there constant. Recent work at Ohio State University[156] has demonstrated a very large IR drop in an artificial crevice. The tests were on a Ti-8-1-1 alloy in 0.6N KI. It was found that applied potentials at the mouth of the crevice between -1842 mV(SCE) and +2158 mV(SCE) produced corresponding potentials between only -392 mV(SCE) and +458 mV(SCE) at the root of the crevice. These results cannot be applied directly to a stress corrosion crack because differences in geometry must be considered but they do indicate that sizeable IR drop is likely inside a crack.

What these observations mean in terms of an actual crack is illustrated in Figure 38. This shows a crack propagating with an applied surface potential, E_S, of -500 mV(SCE). The result of applying these two unequal potentials on the same metal is that there is a net flow of electrons through the metal from the crack tip to the surface. This produces a net flow of positive (anodic) current through the solution from the crack tip to the bulk. This ionic current could be carried by negative ions moving into the crack or by positive ions moving out of

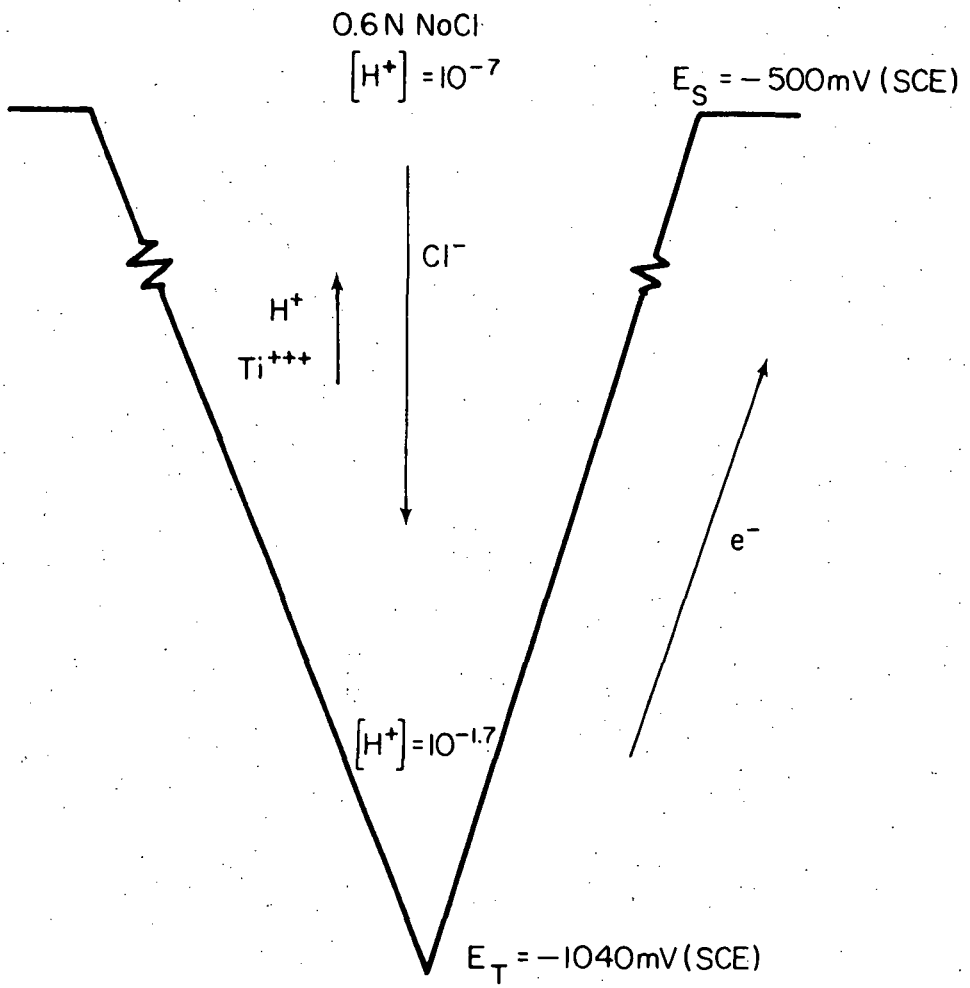

Figure 38 - Schematic Representation of a Crack Propagating in Neutral NaCl with an Applied Surface Potential of -500 mV(SCE)

the crack. In the present example, this would result in a net flux of Cl^- ions into the crack and or H^+ and Ti^{3+} ions out of the crack. Increasing the applied surface potential (noble direction) would increase these driving forces and increase the measured anodic current coming out of the crack. This explains the observed increase in current with applied potential. The fact that the increase is linear indicates that the current flow is controlled by the rate of migration of the ions into or out of the crack and not by the rate of a surface reaction.

The fact that the crack velocity also increases linearly, along with the current, as the potential is increased must be taken as strong evidence that the cracking rate is controlled by the flux of chloride ions to the crack tip. (Unless it is controlled by the flux of hydrogen ions out of the crack which is certainly unlikely.) These observations are, of course, strong support for the stress-sorption theory.

However, the inseparability of the two theories (Chapter II, section 5) becomes very clear when it is discovered that this increase in the measured anodic current can be rationalized to produce an increase in crack velocity via a cathodic mechanism. The rationale is as follows: Suppose the reactions at the crack tip are 22, 23 and 21. These are occurring rapidly and are independent of the applied surface potential. Assume that the rate of reaction is limited by the availability of Cl^- ions, and that the crack is propagating by the absorption of hydrogen produced by the reduction process (reaction 21). Now when the potential of the surface is increased, the availability of Cl^- ions at the tip increases. This increases the rate of reaction 22, which consequently increases the concentration of hydrogen ions via reaction 23, and thus, the cracking rate.

This rationalization is contingent on the assumption that the potential at the crack tip remains constant even when a noble potential is applied to the surface. If the potential at the tip increases with the applied surface potential then it becomes very hard to explain the accompanying increase in crack velocity via the hydrogen embrittlement mechanism. Changes in potential affect electrochemical reaction rates exponentially. So it is extremely doubtful that the cathodic hydrogen reduction reaction could go faster at a more noble potential no matter what the concentration of hydrogen ions.

This observed dependence of the crack velocity on the applied potential continues as the potential is shifted negatively (active direction) until, at a potential of about -1000 mV(SCE) the crack stops propagating altogether. Consider the stress-sorption theory first. It does not involve a direct electrochemical reaction and hence this observation cannot be explained merely as an example of cathodic protection in the classic sense. However cracking can be stopped if Cl^- ions become unavailable or if their concentration decreases below some critical value. In this connection, an applied potential of -1000 mV(SCE) or lower would eliminate the driving force for migration of Cl^- ions into the crack tip. However, a much more fundamental explanation, related

to the adsorption process itself, is possible. The tendency for positive or negative ions to adsorb on a metal surface depends on the charge of the surface. If the surface has a positive charge then negative ions will adsorb on it whereas if the surface is charged negatively then positive ions will adsorb on it. As the electrode potential is decreased from noble values a point is reached where the net charge on the surface changes from positive to negative. This is called the potential of zero charge, E_{pzc}. From the standpoint of cracks propagating by stress-sorption, at potentials below E_{pzc} negative Cl^- ions will no longer be adsorbed and the propagation will stop. The potential of zero charge has not been measured for titanium. However its value can be estimated from the electronic work function. Petrenko[145] has made this calculation and reported a value of -942 mV(SCE). This is a very negative value and indicates that titanium is positively charged over most of the normal potential range. Since this value is only an estimate, the actual value could be slightly more negative and correlate well with the observed cracking behavior.

Advocates of the hydrogen embrittlement theory have explained the cathodic protection by suggesting that at very negative potentials passive films are formed on the surface at the crack tip by the presence of OH^- ions.[140] These films then prevent the ingress of hydrogen. This rationalization is not consistent with the results of the present investigation. While it was observed that passive films are very effective in reducing the rate of hydrogen embrittlement (see Figure 19) the hypothesis that these films are formed preferentially as the potential is decreased cannot be accepted. There are many reasons for this assertion. First, it is unclear why the interruption of an open circuit cracking process by the application of a cathodic potential should produce OH^- ions. They are produced by the reduction of H_2O in alkaline solutions and the crack tip is very acidic. Secondly, film formation is an anodic process. If the films are metal oxides then anodic currents are required to oxidize the metal atoms. Even if passivation is due to adsorption of ions, e.g. OH^-, the process is faster at noble potentials. Shifting the potential in the active direction makes the charge on the metal surface less positive, thus making it more difficult for the passivating ions to adsorb. Therefore, it seems highly unlikely that a film that was absent in a crack tip under open circuit conditions would suddenly be formed when a cathodic potential was applied.

On the other hand, there is much evidence that oxide films on titanium are reduced at cathodic potentials. Increased dissolution rates have been found when cathodic currents were applied (Chapter I, section 10). In a recent paper Pourbaix, Marek and Hochman[157] found that a white surface layer separated and dissolved after a titanium specimen had been held for about one-half hour at -1242 mV(SCE) in 12N HCl. This was accompanied by rapid dissolution of the metal. In the present investigation in 5N HCl, a change in the current in the anodic direction was observed when wires were strained at -1000 mV(SCE) but not when they were strained at -850 mV(SCE). This observation was

suggested to be due to the reduction of a lower oxide, TiO or Ti_2O_3, to a hydride, TiH, (see Table 1).

It is contended that the absence of an oxide film may cause the crack to stop propagating. The reason is that the oxide film is necessary to keep the crack tip sharp. Since electrochemical dissolution is occurring at the crack tip the crack is very likely to become blunted by corrosion unless the new surface becomes rapidly passivated. The necessity for rapid passivation at the crack tip was considered in detail by Hillig and Charles[158] and reported by Beck.[46] Continual, rapid formation of oxide film on the sides of the crack forces the embrittling reaction, which may be either Cl^- adsorption or H absorption, to occur at the extreme tip of the crack. If the crack is propagating by adsorption of Cl^- ions then a blunt crack tip would prevent the Cl^- ions from adsorbing preferentially at the region of highest stress. In the same way, the adsorption of hydrogen would occur over a larger area. Since the diffusion of hydrogen is slow the stresses could be relieved by plastic flow ahead of the tip before enough hydrogen accumulated to promote a cleavage crack. Also oxide formation is an important source of H^+ ions. The solution at the crack tip is not aggressive enough to keep the corrosion reaction going indefinitely. Soon the blunt tip would passivate and the reactions would stop.

It is important to keep in mind here, that the "absence" of the oxide film means that rate of formation of the film is slow enough so that the crack becomes blunted. The film would certainly be expected to form eventually since the electrolyte in the crack, even at the tip, is only mildly aggressive toward titanium. For example, the passive film on titanium will reform spontaneously after it is removed in HCl solutions of strengths up to between 1 and 2 normal whereas a pH of 1.7 at the tip of the crack corresponds to less than 0.1N.

There is no experimental information in the stress corrosion literature concerning the possible role of a surface hydride in crack propagation. However, the results of the present investigation indicate that surface hydrides play a primary role in the electrochemistry of titanium in acid solutions. Therefore, it is imperative that the possibility of hydride formation in the crack be considered.

If a hydride forms it is most likely to form at the crack tip because the hydrogen ion concentration is the highest there. Thus it is pertinent to consider the implications of a surface hydride at the crack tip.

First, it is possible, as was suggested in Chapter II, section 5, that the crack could propagate by repeated mechanical fracture of a brittle hydride. However, if this mechanism is operative then it is difficult to explain the cathodic protection zone. The rate of hydride formation increases as the potential decreases. Therefore, if hydrides are brittle enough that their formation at the crack tip is a sufficient condition for cracking then cracks should propagate faster at cathodic

potentials. Also the results of the straining experiments in the present investigation indicate that the presence of a hydride on the metal surface may have a strengthening effect.

It was also suggested in Chapter II, section 5 that the formation of a hydride at very negative potentials could prevent the ingress of hydrogen into the metal and thus account for the cathodic protection zone. It is not possible to confirm or refute this hypothesis with the available information. In the present investigation the rate of hydrogen embrittlement increased drastically as the potential decreased (active direction) with no indication that a hydride in any way slowed the process. However this result was interpreted in terms of the reduction of an oxide and does not represent a comparison between a hydride and a bare titanium surface. In the same light, there is evidence from the literature and from the results of the present investigation that the hydrogen reduction reaction goes faster on a hydride surface than on a "titanium" surface. But this "titanium" surface is certainly not a bare titanium surface.

The fact that hydrides have not been observed on the fracture surfaces is easily explained since a thin hydride formed initially at the crack tip would almost certainly be oxidized on the crack walls as the propagation proceeds (see Table 1, reactions s-z).

In summary, the salient points of this discussion on crack propagation are as follows: (1) There is no support from the present investigation for the existence of large enough currents to propagate the cracks by pure anodic dissolution. (2) There is evidence that the diffusivity of hydrogen in the high concentration area at the crack tip may be higher than previously thought. This helps explain the high crack velocity via the hydrogen mechanism. (3) There is strong evidence that the crack velocity is controlled by the rate of migration of Cl^- ions to the crack tip. (4) There is no support from the present investigation that oxides are formed at very negative potentials. On the contrary, evidence is presented that the oxide may be reduced at these potentials. The absence of the oxides suggests an alternative explanation for the cathodic protection zone. (5) The two cracking theories are so interwoven that it is possible to explain although sometimes rather tenuously, all the available experimental results using either theory. (6) The possible role of a surface hydride in the cracking process must be considered.

Due to the voluminous amount of work reported in the literature concerning hydrogen embrittlement of titanium and its application to stress corrosion this theory must be considered the foremost theory for the SCC of titanium in aqueous solutions. Most of the aspects of the cracking, particularly the physical and mechanical aspects, can be explained and experimentally verified, using the hydrogen theory. On the other hand there is very little data reported in the literature which can be directly related to the stress-sorption theory. Indeed the main difficulty with this theory is that it appears immune to experimental evaluation. It is very difficult to design an experiment which will either verify or refute it.

3. Future Work

Since the results of this investigation are inconclusive as to the cracking model it is important to consider other experiments which may help to pin down the mechanism. There are two, as yet unanswered, questions which are crucial in separating the two cracking models. (1) Is the microscopic cracking process continuous or discontinuous? Stress sorption cracking would be continuous while hydrogen cracking would be discontinuous. Experimental work in the area of accoustical emissions is needed to answer this question. (2) Does the potential at the crack tip change when the external potential is changed? A noble shift in potential at the crack tip resulting from an applied noble potential would be very hard to explain via the hydrogen theory. The potential at the crack tip can be measured using microelectrodes. Experimental work is needed to improve the reliability of this technique.

Another aspect of cracking which needs more study from the standpoint of the hydrogen theory is the role of the Cl^- ion. It is clear that the presence of Cl^- ions is necessary for cracking to occur. The hypothesis that the Cl^- ions are used to produce H^+ ions via a hydrolysis reaction appears rather tenuous since the H^+ ions should be produced in the absence of Cl^- ions by the oxide formation reactions. If the hydrogen mechanism is operative it would seem more likely that the Cl^- ions are directly involved in the absorption of hydrogen. Experimental work is needed to evaluate this postulate. For example, the rate of hydrogen pickup as a function of chloride ion concentration could be measured.

More experimental work on the role of a surface hydride in both the initiation and propagation processes is definitely needed. In this connection it is suggested that a hydride be synthesized in the laboratory. A method for doing this was outlined by Sukhotin and Tungusova.[41] The properties of the hydride could then be measured independently. For example, dissolution rates could be monitored as a function of environment and stress; the rate of hydrogen reduction on the hydride surface could be measured with a known surface roughness. Other experiments designed to study the rate of formation and growth of hydrides on titanium would be very informative. For example, the difference in growth rates in H_2SO_4 versus HCl could be determined. From the standpoint of initiation, the growth of a hydride during cathodic charging in neutral solutions should be studied. Mechanically polished specimens would be most useful for these experiments. The effect of a surface hydride on the absorption of hydrogen could be assessed using a rotating electrode apparatus with an abrasive added to the solution. With this technique it may be possible to compare the rate of hydrogen pickup in a static situation where a hydride is present to the rate when abrasion of the surface keeps the hydride from forming.

The results of the present investigation indicate that anodic reactions may be occurring at appreciable rates during cathodic polarization. These rates could be effectively assessed by measuring dissolution rates analytically as a function of applied potential.

VII. CONCLUSIONS

The conclusions resulting from this investigation are listed below.

1. Surface hydrides play a critical role in the electrochemical behavior of titanium in concentrated acid solutions.

2. There is strong evidence that titanium is protected by an oxide film in concentrated acid solutions, even when it is in the "active" condition.

3. Polarization of Ti-8-1-1 wires in 5N HCl at a potential of -200 mV(SCE) results in the formation of a different oxide than that formed at potentials of +200 mV(SCE) or above.

4. The Tafel slope for the cathodic polarization of Ti-8-1-1 in 5N HCl was measured to be 0.1 volts per decade of current. A reverse polarization scan following exposure at very negative potentials results in a large increase in the rate of hydrogen reduction but does not change the Tafel slope.

5. Prolonged exposure of Ti-8-1-1 wires to 5N HCl results in their embrittlement due to the absorption of hydrogen. The rate of hydrogen embrittlement increases as the potential is made more negative. This appears to be due to the reduction of a surface oxide.

6. The presence of a passive film, formed by pre-polarization at +500 mV(SCE), greatly reduces the rate of hydrogen embrittlement upon subsequent exposure at -850 mV(SCE). Films formed in air at room temperature are not effective in reducing the rate of hydrogen embrittlement.

7. Measurements on a wire embrittled at -850 mV(SCE) indicated that the effective distance over which embrittlement occurred was substantially greater than the distance over which hydrogen diffusion through the alpha phase could have occurred.

8. The magnitudes of current changes during straining of the Ti-8-1-1 wires in 5N HCl were too small to produce support for the existence of strain-induced dissolution rates large enough to account for the rapid crack velocities observed for titanium stress corrosion in aqueous solutions.

9. Straining of Ti-8-1-1 wires at -1000 mV(SCE) produced large current transients in the anodic direction. Anodic transients were not observed at less negative cathodic potentials.

APPENDIX

Consider an electrochemical reaction in which a single electron is transferred. For example,

$$(43)\quad M^+ + e^- = M$$

The rate of this reaction is given by the current flowing. In the forward (cathodic) direction the rate, i_c, is described by the following equation:

$$(44)\quad i_c = [C_{M^+}]\left[\frac{kT}{h}\exp\frac{-\Delta G_c^{\dagger}}{RT}\right]\left[F\exp\frac{-\beta F\Delta\phi}{RT}\right]$$

To simplify the description, the equation has been separated into three general terms. The first term, C_{M^+} is self-explanatory and is the concentration of metal ions that can be reduced. The second term is derived from the Absolute Reaction Rate Theory and is the chemical rate constant for the reaction in the cathodic direction. It describes the rate of the reaction in the absence of an electric field. The specific parts of the term are familiar. T is the absolute temperature; k is the Boltzmann constant; h is Planks constant; $\Delta G_c^{\dagger}$ is the activation energy for the forward direction; R is the Universal Gas Constant. The third term describes how the reaction rate is affected by the potential difference across the metal/solution interface. F is the Faraday constant which relates the flux of material to a current flow. $\Delta\phi$ is the actual unmeasurable potential difference between the metal and the solution. β is called the symmetry coefficient and represents the fraction of the electrical energy (resulting from the potential difference $\Delta\phi$) that actually affects the rate of the forward reaction.

Equation 44 is not convenient for experimental analysis because the potential term, $\Delta\phi$, is unmeasurable. Therefore, the overpotential, η, is defined.

$$(45)\quad \eta = \Delta\phi - \Delta\phi_e$$

$\Delta\phi_e$ is the actual unmeasurable potential difference between the metal and the solution when the reaction is in equilibrium. The overpotential can be measured experimentally. Putting equation 45 into equation 44, the rate becomes

$$(46)\quad i_c = FC_{M^+}\frac{kT}{h}\exp\frac{-\Delta G_c^{\dagger}}{RT}\exp\frac{-\beta F\Delta\phi_e}{RT}\exp\frac{-\beta F\eta}{RT}$$

This can be simplified to

$$(47)\quad i_c = C_{M^+}\,\vec{k}\,\exp\frac{-\beta F\eta}{RT}$$

where

$$\vec{k} = F\,\frac{kT}{h}\,\exp\frac{-\Delta G_c^{\dagger}}{RT}\,\exp\frac{-\beta F\Delta\Phi_e}{RT}$$

Thus $\vec{k}$ is the electrochemical rate constant for the reaction going in the forward direction. It contains both chemical and electrochemical terms and describes the intrinsic tendency for the reaction to occur in the absence of an external driving force (η).

Similarly, the rate of the reaction in the reverse (anodic) direction is given by

$$(48)\quad i_a = FC_M\,\frac{kT}{h}\,\exp\frac{-\Delta G_a^{\dagger}}{RT}\,\exp\frac{(1-\beta)F\Delta\Phi_e}{RT}\,\exp\frac{(1-\beta)F\eta}{RT}$$

where C_M = the concentration of metal atoms that can be oxidized

$\Delta G_a^{\dagger}$ = the chemical actuation energy for the reverse reaction

$(1-\beta)$ = the fraction of electrical energy which affects the rate of the reverse reaction.

and

$$(49)\quad i_a = C_M\,k\,\exp\frac{(1-\beta)F\eta}{RT}$$

where

$$\overleftarrow{k} = F\,\frac{kT}{h}\,\exp\frac{-\Delta G_a^{\dagger}}{RT}\,\exp\frac{(1-\beta F)\Delta\Phi_e}{RT}$$

When more than one electron is involved in the reaction the symmetry coefficient is replaced by a transfer coefficient, α, which includes a term for the number of electrons transferred.

For a complete derivation and description of these electrochemical kinetic equations the reader is referred to J. O'M. Bockris and A. K. N. Reddy, Modern Electrochemistry Vol 2 Plenum Press: New York (1970).

REFERENCES

1. M. Pourbaix, Atlas of Electrochemical Equilibria in Aqueous Solutions Pergamon Press: New York (1966).

2. N. D. Tomashov and R. M. Al'tovskii, Corrosion 19, 217t (1963).

3. M. Stern and H. Wissenberg, J. Electrochem. Soc. 106, 755 (1959).

4. M. Stern and H. Wissenberg, J. Electrochem. Soc. 106, 759 (1959).

5. N. D. Tomashov and E. N. Mirolyubov, eds., Corrosion of Metals and Alloys Collection No. 2 Israel Program for Scientific Translations: Jerusalem, p. 71 (1966).

6. J. E. Reinoehl, Ph.D Dissertation The Ohio State University (1967).

7. R. Otsuka, Sci. Papers I.P.C.R. 54, 97 (1960).

8. N. D. Tomashov, R. M. Al'tovskii and M. Ya Kushnerev, Dokl. Akad. Nauk SSSR 141, 913 (1961).

9. B. Stalinski and Z. Buganski, Bull. Acad. Polon. Sci. Ser. Chim. 10, 247 (1962).

10. T. R. P. Gibb, J. J. McSharry and R. W. Bragdon, J. Am. Chem. Soc. 73, 1751 (1951).

11. R. V. Tsvetnova, S. L. Dyatkina, S. N. Sheremet'eva, A. R. Kel'n and A. I. Krasil'shchikov, Russian J. Phys. Chem. 37, 544 (1963).

12. M. N. Fokin and R. L. Baru, Dokl. Akad. Nauk. SSSR 157, 954 (1964).

13. W. M. Latimer, Oxidation Potentials Second Edition, Prentice-Hall: Englewood Cliffs, N. J. (1952).

14. A. M. Sukhotin, Trudy XIV CICE. (1963).

15. D. Franz and H. Gohr, Ber. Buns. Ges. Physik. Chem. 67, 680 (1963).

16. J. W. Hickman and E. A. Gulbransen, Anal. Chem. 20, 158 (1948).

17. J. Yahalom and J. Zahavi, Electrochimica Acta 15, 1429 (1970).

18. N. D. Tomashov, R. M. Al'tovskii and A. G. Arakelov Dokl. Acad. Nauk. SSSR 121, 885 (1958).

19. F. H. Beck and M. G. Fontana "Stress Corrosion Cracking of Titanium Alloys" Ohio State University Research Foundation Report 2267-5 Grant No. NGR 36-008-051, March 1969.

20. N. D. Tomashov, R. M. Al'tovskii and M. Ya. Kushnerev, Zav. Lab. 3 (1960).

21. N. D. Tomashov, R. M. Al'tovskii, A. V. Prosuirin and R. P. Shamgunova, Collection The Corrosion and Protection of Constructional Materials, Moscow p. 151 (1961).

22. P. H. Morton and W. M. Baldwin, Trans. ASM 44, 1004 (1953).

23. S. Owaga and D. Watanabe, Sci. Rep. Res. Inst. Tohoku Univ. 2, 184 (1955).

24. O. Rudiger, W. R. Fischer and W. Knorr, Zs. Metallukunde 47, 8 (1956).

25. G. Sanderson and J. C. Scully, Corros. Sci. 6, 541 (1966).

26. R. Otsuka, J. Sci. Res. Inst. 51, 73 (1957).

27. R. Otsuka, J. Sci. Res. Inst. 49, 319 (1955).

28. M. B. Straumanis and P. C. Chen, Corrosion 7, 229 (1951).

29. S. Morioka and A. Umezono, J. Japan Inst. Metals 20, 407 (1956).

30. N. D. Tomashov, R. M. Al'tovskii and M. Ya. Kushnerev, Zavodskaya Laboratoriya 26, 298 (1960).

31. R. C. Menard, J. Opt. Soc. of America 52, 427 (1962).

32. D. L. Johnson and L. C. Tao, Surface Science 16, 390 (1969).

33. V. V. Andreeva, Corrosion 20, 35t (1964).

34. S. Ogawa and D. Watanabe, J. Japan Inst. Metals 18, 523 (1954).

35. M. Levy and G. N. Skover, J. Electrochem. Soc. 116, 323 (1969).

36. N. T. Thomas and K. Nobe, J. Electrochem. Soc. 116, 1748 (1969).

37. R. D. Armstrong, J. A. Harrison, H. R. Thirsk and R. Whitfield, J. Electrochem. Soc. 117 1003 (1970).

38. N. Hackerman and C. D. Hall Jr., J. Electrochem. Soc. 101, 321 (1954).

39. V. V. Andreeva and V. I. Kazarin, Proc. Acad. Sci. USSR, Phy. Chem. Sec. 121, 577 (1958).

40. N. D. Tomashov, G. P. Chernova and R. M. Al'tovskii, Russian J. Phys. Chem. 35, 523 (1961).

41. A. M. Sukhotin and L. I. Tungusova, Zashchita Metallou 4 8 (1968)*

42. N. D. Tomashov, V. N. Modestova, R. P. Vasil'eva and N. I. Stroganova, Zashchita Metallov 5, 496 (1969).

43. N. D. Tomashov, V. N. Modestova, V. V. Usova, N I. Stroganova, T. I. Kudryashova and R. P. Vasil'eva, in Hydrogenation of Metals and the Control of Hydrogen Brittleness Mosk. Dom. Nauchn. - Tekh: Propagandy, Moscow, p. 123 (1968).

44. N. D. Tomashov, and R. M. Al'tovskii, "Investigation of Self-Passivation of Titanium in Acid, Neutral and Alkaline Media" in Corrosion of Metals and Alloys Collection No. 1 N. D. Tomashov, ed., Metallurgisdat: Moscow, p. 141 (1963).

45. J. W. Oliver and J. W. Ross, J. Am. Chem. Soc., 85, 2565 (1963).

46. T. R. Beck, "Electrochemical Models for SCC of Titanium" NATO Conference on the Theory of Stress Corrosion Cracking in Alloys Ericerira, Portugal, March, 1971.

47. A. P. Brynza, L. I. Gerasyutina, E. A. Zhivotovskii, and V. P. Fedash, Zashchita Metallov 5, 15 (1969).

48. N. D. Tomashov, R. M. Al'tovskii and G. P. Chernova, J. Electrochem. Soc. 108, 113 (1961).

49. H. Togano, H. Sasaki and Y. Kanda, J. Japan Inst. Metals 33 1280 (1969).

50. D. Schlain and J. S. Smatko, J. Electrochem. Soc. 99, 417 (1952).

51. A. P. Brynza and V. P. Fedash, Zashchita Metallov 4 252 (1968).

52. M. Levy, Corrosion 23, 236 (1967).

53. N. T. Thomas and K. Nobe, J. Electrochem. Soc. 117, 621 (1970).

54. G. M. Kirkin and N. P. Zhuk, Zashchita Metallov 1 380 (1965).

55. S. Morioka and A. Umezono, J. Japan Inst. Metals 20, 403 (1956).

*English translation of Zashchita Metallov is available as a periodical under the title Protection of Metals.

56. J. M. Peters and J. R. Myers, Corrosion 23, 326 (1967).

57. M. E. Straumanis, S. T. Shih and A. W. Schlechten, J. Phys. Chem. 59, 317 (1955)

58. R. V. Tsvetnova and A. I. Krasil'shchikov, Zh. Fiz. Khim. 39, 201 (1965).

59. Ya. M. Kolotyrkin and G. M. Florianovich, Zashchita Metallov 1, 7 (1965).

60. A. N. Frumkin, V. N. Korshunov and Z. A. Iofa, Dokl. Akad. Nauk. SSSR 141, 413 (1961).

62. J. O'M. Bockris and A. K. N. Reddy, Modern Electrochemistry Vol. 2 Plenum Press: New York, p 1017 (1970).

63. H. H. Uhlig, Corrosion Science 7, 325 (1967).

64. H. H. Uhlig, The Corrosion Handbook, New York (1948).

65. V. M. Knyazheva and Ya. M. Kolotyrkin, Dokl. Akad. Nauk. SSSR 114, 1265 (1957)

66. N. D. Tomashov and N. M. Strukov, in Corrosion and Protection of Structural Alloys Part 1 A. D. Mercer ed., National Lending Library for Science and Technology: Boston Spa, Yorkshire, England, p. 95 (1968).

67. V. M. Novakovskii and Yu. A. Likhachev, Zashchita Metallov 1, 13 (1965).

68. A. I. Oshe, Ya. Ya. Kulyavik, T. I. Popova and B. N. Kabanov, Elektrokhimiya 2, 1485 (1966).

69. A. I. Oshe and B. N. Kabanov, Zashchita Metallov 4, 260 (1968).

70. A. N. Chemodanov, Ya. M. Kolotyrkin and M. A. Dembrovskii, Elektrokhimiya 5, 533 (1969).

71. V. M. Novakovskii and V. I. Ovcharenko, Zashchita Metallov 4, 656 (1968).

72. G. G. Kossyi, V. M. Novakovskii and Ya. M. Kolotyrkin, Zashchita Metallov 5, 210 (1969).

73. R. V. Tsvetnova and A. I. Krasil'shchikov, Zashchita Metallov 2, 295 (1966).

74. T. Murata, Ph.D Dissertation The Ohio State University (1971).

75. J. C. Griess Jr., Corrosion 24, 96 (1968).

76. J. O'M. Bockris and A. K. N. Reddy, Modern Electrochemistry Vol. 1 Plenum Press: New York, p. 547 (1970).

77. N. Sato and M. Cohen, J. Electrochem. Soc. 111 512 (1964).

78. M. B. Rockel, Private Communication.

79. T. P. Hoar, Trans. Inst. Metal Finishing 39, 166 (1962).

80. G. F. Savchenkov and L. A. Uvarov, Zashchita Metallov 1 636 (1965).

81. D. A. Vermilyea, "Anodic Films" in Advances in Electrochemistry and Electrochemical Engineering Volume 3 P. Delahay and C. W. Tobias, eds. Interscience: New York, p. 211 (1963).

82. J. Askill, Tracer Diffusion Data for Metals, Alloys and Simple Oxides Plenum: New York (1970).

83. N. D. Tomashov, V. N. Modestova and A. S. Aratol'yeva, "The Effect of Current Density on Hydrogen Embrittlement and Corrosion of Titanium Alloys" (ref. 44) p. 176.

84. A. F. Karasev and A. I. Stabrovskii, Zashchita Metallov 6, 324 (1970).

85. G. M. Kirkin and N. P. Zhuk, Zashchita Metallov 1, 648 (1965).

86. J. B. Rittenhouse, Trans. ASM. 51, 870 (1959).

87. M. G. Fontana and N. D. Greene, Corrosion Engineering McGraw-Hill: New York, p. 177 (1967).

88. H. B. Bomberger, "The Corrosion Resistance of Titanium" RMI TR D-15 Reactive Metals, Inc. March 28, 1966.

89. Ya. N. Kolotyrkin and V. A. Strunkin, Zashchita Metallov 6, 511 (1970).

90. N. G. Feige and T. J. Murphy, "Fracture Behavior of Titanium Alloys in Aqueous Environment" WESTEC Conference, 1966.

91. D. Schlain and J. S. Smatko, J. Electrochem. Soc. 99, 417 (1952).

92. H. H. Uhlig and A. Geary, J. Electrochem. Soc. 101, 215 (1954).

93. S. H. Weiman, Corrosion 22, 98 (1966).

94. V. V. Andreeva and E. A. Yakovleva, (ref. 66) p. 142.

95. N. D. Tomashov, G. P. Chernova and T. V. Matveeva, Zashchita Metallov 6, 145 (1970).

96. Yu. S. Ruskol and I. Ya Klinov, Zashchita Metallov 4, 495 (1968).

97. G. M. Kirkin and N. P. Zhuk, Zashchita Metallov 1, 380 (1965).

98. V. A. Strunkin, E. N. Poret and Kh. L. Tseitlin, Zashchita Metallov 5, 265 (1969).

99. A. F. Karasev and A. I. Stabrovskii, Zashchita Metallov 6, 324 (1970).

100. T. R. Beck, Proceedings of Conference on Fundamental Aspects of Stress Corrosion Cracking at The Ohio State University, R. W. Staehle, ec., NACE, Houston, P. 605 (1969).

101. E. N. Pugh, J. A. S. Green and A. J. Sedricks, "Current Understanding of Stress Corrosion Phenomena" RIAS Technical Report 69-3 March, 1969.

102. M. J. Blackburn and J. C. Williams, (Ref. 100) p. 620.

103. D. T. Powell and J. C. Scully, Corrosion 24, 151 (1968).

104. N. G. Feige and T. J. Murphy, "Environmental Effects on Titanium Alloys" TMCA Second Annual Conference, April, 1966.

105. G. Sanderson and J. C. Scully, "Room Temperature Stress Corrosion Cracking of Titanium Alloys" Nature, p. 179, July 9, 1966.

106. A. J. Sedriks, P. W. Slattery and E. N. Pugh, (ref. 100) p. 673.

107. B. F. Brown, et. al., "Marine Corrosion Studies, Third Interim Report of Progress," NRL Memorandum Report 1634, July, 1965.

108. "A Study of the Stress Corrosion Cracking of Titanium Alloys in Sea Water with Emphasis on the Ti-6Al-4V and Ti-8Al-1Mo-1V Alloys," Research Report No. R471, Project No. 93002, Reactive Metals, Inc., Oct. 18, 1965.

109. M. H. Peterson, B. F. Brown, R. L. Newbegin, and R. E. Groover, Corrosion 23, 142 (1967).

110. J. D. Jackson, and W. K. Boyd, "Stress-Corrosion and Accelerated Crack-Propagation Behavior of Titanium and Titanium Alloys," DMIC Technical Note, Battelle Memorial Institute, Feb. 1, 1966.

111. S. R. Seagle, R. R. Seeley and G. S. Hall, "The Influence of Composition and Heat Treatment on the Aqueous Stress Corrosion of Titanium," Research and Development Report 492, Reactive Metals, Inc., March 15, 1967.

112. J. D. Boyd, W. K. Boyd, R. A. Wood, and R. I. Jaffee, "The Effect of Composition on the Mechanism of Stress-Corrosion Cracking of Titanium Alloys in N_2O_4 and Aqueous and Hot-Salt Environments, "Second Quarterly Progress Report to NASA, Contract No. NASA-100 (09) Battelle Memorial Inst., June 14, 1967.

113. M. F. Amateau, E. A. Steigerwald, "The Relationship between Plastic Deformation and Fracture in Alpha Titanium," Equipment Laboratories TRW, Inc., June, 1966.

114. D. G. Howe, "Effects of Vacuum and Inert Atmosphere Heat Treatments on the Stress-Corrosion-Cracking Resistance of Several Titanium Alloys," Data Sheets for Presentation at Advanced Research Projects Agency Review, Lehigh University, August 1-2, 1966.

115. I. R. Lane, O. L. Cavallaro, and A. G. S. Morton, "Fracture Behavior of Titanium in the Marine Environment," U. S. Navy, MEL Report 231/65, July, 1965.

116. J. A. Kies, et. al. "Fracture Testing of Weldments" in Fracture Toughness Testing and Its Applications ASTM (1965).

117. H. P. Leckie, "Stress Corrosion Characteristics of a Ti-7Al-2Cb-1Ta Alloy," Annual Meeting of AIME, February, 1967.

118. C. M. Chen, F. H. Beck and M. G. Fontana Corrosion 27, 77 (1971).

119. D. N. Williams, R. A. Wood, E. L. White, W. K. Boyd, and H. R. Ogden, "Studies of the Mechanism of Crack Propagation in Salt Water Environments of Candidate Supersonic Transport Titanium Alloy Materials, "Final Report SST-66-1, BMI, Federal Aviation Agency Contract FA-SS-66-1, (January, 1966).

120. E. G. Haney, "Investigation of Stress Corrosion Cracking of Titanium Alloys, "Semi-Annual Progress Report No. 1, to NASA, Contract NGR-39-008-014, Mellon Institute, Nov. 30, 1966.

121. B. F. Brown, C. T. Fujii and E. P. Dahlberg, J. Electrochem. Soc. 116, 218 (1969).

122. B. F. Brown, "Solution Chemistry within Stress Corrosion Cracks in Titanium 8-1-1 Alloy" International Symposium on Stress Corrosion Mechanisms in Titanium Alloys at the Georgia Institute of Technology, Atlanta, Georgia, January, 1971.

123. F. H. Beck and M. G. Fontana, (ref. 19) Report 2267-2, July, 1967.

124. H. W. Pickering, and P. R. Swann, Corrosion 19, 373t (1963).

125. P. R. Swann, and H. W. Pickering, Corrosion 19, 369t (1963).

126. P. R. Swann, Corrosion 19, 102t (1963).

127. M. J. Blackburn, Trans. ASM 59, 694 (1966).

128. D. Tromans, and J. Nutting, Corrosion 21, 143 (1965).

129. T. P. Hoar, (ref. 100) p. 98.

130. T. P. Hoar and J. C. Scully, J. Electrochem. Soc. 11, 348 (1964).

131. H. H. Uhlig, (ref. 100) p. 86.

132. D. N. Williams, J. Inst. Metals 91, 147 (1962-63).

133. P. Cotterill, "The Hydrogen Embrittlement of Metals" Progress in Materials Science Vol. 9 Pergamon Press Ltd., 1961.

134. J. D. Boyd, et. al., (Ref. 112) Fourth Quarterly Progress Report, Feb. 29, 1968.

135. J. D. Boyd, et. al., (Ref. 112) Fifth Quarterly Progress Report, Aug. 26, 1968.

136. J. D. Boyd, et. al. (Ref. 112) Annual Summary Report, Aug. 26, 1969.

137. J. D. Boyd, Trans ASM 62, 977 (1969).

138. G. Sanderson, D. T. Powell and J. C. Scully, (ref. 100) p. 638.

139. A. J. Forty, in Physical Metallurgy of Stress Corrosion Fracture T. N. Rhodin, ed. Interscience: New York p. 99 (1959).

140. J. C. Scully, "The Stress Corrosion Cracking of α Titanium Alloys in Aqueous and Methanolic Environments" (ref. 122).

141. J. McBreen and M. A. Genshaw, (ref. 100) p. 51.

142. D. A. Mauney and E. A. Starke, Corrosion 25, 177 (1969).

143. E. L. Owen, Ph.D Dissertation The Ohio State University (1970).

144. V. M. Artemova, Elektrokhimiya 3, 1219 (1967).

145. A. T. Petrenko. Russian J. Phys. Chem. 36, 815 (1962).

146. Ya. M. Kolotyrkin and P. S. Petrov. Zh. Fiz. Khim. 31, 659 (1957).

147. J. O'M. Bockris and A. K. N. Reddy, (Ref. 62) Vol. II p. 1231.

148. R. E. Elson, H. C. Hornig, W. L. Jolly, J. W. Kury, W. J. Ramsey and A. Zalkin, "Some Physical Properties of the Hydrides" University of California Radiation Laboratory, Livermore, California UCRL-4519 June, 1956.

149. R. E. Meyer, J. Electrochem. Soc. 107, 847 (1960).

150. R. E. Meyer, J. Electrochem. Soc. 110, 167 (1963).

151. F. A. Posey, G. H. Cartledge and R. P. Yaffe, J. Electrochem. Soc. 106, 582 (1959).

152. N. D. Tomashov, V. N. Modestova, S. T. Glazunov, Ye. A. Borisova and V. L. Zotov, "Investigation of Hydrogen Embrittlement of α-Titanium Alloys in Cathodic Polarization" (ref. 44) p. 167.

153. R. J. Wasilewski and G. L. Kehl, Metallurgia 225, Nov., 1954.

154. J. Crank, The Mathematics of Diffusion Oxford: London p. 67 (1956).

155. H. R. Gray, "Role of Hydrogen in Hot-Salt Stress-Corrosion of a Titanium Alloy" (ref. 122).

156. M. G. Fontana, "Corrosion Cracking of Metallic Materials" The Ohio State University, Department of Metallurgical Engineering Technical Report AFML-70-2. January, 1970. p. 20.

157. A. J. E. Pourbaix, M. Marek and R. F. Hochman, "Electrochemical Behavior of Ti at Low pH and Low Electrode Potentials" (ref. 122)

158. W. B. Hillig and R. J. Charles, "Surfaces, Stress-Dependent Surface Reactions and Strength of High-Strength Materials" V. F. Zackay ed. John Wiley: New York (1965).

159. T. Murata, Masters Thesis The Ohio State University (1968).

160. T. P. Hoar and J. G. Hines, Stress Corrosion Cracking and Embrittlement W. D. Robertson, ed., John Wiley: New York, p. 107 (1956).

161. L. Yang, G. T. Horne and G. M. Pound, Physical Metallurgy of Stress Corrosion Fracture T. N. Rhodin, ed. Interscience: New York p. 29 (1959).

162. K. Nobe, E. Baum and W. F. Seyer, J. Electrochem. Soc. 108, 97 (1961).

163. H. W. Pickering, Acta Met 13, 437 (1965).

164. T. C. Finley and J. R. Myers, Corrosion 26, 150 (1970).

165. W. D. France, Jr., Corrosion 26, 189 (1970).

166. N. D. Tomashov and Yu. M. Ivanov, Zashchita Metallov 1, 36 (1965).

167. J. E. Slater, "Mechano-Chemical Phenomena in Stainless Alloys" Ph.D Dissertation, University of Cambridge (1970).

168. L. Graf and G. Springe (ref. 100) p. 335.

169. A. R. Despic, R. G. Raicheff and J. O'M. Bockris, J. Chem. Phys. 49, 926 (1968).

170. A. Windfeldt, Electrochemica Acta 9, 1139 (1964).

171. A. Windfeldt, Electrochemica Acta 9, p. 1295 (1964).

172. J. C. Giddings, A. G. Funk, C. J. Christensen, and H. Eyring, J. Electrochem. Soc. 106 91 (1959).

173. T. P. Hoar and J. R. Galvele, Corrosion Science 10, 211 (1970).

174. R. J. Clark, The Chemistry of Titanium and Vanadium Elsevier: New York (1968).

175. N. D. Tomashov and G. P. Chernova, Passivity and Protection of Metals Against Corrosion Plenum Press: New York p. 13 (1967).

176. W. A. Tiller and R. Schrieffer, Scripta Metallurgica 4, 57 (1970).

177. H. G. Nelsen, D. P. Williams, and A. S. Tetelman, Met. Trans. 2, 953 (1971).